Proteomic and functional analysis of the *Drosophila melanogaster* centrosome identifies a novel role in cell cycle control

Dissertation

zur Erlangung des akademischen Grades des
Doktors der Naturwissenschaften (Dr. rer. nat.)

eingereicht im Fachbereich Biologie, Chemie, Pharmazie
der Freien Universität Berlin

vorgelegt von

Hannah Müller
aus Troisdorf

Juni 2008

1. Gutachter: PD Dr. Bodo Lange
2. Gutachter: Prof. Dr. Ansgar Klebes

Disputation am: 10.Oktober 2008

Acknowledgements

First of all, I would like to thank Bodo Lange for his patient supervision and mentoring, his guidance and support throughout the years.

I thank Hans Lehrach and the people working in his department, who were always open for discussions and provided an excellent scientific environment.

I am grateful to Ansgar Klebes for being a member of my committee and reviewer of my thesis.

Special thanks go to our group, who accompanied me during my time as a PhD student, for creating this unique atmosphere, for inspiring discussions and lots of help, support and fun. Particularly, I thank Karin Habermann, Verena Lehmann and Marie-Laure Fogeron for their indispensable co-work during the experimental part of my PhD project and Thomas Kessler for critical reading of this thesis and useful advice.

I very much appreciate the good collaboration with Sandra Steinbrink and Michael Boutros during the ‘centrosome proteome project’.

I am thankful to Lukas Chavez and Axel Rasche for sharing their office with me and constantly encouraging me during the past few weeks.

I thank my family and friends for supporting me and for reminding me of the most important things in life.

Contents

List of publications enclosed in this thesis

Lehmann V, Müller H, Lange BMH. 2005. Immunoisolation of centrosomes from *Drosophila melanogaster*. Current Protocols in Cell Biology. Chapter 3: Unit 3.17.

Müller H, Mirgorodskaya E, Steinbrink S, Lehmann V, Habermann K, Gustavsson N, Lehrach H, Gobom J, Boutros M, Lange BMH. 2008. Proteome analysis identifies functionally conserved protein components important for centrosome structure and cellular signalling in *Drosophila* and human. Submitted.

Müller H, Fogeron ML, Lehmann V, Lehrach H, Lange BMH. 2006. A Centrosome-Independent Role for γ-TuRC Proteins in the Spindle Assembly Checkpoint. Science, 314: 654-656

1 Introduction

1.1 The centrosome

Theodor Boveri first described the centrosome in 1901 and named it on the basis of its location near the cell centre (Boveri, 1901). He observed that the centrosomes focused the ends of thin cytoplasmic fibres in interphase cells and bipolar spindles in mitotic cells. Boveri correlated the occurrence of supernumerary centrosomes with the assembly of multipolar mitotic spindles and cancer. He hypothesized that centrosomes play a role in aneuploidy resulting from missegregation of chromosomes during cell division (Boveri, 1914). Today the centrosome is characterised as the primary microtubule-organizing centre (MTOC) in eukaryotic cells. The centrosome plays a role in fundamental cellular functions like mitosis, cytokinesis, intracellular transport, cell polarity and positioning of other cell organelles. Apart from these microtubule-dependent processes it is implicated in cell cycle regulation and signal transduction pathways relating to DNA damage, stress response and differentiation (Lange, 2002). Centrosomal aberrations have been shown to occur in various diseases like cancer and several genetic disorders (see chapter 1.6).

The centrosome consists of two centrioles that are embedded in a complex protein matrix, the pericentriolar material (PCM) (Fig.1). The composition of the PCM is largely unknown. Moreover, the PCM is highly dynamic and its protein composition changes depending on the cell cycle stage (Kalt & Schliwa, 1993).

Centrioles are cylindrical structures in orthogonal configuration with interconnecting fibres at their proximal ends. A centriolar pair consists of a mature centriole (mother centriole) and an immature centriole that is assembled during the previous cell cycle (daughter centriole). A mammalian centriole consists of nine microtubule triplets held together by linker proteins. The mother centriole has nine distal and nine subdistal appendages, which anchor cytoplasmic microtubules or dock to membranes (Paintrand *et al*., 1992). The centriole of the early *Drosophila melanogaster* embryo lacks appendages and consists of a ring of nine singlet microtubules (Moritz *et al.*, 1995) or doublet microtubules (Callaini *et al*., 1997) surrounding one central tube.

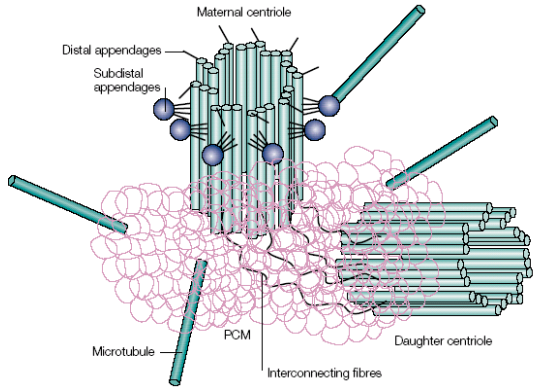

Figure 1: Structure of the centrosome
The illustration shows a pair of centrioles connected by fibres. The mother centriole has subdistal and distal appendages. The centrioles are embedded in pericentriolar material that is essential for microtubule nucleation.
(Doxsey, 2001)

In contrast to other cell organelles the centrosome is not enclosed by a membrane. Thus, it is still unclear what holds the centrosome together. A scaffold structure has been proposed to serve as the basis for centrosomal cohesion (Schnackenberg *et al*., 1998, Moritz *et al*., 1998). The scaffold is described as a stable protein matrix that resists extraction with high concentration of potassium iodide. Soluble PCM components assemble onto the scaffold to form an intact centrosome. Which proteins build the scaffold structure remains to be elucidated.

Centrosomes are present in higher eukaryotic cells with the exception of female meiotic cells in e.g. *Drosophila* (Theurkauf & Hawley, 1992) or mouse (Szollosi *et al*., 1972) and higher plant cells (reviewed by Schmit, 2002). Even though centrosomal proteins are evolutionary conserved, the microtubule-organizing centre differs morphologically between species. The functional equivalent of the centrosome in yeast is the spindle pole body (SPB). The SPB is a cylindrical multilaminate organelle embedded in the nuclear envelope. It consists of three plaques: an outer cytoplasmic plaque, a central plaque in the plane of the nuclear membrane and an inner plaque within the nucleus (Rout & Kilmartin, 1990). The MTOC in slime molds like *Dictyostelium discoideum* is termed nucleus-associated body (NAB) (Roos, 1975). The NAB has a multilayered, box-shaped core that is embedded in an amorphous corona (Omura & Fukui, 1985) and lacks centrioles (Heath, 1981). Basal bodies are related to centrioles and serve as the template for the axoneme, the basic structure of all eukaryotic cilia and flagella. In the green algae *Chlamydomonas* the same organelle functions as a flagellar basal body during interphase and as centriole at the spindle pole during cell division.

The next sections focus mainly on the centrosome in *Drosophila melanogaster* and *Homo sapien*s because the experimental work in this thesis concerns the isolation,

identification and functional characterisation of centrosomal proteins of these two organisms.

1.2 Isolation of centrosomes

Although many centrosomal components have been identified, a comprehensive molecular characterisation of the centrosome in *Drosophila* has not been accomplished yet. The centrosome represents only a minor proportion of the cell proteome as it is small and is present in a single copy per cell. Therefore, an enrichment of centrosomes is the prerequisite for the molecular characterisation of the organelle. The limiting factor for such analysis was the lack of an isolation method that enriches centrosomes thousand-fold and at the same time sufficiently reduces contamination with other cellular components.

A number of methods have already been established to isolate centrosomes from diverse organisms, tissues or cultured cells. These include the isolation from human lymphoblastoma KE37 cells (Moudjou & Bornens, 1994), mouse neuroblastoma N115 and CHO cells (Mitchison & Kirschner, 1984) *Spisula solidissima* oocytes (Palazzo & Vogel, 1999), calf thymus (Komesli *et al*., 1989) and *Drosophila* embryos (Moritz *et al*., 1995). Like the isolation of spindle pole bodies from yeast (Rout & Kilmartin, 1990) all these methods are based on cell organelle enrichment via density gradient centrifugation. Lange *et al*. (2000) developed a new efficient immunoisolation technique that further improves the enrichment of centrosomes. With this method, centrosomes are first isolated in sucrose step gradients from syncytial *Drosophila* embryos. Subsequently, centrosomes are affinity purified using magnetic beads that are coupled to centrosome-specific antibodies (Lange *et al*., 2000). Within the experimental part of this thesis, this method has been further optimized (see chapter 2.1 and 3.1). The immunoisolation of centrosomes results in highly enriched centrosomal preparations that can be used for the direct identification of centrosomal proteins by mass spectrometry techniques. Hence, this approach makes a direct biochemical dissection of the centrosome feasible and provides the basis for a systematic functional analysis of the centrosomal proteome.

1.3 Identification of centrosomal proteins

During the past ten years remarkable progress has been made in defining the structure and the molecular composition of the centrosome. Several approaches to identify centrosomal proteins have been developed. Initially, Calarco-Gillam *et al*. used a human autoantibody that marked an antigen in the PCM (Calarco-Gillam *et al*., 1983). Thereafter, a number of centrosomal proteins have been identified based on using autoimmune sera and subsequent production of centrosome-specific antibodies. The application of organelle isolation and subsequent mass spectrometric analysis allowed identification of further centrosomal or centriolar proteins and related structures like basal bodies, cilia and flagella. This approach was first carried out for the yeast spindle pole body, discovering twelve known and eleven novel spindle pole proteins (Wigge *et al*., 1998). The proteomic analyses of human centrosomes (Andersen et al., 2003) and cilia (Ostrowski *et al*., 2002), basal bodies (Keller *et al*., 2005) and flagella (Pazour *et al*., 2005) of *Chlamydomonas* as well as basal bodies of *Trypanosoma* (Broadhead *et al*., 2006) and nucleus-associated body of *Dictyostelium* (Reinders *et al*., 2006) have identified more than 300 candidate proteins in total. Some of these candidate proteins have been confirmed by localization and mutagenesis studies or RNA interference (reviewed in Bettencourt-Dias & Glover, 2007). A number of studies have taken advantage of recent sequencing and annotation of several genomes using genomics and comparative genomics approaches. The computational subtraction of the non-flagellated proteome of *Arabidopsis* from the shared proteome of the ciliated and flagellated organisms *Chlamydomonas* and human led to the identification of proteins that are involved in ciliary and basal body biogenesis and function (Li *et al*., 2004). A large set of flagellar components was discovered in the genome-wide analysis of transcription levels following deflagellation in *Chlamydomonas* (Stolc *et al*., 2005). Furthermore, a functional whole genome RNA interference (RNAi) screen for proteins involved in mitotic spindle assembly (Goshima *et al*., 2007) revealed novel centrosomal components in *Drosophila*.

Despite all efforts to define the molecular make-up of the centrosome, further molecular characterisation of the centrosome has to be accomplished to reveal the precise functions of the cell organelle and to better understand the implication of the centrosome in fundamental cellular processes. This knowledge will be relevant for understanding the role of the centrosome in signalling pathways of the cell cycle, stress,

differentiation, cell death and the relation of dysregulation of the centrosome cycle and dysfunction of centrosomal proteins to diseases.

1.4 Known centrosomal proteins and their functions

Previous studies have identified several centrosomal components, which can be classified into at least four groups according to their function (Lange, 2002):
(a) Scaffold proteins that maintain the structure of the centrosomes, (b) proteins functioning in microtubule nucleation, (c) anchoring proteins that connect microtubule nucleation proteins to regulatory molecules and (d) regulatory proteins like kinases, phosphatases and signalling molecules.
The centrosome is the only cell organelle in higher eukaryotic cells that has no clear boundary (reviewed by Kalt & Schliwa, 1993). Thus, the basis of centrosomal cohesion, a stable protein matrix has been proposed to serve as a scaffold (Schnackenberg *et al*., 1998, Moritz *et al*., 1998). The scaffold structure persists extraction with high salt concentrations while it looses the ability to nucleate microtubules. The nucleating ability can be restored with embryonic extract, demonstrating that the scaffold builds a basic structure onto which functional subunits are assembled. Ultrastructural analysis of potassium iodide (KI) extracted *Spisula solidissima* centrosomes revealed a latticework of 12-15 nm-diameter filaments that lack centrioles (Schnackenberg *et al*., 1998). Approximately 90% of centrosomal proteins are removed by KI treatment, of the residual 10% that are part of the scaffold structure, only few have been identified so far. One example of a scaffold protein is Odf2 in mammalian cells that is associated with the mother centriole in G0/G1 phase of the cell cycle and with both centrioles toward G1/S phase before centrosome duplication (Nakagawa *et al.*, 2001).
The basic function of the centrosome is microtubule nucleation. Microtubule nucleation is mediated by γ-tubulin and associated proteins, which are localised in the PCM. A model has been proposed in which γ-tubulin is mainly found in two complexes in *Drosophila* (Moritz *et al*., 2000): the γ-tubulin small complex (γ-TuSC) in which two γ-tubulin molecules bind to Grip84 and Grip91 and the γ-tubulin ring complex (γ-TuRC).

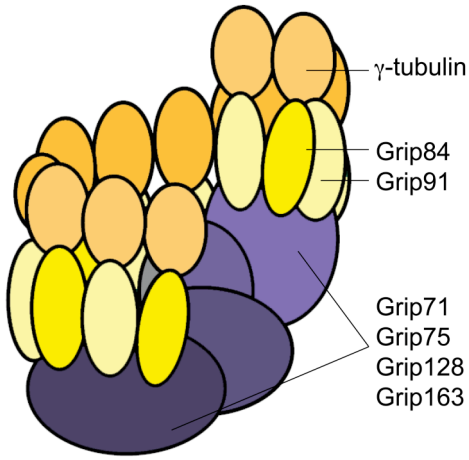

Figure 2: Structure of the γ-TuRC
This model of the γ-TuRC shows the helical arrangement of its components. Two γ-tubulin molecules bind to Grip84 and Grip91 to form γ-TuSC. Six of these complexes associate with the proteins Grip71, Grip75, Grip128 and Grip163.
The γ-TuRC is the starting point for microtubule nucleation.
(Moritz, 2000)

The γ-TuRC consists of six γ-TuSCs that are arranged in a ring structure and associate with the proteins Grip71, Grip75, Grip128 and Grip163 maintaining the configuration of the ring (Fig.2). γ-tubulin is in contact with the minus end of a microtubule protofilament, forming the starting point for microtubule nucleation. A core component of the centrosome is Centrosomin (Cnn) that is responsible for the assembly of other PCM proteins to achieve microtubule-organizing activity in *Drosophila*. Cnn was first identified as a regulatory target of the homeotic genes in *Drosophila* (Heuer & Kaufman, 1995). Functional studies of mutant *Drosophila* embryos revealed that absence of Cnn displaces the PCM core proteins γ-tubulin, CP60 and CP190 from the centrosome and results in a lack of astral microtubules in mitosis (Megraw *et al*., 1999). It has been shown recently that centrosomal localisation of the proteins Aurora A, D-TACC and Msps also depend on Cnn (Zhang & Megraw, 2007).

The centrosome is integrated in multiple signalling pathways (Lange, 2002). It is thought to serve as a docking site that brings regulatory elements in close proximity to each other or to specific centrosomal proteins. This connection is mediated by anchoring proteins. Examples of this protein class are Pericentrin or AKAP450 that contain a functional domain to bind phosphatases or kinases and a PACT (Pericentrin/AKAP450 centrosomal targeting) domain functioning in recruiting proteins to the centrosome (Gillingham & Munro, 2000). In *Drosophila*, the pericentrin-like protein (D-PLP) that contains a PACT domain is essential for efficient recruitment of the PCM components Cnn, D-TACC, CP60, Msps and CP190 to the centrosome (Martinez-Campos *et al*., 2004).

A multitude of regulatory proteins, namely kinases and phosphatases, localise to the centrosome. Protein phosphorylation and dephosphorylation plays an important role in controlling microtubule nucleation ability in different cell cycle stages. During centrosome maturation the kinases Polo and Aurora A among other proteins promote the recruitment of microtubule nucleation factors to prepare for the assembly of the mitotic spindle. This is counteracted through dephosphorylation by protein phosphatases like protein phosphatase 1 (PP1) or protein phosphatase 4 (PP4) (reviewed by Bettencourt-Dias & Glover, 2007).

The view of the centrosome changes from being only a microtubule-organizing centre towards functioning as a regulatory hub connected to cell cycle progression and checkpoint control (see chapter 1.7). Further identification and characterisation of novel centrosomal proteins contributes to a better understanding of these processes. Furthermore, the identification of components of the centrosomal scaffold is necessary to clarify the basis of centrosomal cohesion and therefore important aspects of centrosome function.

1.5 The centrosome cycle

The centrosome duplicates and segregates in synchrony with the cell cycle. A critical feature of the centrosome cycle is to limit centrosome duplication to once per cell cycle. The centrosome duplication cycle in higher animal cells can be subdivided into four distinct steps: centriole disengagement, centriole duplication, centrosome maturation and centrosome separation (Fig.3). Some of these steps can be linked to cell cycle progression through involvement of common regulators.

Centriole disengagement: In G1-phase of the cell cycle the orthogonal configuration of the two centrioles is lost, a process that is referred to as centriole disengagement. It requires the activity of the protease separase that also triggers anaphase by disrupting sister chromatid binding (Tsou & Stearns, 2006). It has been suggested that engagement of the centrioles with each other blocks centrosome re-duplication and that disengagement licenses duplication in the subsequent cell cycle as mechanism to control centrosome number and limit duplication to once per cell cycle (Tsou & Stearns, 2006).

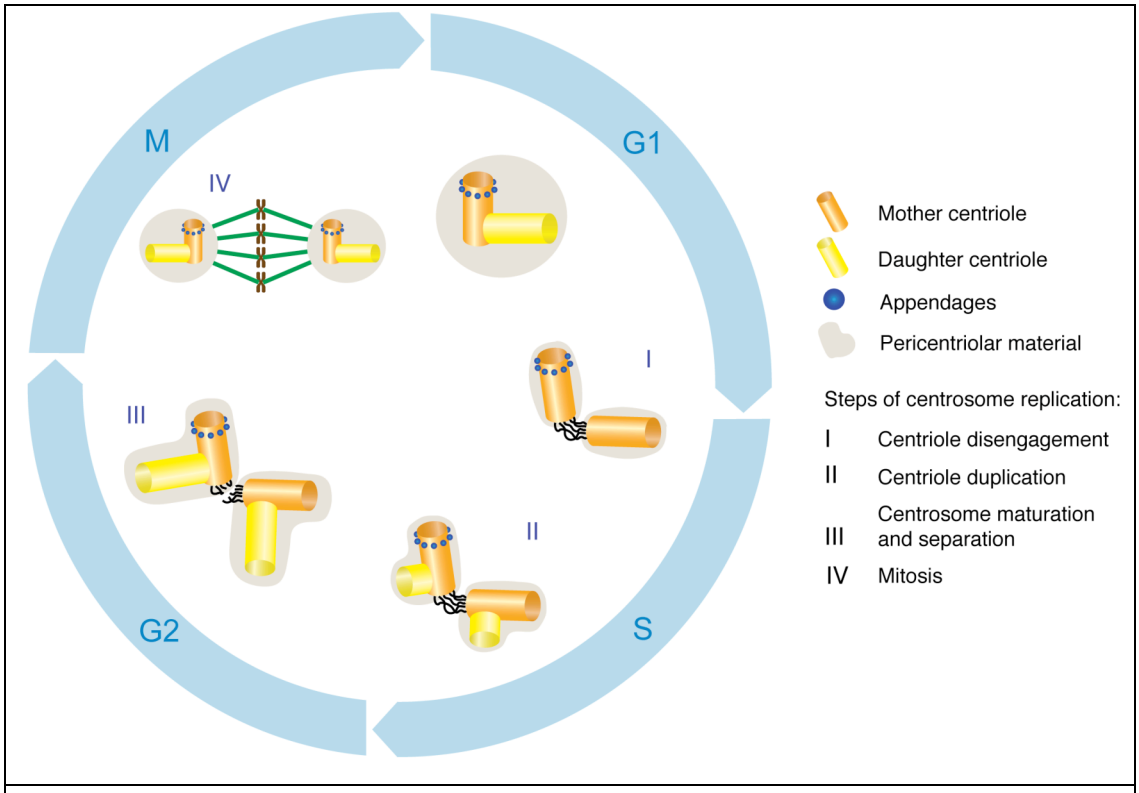

Figure 3: The centrosome cycle
The steps of the centrosome cycle are outlined in this illustration. Centriole disengagement: The orthogonal orientation of the two centrioles breaks down in G1-phase. Centriole duplication: Procentrioles are generated perpendicular to the mother centriole in S-phase and elongate until G2. Centrosome maturation: Additional proteins are recruited to the PCM in preparation of mitosis. Centrosome separation: The linkage between the centrioles disassembles prior to mitosis. Centrosome separation results in two centrosomes containing two centrioles each that build the spindle poles.

Centriole duplication: Procentrioles are generated perpendicular to the mother centriole in S-phase and elongate until G2. Initiation of centriole duplication requires the cell cycle kinase Cdk2 together with cyclin E and cyclin A in *Xenopus* egg extracts (Hinchcliffe *et al.*, 1999) and mammalian cells (Meraldi *et al.,* 1999; Matsumoto *et al.*, 1999). The protein nucleophosmin, which is abundantly found in the nucleolus (Szebeni & Olson, 1999) also localises to spindle poles after nuclear envelope breakdown and is a primary target for phosphorylation by Cdk2/cyclin E in order to initiate centriole duplication (Okuda *et al.*, 2000). The Cdk2/cyclin E complex is also known to induce DNA replication (reviewed in Ekholm *et al.*, 2000). Cdk2/cyclin E triggers initiation of DNA synthesis by phosphorylation of the retinoblastoma protein (Rb). Phosphorylated Rb dissociates from E2F transcription factor resulting in transcription of genes necessary for initiation of DNA synthesis (Nevins, 1992). A recent study shows that uncoupling of nuclear cycle and centrosome cycle occurs as a consequence of RNAi-

mediated protein depletion of mitotic cyclins in early *Drosophila* embryos (McCleland & O'Farrell, 2008). The activation of Cdk2/cyclin E is a key event for the coordinated initiation of centriole duplication and DNA replication.

Further proteins that are essential for centriole duplication have been identified in *C.elegans*. Consecutive recruitment of SPD-2, the kinase ZYG-1 and the SAS-6 – SAS-5 complex leads to formation of the central tube onto which singlet microtubules are assembled (Pelletier *et al*., 2006, Delattre *et al*., 2006). This mechanism is likely to be conserved because the involved proteins (except ZYG-1) have orthologues in other species (Azimzadeh & Bornens, 2007). Plk4, a member of the Polo kinase family, has been proposed to be a functional equivalent of ZYG-1 because it positively regulates centriole duplication in *Drosophila* and human (Bettencourt-Dias *et al*., 2005; Habedanck *et al*., 2005).

Centrosome maturation: During the G2-phase and mitosis numerous proteins are recruited to the PCM. The process of centrosome maturation depends on mitotic kinases like Aurora A (Hannak *et al*., 2001; Berdnik & Knoblich, 2002), Polo (Fry *et al*., 2000) or Nek2 (Fry *et al*., 1998). Centrosomal proteins are phosphorylated and the ability to nucleate microtubules increases due to enhanced recruitment of γ-tubulin ring complexes (reviewed by Palazzo *et al*., 2000). In addition, centrosomal microtubules are stabilized by activation of D-TACC – Msps complexes through phosphorylation by Aurora A in *Drosophila* (Barros *et al*., 2005). The increase in microtubule nucleation capacity and the stabilization of centrosomal microtubules is a prerequisite for assembly of the mitotic spindle.

Centrosome separation: Centrosome separation results in the generation of two spindle poles containing two centrioles each. The linkage between the mother centrioles disassembles in response to phosphorylation of linker proteins such as C-Nap1 (Mayor *et al*., 2000) and Rootletin (Bahe *et al*., 2006).

In conclusion, regulators of the cell cycle also participate in regulating the centrosome cycle. Thus, timing and progression of both centrosome and cell cycle are coordinated, demonstrating the interdependence of cell cycle and centrosome cycle.

1.6 The centrosome in disease

The importance of the centrosome and its components is reflected by its implication in several human diseases like cancer, ciliary diseases or neurodegenerative disorders. Examples for the role of centrosomal aberrations or dysfunction of centrosomal proteins in human diseases are summarised in the following section.

1.6.1 Cancer

The transformation of a normal cell into a cancer cell is likely to result from the accumulation of mutations in multiple genes (Hanahan & Weinberg, 2000). These mutations cause malignant phenotypes like immortalization, mitogen-independent growth, anchorage-independent growth or loss of tissue specificity (Fukasawa, 2005). Tumourigenesis involves uncontrolled cell proliferation and metastasis. Characteristic of tumour cells is genomic instability resulting from aneuploidy, chromosome translocation, gene amplification and mutation (Cheng & Loeb, 1997).

Centrosome abnormalities occur in many types of human cancers. These abnormalities include numerical aberrations, increase in centrosome size, formation of acentriolar bodies and alteration of phosphorylation state of PCM components. Increased and decreased recruitment of γ–TuRCs cause altered microtubule nucleation capacity and therefore affect shape, polarity and motility of tumour cells (Lingle *et al.*, 2002). Supernumerary centrosomes (extra-copies of centrosomes) are observed in almost all types of cancers. If more than two centrosomes are present in a cell, multipolar mitotic spindles are formed. This increases the frequency of chromosome segregation errors that lead to higher tumour progression rate and to genomic instability, as suggested for example for pancreatic cancer by Shono *et al*. (2001). Deregulation of centrosome duplication, cytokinesis failure, cell fusion or *de novo* genesis were proposed as possible reasons for occurrence of supernumerary centrosomes (Nigg, 2006).

The relevance of the tumour suppressor gene p53 for centrosome number control indicates a relation between deregulation of the centrosome duplication cycle and cancer. p53 is frequently mutated in human cancers. It is activated as a consequence of DNA damage and regulates key processes like DNA repair, cell cycle arrest and apoptosis in order to suppress cancer (reviewed by Riley *et al*., 2008). p53 has been linked to control of centrosome duplication, because p53 deficiency in mouse cells was shown to result in centrosome overduplication (Fukasawa, 1996; Fukasawa, 1997).

The tumour suppressor genes BRCA1 and BRCA2 are both implicated in DNA repair (Moynahan *et al*., 1999; Kerr & Ashworth, 2001) and bind to Rad51, which plays a role in repair of DNA double-strand breaks (Scully *et al*., 1997; Mizuta *et al*., 1997). Deficiency of BRCA1 (Xu *et al*., 1999), BRCA2 (Tutt *et al*., 1999) and Rad51 (Bertrand *et al*., 2003) results in supernumerary centrosomes, therefore providing a link between DNA damage/repair and centrosome duplication.

So far, it is unclear if overduplication of centrosomes is a cause or a consequence of tumourigenesis. However, the existence of supernumerary centrosomes in pre-cancerous lesions supports the view that overduplication of centrosomes might be an early event in tumourigenesis (Nigg, 2006).

1.6.2 Ciliary diseases

Centrioles are structurally related to basal bodies, which generate cilia and flagella (reviewed by Kilburn & Winey, 2008). Motile cilia and flagella are important for cell locomotion and transport of material over cell surfaces. Cilia play a role in processes important for development and health like determination of left-right asymmetry, kidney function and photoreception. The primary cilium in vertebrate cells is a non-motile cilium that provides sensory and signalling functions (reviewed by Marshall & Nonaka, 2006). Dysfunction of basal body/centriole and cilia associated proteins leads to human diseases. An example for a ciliary disease is the Bardet-Biedl syndrome (BBS). BBS is a multisystemic disorder characterized by retinal dystrophy, renal dysfunction, obesity, polydactyly and numerous developmental and behavioural defects (Beales *et al*., 1999). Mutations in several genes (BBS1 – BBS12) have been linked to the syndrome. At least four of the twelve known mammalian BBS proteins localize to centrosomes and basal bodies (Ansley *et al*., 2003; Kim *et al*., 2004; Li *et al*., 2004, Kim *et al*., 2005). BBS4 for instance localizes to centriolar appendages and interacts with the protein PCM1. PCM1 is thought to be involved in recruiting proteins to the centrosome that are necessary for centrosome duplication as well as microtubule organization and anchoring (Dammermann & Merdes, 2002). Silencing or expression of truncated forms of BBS4 (similar to those found in BBS) induces mislocalisation of PCM1 which detaches microtubules from the centrosome, arrests the cell in the cell cycle, leads to apoptotic cell death and finally contributes to the BBS phenotype (Kim *et al*., 2004).

1.6.3 Neurodegenerative disorders

The observation that proteasomes are concentrated at the centrosome and that proteasomal components co-purify with γ-tubulin in centrosomal fractions after sucrose gradient centrifugation has led to the description of the centrosome as a proteolytic centre (Wigley *et al*., 1999) and to its association with Parkinson's disease. Dysfunction of protein degradation at the proteasome is implicated in several neurodegenerative disorders like Parkinson's disease (reviewed by Badano, 2005).

Furthermore, the centrosome is implicated in the neurodegenerative disorder Huntington's disease. The centrosome is organising the microtubule cytoskeleton and therefore plays a role in intracellular transport and positioning of proteins and cell organelles. Neuronal defects that are observed in Huntington disease are thought to result from defects in microtubule-dependent vesicle transport (Gutekunst *et al*., 1995), which links the centrosome to this disease. In addition, the huntingtin protein that causes Huntington's disease by expansion of a polyglutamine repeat, interacts indirectly with PCM1 (Engelender *et al*., 1997).

1.6.4 Genetic disorders

Lissencephaly is a human brain malformation manifested by a smooth cerebral surface and abnormal neuronal migration. Mutations in the genes LIS1 (Reiner *et al*., 1993) and DCX (Gleeson *et al*., 1998) cause lissencephalic phenotypes and contribute to neuronal migration defects in Miller-Dieken syndrome. Both proteins localize to centrosomes.

Mutations in centrosomal genes CDK5RAP2 (Bond *et al*., 2005), ASPM (Shen *et al*., 2005) and CENPJ (Bond *et al*., 2005) have been identified in primary microcephaly. A recent study reveals that a mutation of Pericentrin (PCNT) causes primordial dwarfism (Rauch *et al*., 2008). Pericentrin is part of the PCM and anchors γ-tubulin and is therefore essential for maintaining centrosome function (Takahashi *et al*., 2002). The absence of Pericentrin in patients' cells resulted in disorganized mitotic spindles and chromosome segregation defects (Rauch *et al*., 2008).

Numerical aberrations or dysfunction of centrosomal proteins often occur in disease. It has been shown that dysfunction of a centrosomal protein causes for example primordial dwarfism. In terms of cancer, there is a debate on cause or consequence of

centrosome overduplication (Nigg, 2002). Hence, more and more evidence is provided for a close link of the centrosome to genetic diseases. Future work needs to elucidate the molecular basis of such diseases and the role of centrosomal proteins in their development.

1.7 The spindle assembly checkpoint

The cell cycle is divided into (a) interphase consisting of the G1 phase, S phase and G2 phase and (b) mitosis. In G1 and G2 phase, the so-called gap phases, the cell grows, synthesizes proteins and assembles organelles. During S phase the DNA is replicated in preparation for cell division. In mitosis the cytoplasm and chromosomes are equally distributed between the two daughter cells. The precision of chromosome distribution is crucial for the cell to maintain genomic stability. Errors in this process might lead to either cell death or malignant transformations (Nigg, 2001).

Therefore, the cell cycle is controlled by a checkpoint system that monitors the process of cell division and is able to delay cell cycle progression in order to correct defects like DNA damage or incomplete mitotic spindle assembly. The transition of metaphase to anaphase during mitosis is controlled by the spindle assembly checkpoint (SAC). The SAC is explained in detail in the following section because a part of this thesis provides evidence for a molecular role of γ-TuRC proteins in the activation of the spindle assembly checkpoint (Fig. 4).

During prometaphase the spindle microtubules bind to the kinetochores, which are specialised protein structures that assemble on the centromere of each chromosome. In metaphase the pairs of sister chromatids are aligned in the metaphase plate and attached to spindle microtubules emanating from opposite poles. The sister chromatids are held together by a multisubunit protein complex called cohesin (Michaelis *et al*., 1997). The cohesin-mediated cohesion is protected by the protein Shugoshin (Salic *et al*., 2004) that also plays a role in centriole cohesion (Wang *et al*., 2008).

At the onset of anaphase, sister chromatids become separated and pulled towards the spindle poles. The separation of sister chromatid requires the activation of the anaphase-promoting complex/cyclosome (APC/C), a multiprotein E3 ubiquitin ligase, by Cdc20. APC_{Cdc20} ubiquitylates securin, which is an inhibitor of the protease separase, thereby targeting it for degradation by the proteasome (reviewed by Castro *et al*., 2005).

Degradation of securin releases the protease separase that cleaves the cohesin complex and enables sister chromatid separation (Uhlmann *et al*., 1999).

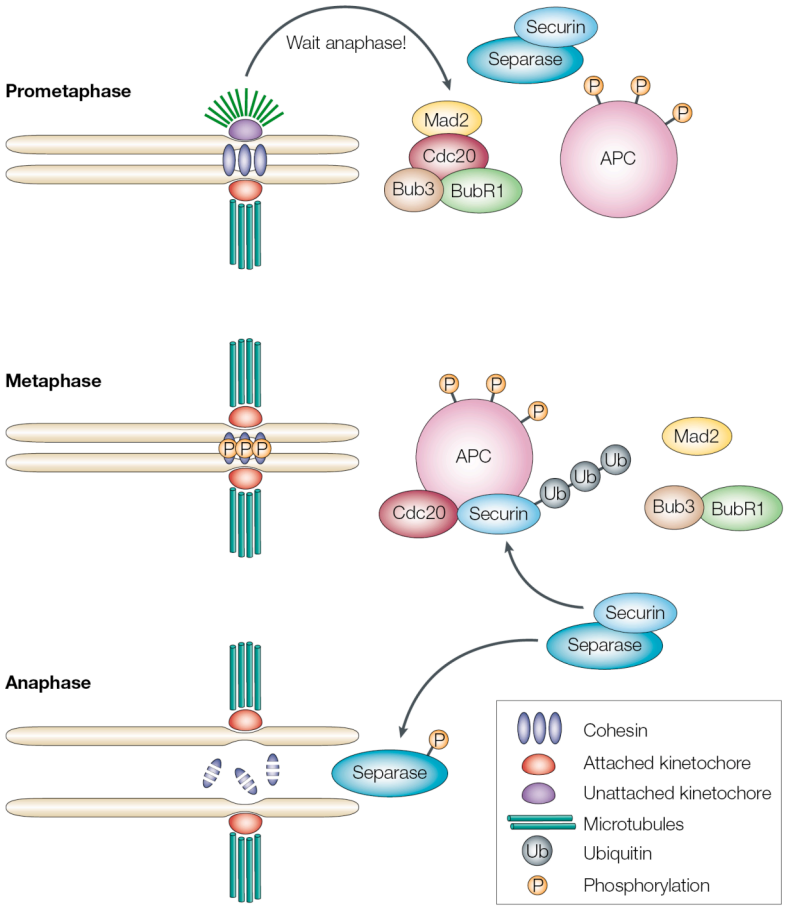

Figure 4: The spindle assembly checkpoint prevents transition from metaphase to anaphase
At the onset of anaphase, sister chromatids are separated and pulled to the opposite poles if kinetochores are bipolar attached to spindle microtubules. Unattached kinetochores can be sensed by the Mad and Bub spindle assembly checkpoint proteins that generate a diffusible "wait"-signal. Cdc20 forms APC-inhibitory complexes with BubR1, Bub3 and Mad2. Once all kinetochores are attached, the spindle assembly checkpoint is turned off and Cdc20 activates APC. APC ubiquitylates the separase inhibitor securin, thereby targeting it for proteolysis. Separase is released and cleaves cohesin complexes that mediate chromatid cohesion causing sister chromatids to separate.
(Musachio & Hardwick, 2002)

The equal distribution of chromosomes to the daughter cells depends on the correct bipolar attachment of all kinetochores to the mitotic spindle. The SAC is a surveillance mechanism that delays anaphase onset by maintaining sister chromatid cohesion. It senses the existence of misaligned sister chromatids by either lack of attachment or tension that is generated by pulling forces of the mitotic spindle (reviewed by Musachio & Hardwick, 2002). The highly conserved core spindle assembly checkpoint proteins

are Mad1, Mad2, BubR1, Bub1, Bub3 and Mps1. Mad1 and Bub1 are stably associated with unattached kinetochores, BubR1 and Mad2 are proposed to function as a diffusible signal that prevents anaphase onset (Howell *et al*., 2004). Cdc20-activation of APC/C is the key target of the SAC. BubR1, Bub3, Mad2 and Cdc20 have been proposed to form APC/C-inhibitory complexes (reviewed by Yu, 2007) preventing securin from being degraded. Consequently, sister chromatid cohesion is preserved and anaphase onset is delayed until all chromosomes are bipolar attached to the mitotic spindle. Once all kinetochores are attached, APC/C can be activated. In addition to securin, APC/C targets cyclin B for degradation via the proteasome pathway. This degradation leads to inactivation of the Cdk1/cyclin B complex, which is essential for exit from mitosis (Glotzer *et al*., 1991).

It has been suggested that the centrosome is implicated in mitotic progression: The centrosome is involved in the metaphase-anaphase transition via cyclin B. The degradation of cyclin B starts at the spindle pole and extends to the mitotic spindle in Drosophila embryos (Huang & Raff, 1999). In the Drosophila mutant "centrosome fall off" (cfo), in which centrosomes are displaced from the spindle pole, degradation of cyclin B occurred at the centrosome but not at the mitotic spindle, resulting in anaphase arrest (Wakefield *et al*., 2000).

In addition, a function for the centrosomal proteins γ-tubulin in *Aspergillus nidulans* (Prigozhina *et al*., 2004) and pericentrin in *Schizosaccharomyces pombe* (Rajagopalan *et al*., 2004) in cell cycle transitions and establishing or maintaining a mitotic checkpoint has been proposed. Furthermore, within this thesis the role of γ-TuRC proteins in the spindle assembly checkpoint in *Drosophila* and human has been shown (Müller *et al*., 2006).

In conclusion, the view of the centrosome as an organelle that is solely responsible for organisation and anchoring of microtubules is incomplete. Centrosomes and centrosomal proteins independently of the centrosome structure also function in regulation of the cell cycle and are integrated in disease related signalling pathways.

1.8 Aim of this project

In spite of the fact that the centrosome has been suggested to have many important cellular functions and is implicated in the development of several genetic diseases, its molecular structure and composition remains unclear so far. Hence, to have a better knowledge of the precise molecular role of centrosome components, it was the aim of this project to carry out a comprehensive biochemical analysis of the centrosomal proteome from *Drosophila melanogaster* using whole cell organelle isolation followed by the functional characterisation of all identified components.

A prerequisite for the elucidation of the centrosome protein composition was to optimise the isolation procedure in order to obtain highly enriched preparations. It was the first goal to improve an immunoisolation technique of this cell organelle. The next steps were the identification of centrosomal proteins using mass spectrometry and their functional characterisation through protein depletion in *Drosophila* SL2 cells using RNAi. The following phenotype analysis was directed at identifying proteins that are relevant for centrosome segregation, replication, maturation, altered cell cycle distribution and aberrant chromosome segregation when depleted. Finally, this work aimed at analysing the function of the classical microtubule nucleation proteins, the γ-TuRC proteins, in activation of the spindle assembly checkpoint. A possible interaction of γ-TuRC proteins with spindle assembly checkpoint proteins was tested on a biochemical (immunoprecipitation in *Drosophila* and tandem-affinity-purification in human cells) and on a functional level (RNAi).

2 Synopses of Publications

2.1 Immunoisolation of Centrosomes from *Drosophila melanogaster*

Verena Lehmann, Hannah Müller, Bodo MH Lange. 2005. Current Protocols in Cell Biology, Chapter 3: Unit 3.17.

One of the main objectives of this project was the identification of the centrosomal proteome in *Drosophila*. The lack of an affinity-isolation technique that yields highly enriched preparations and minimizes contamination prevented a comprehensive proteomic analysis of the centrosome so far. Hence, the aim was to further develop the isolation method established by Lange *et al*. (2000).

The isolation procedure that is described here uses the syncytial stage of the *Drosophila* embryo as starting material, which is advantageous for several reasons: (a) At this stage the embryo is highly mitotic. As the centrosome is very dynamic in terms of protein composition, the amount of pericentriolar material peaks during mitosis. Therefore, isolation of centrosomes from this stage results in high protein yields. (b) The embryo is not cellularised yet. Cell organelles and the cytoskeleton are not enclosed by membranes. (c) Using *Drosophila* embryos is time and cost efficient, because large amounts of starting material can be produced within a few hours with a relative simple setup. (e) Large quantities of starting material can be obtained (up to 60 g a day) facilitating the purification of µg quantities of affinity purified centrosomes that can be characterised in coomassie stained gels followed by MS analysis.

The first step enriches centrosomes from *Drosophila* embryo extract using classic sucrose gradient centrifugation. In a second step centrosomes are further purified by means of immunomagnetic separation, which is crucial to obtain highly enriched centrosomes that can be used for subsequent biochemical analyses, mass spectrometry or functional characterisation. The method described here differs from the one originally described in Lange *et al*. (2000) since an anti-Cnn antibody was used for affinity purification, which was chemically crosslinked to magnetic beads allowing further enrichment of centrosomes while avoiding IgG sample contamination. This method makes proteomic analysis of centrosomes feasible, because it significantly increases the enrichment of centrosomes and reduces contamination by other cellular fractions.

2.2 Proteome analysis identifies functionally conserved protein components important for centrosome structure and cellular signalling in *Drosophila* and human

Hannah Müller, Ekaterina Mirgorodskaya, Sandra Steinbrink, Verena Lehmann, Karin Habermann, Niklas Gustavsson, Hans Lehrach, Johan Gobom, Michael Boutros, Bodo MH Lange. 2008. Submitted.

The aim of this project was to identify the composition of the centrosomal proteome in *Drosophila melanogaster* and to functionally characterise its components. To better understand how the centrosome is implicated in different signalling pathways, the functional role of the centrosomal candidate proteins in centrosome structure maintenance, centrosome replication, segregation and cell cycle progression was analysed.

Immunoisolated centrosomes of *Drosophila* embryos were subjected to proteomic analysis by Nano-LC and MALDI mass spectrometry. 260 centrosomal candidate proteins were identified and subsequently characterised by RNAi protein depletion. The resulting phenotypes were analysed via immunofluorescence microscopy and FACS. In detail, we examined the effects of depletion of the candidate proteins on centrosome number and morphology, mitotic index and cell cycle progression. We classified proteins in clusters, which are relating to distinct functions in centrosome integrity, centrosome cycle or cell cycle progression. Depletion of 61 proteins affected the centrosome, of which 28 were novel centrosomal candidate proteins. We distinguished three classes of aberrant centrosomal morphology: large centrosomes (26 proteins), small centrosomes (6 proteins) and fuzzy centrosomes (4 proteins). A change in centrosome size is likely to result from defects in centrosome maturation or segregation, as well as irregular number of centrioles or fragmentation of the centrosome. Altered centrosome shape or a complete lack of centrosomes (20 proteins) can be the consequence of depletion of a protein that plays a role in maintenance of the centrosome structure. Centrosome segregation defects after protein level reduction might result in mitotic cells with one centrosome (28 proteins) and overduplication of centrosomes can lead to mitotic cells with more than three centrosomes (5 proteins).

Several proteins that we identified to function in centrosome segregation, replication or integrity have been reported to play a role in other cellular processes like nuclear

import, receptor tyrosine kinase signalling and contractile ring formation. This demonstrates the implication of the centrosome in multiple cellular signalling pathways.
FACS analysis and determination of the mitotic index of cells depleted of centrosomal candidate proteins provided evidence for the centrosomes role in cell cycle progression, cell proliferation and cell viability. Predominant phenotypes resulting from protein depletion were viability defects (20 proteins), cytokinesis defects (28 proteins), cell cycle arrest in G1/G0-phase (9 proteins) or mitosis (20 proteins).
A number of proteins functioning in RNA-binding and transport were identified in the proteomic analysis. Depletion of these proteins often affected centrosome integrity or segregation. Together with the recent discovery of RNA in the centrosome (Alliegro *et al.* 2006) this suggests a possible role of RNA in centrosomal cohesion.
The centrosome is an evolutionary conserved organelle. Database searches showed that 75% of the identified proteins have human orthologues. In addition to sequence conservation, functional conservation was shown by small interfering RNA (siRNA) depletion of a subset of human orthologues in human U2OS cells, that play a role in structure maintenance in *Drosophila* SL2 cells. SiRNA of five orthologues resulted in a centrosome-related phenotype, confirming a structural role of these proteins in human cells.
In summary, we defined the centrosomal proteome and functionally characterised the identified candidate proteins. We assigned novel functions to 28 proteins, relating to centrosome replication and morphology and showed that centrosome-associated proteins play a role for cytokinesis and cell cycle progression. Furthermore, we provided evidence for molecular links of centrosomal proteins to diverse cellular signalling pathways such as cytokinesis and nuclear signalling.

2.3 A Centrosome-Independent Role for γ-TuRC Proteins in the Spindle Assembly Checkpoint

Hannah Müller, Marie-Laure Fogeron, Verena Lehmann, Hans Lehrach, Bodo MH Lange. 2006. Science, 314: 654-656

Classically, the γ-TuRC proteins function in microtubule nucleation. This work provides evidence for a novel role of γ-TuRC proteins in cell cycle control. The implication of these proteins in the activation of the spindle assembly checkpoint was investigated on a biochemical and on a functional level. RNAi protein depletion of the γ-TuRC components γ-tubulin, Grip84, Grip91 and Grip71 resulted in aberrant centrosome number, defects in spindle morphology and an increase of mitotic index, indicating mitotic arrest and therefore spindle assembly checkpoint activation. Simultaneous depletion of Cnn and Grip71 revealed that the mitotic arrest following γ-TuRC depletion can be triggered in the absence of an intact centrosome structure.

The spindle assembly checkpoint is triggered through sensing of misaligned sister chromatids by either lack of attachment between the kinetochore and spindle microtubules or lack of tension within the mitotic spindle (see chapter 1.7). To determine if the γ-TuRC is part of a signalling complex activating the spindle assembly checkpoint, we investigated a possible interaction of γ-TuRC proteins with spindle assembly checkpoint components. On the biochemical level, immunoprecipitation of γ-tubulin from *Drosophila* embryo extract as well as tandem-affinity purification from human cells (HEK293) showed an evolutionary conserved interaction with Cdc20 and BubR1. On a functional level, we depleted the checkpoint components simultaneously with γ-tubulin using RNAi. γ-tubulin depletion mediated checkpoint arrest was not triggered when Mad2, Mps1- or BubR1-levels were reduced, demonstrating the functional importance of their interaction and that γ-tubulin absence triggers a spindle assembly checkpoint. The co-depletion of Cdc20 and γ-tubulin resulted in a cumulative increase of the mitotic index compared to Cdc20 single knock-down, which corroborates a functional interaction consistent with the biochemical data. We suggest that reduction of γ-tubulin levels triggers activation of spindle assembly checkpoint in addition to missing kinetochore microtubule attachment or lack of tension.

To investigate the contribution of kinetochore and γ-TuRC to spindle checkpoint activation we depleted the structural kinetochore component CID using RNAi. CID is

required for kinetochore assembly and is localised close to the inner plate of the kinetochore. Reduction of this protein led to displacement of the chromosomes from the metaphase plate and increased mitotic index, suggesting activation of the spindle assembly checkpoint due to microtubule-kinetochore attachment defects. Simultaneous depletion of γ-tubulin and CID causes a further increase in mitotic index, therefore indicating an activation of the spindle assembly checkpoint through an additional signal. The study provides evidence for a role of the γ-TuRC in spindle checkpoint activation independent of centrosome localisation or centrosome integrity. γ-tubulin interacts biochemically and functionally with spindle assembly checkpoint components and this interaction is evolutionary conserved between human and *Drosophila*.

Immunoisolation of Centrosomes from *Drosophila melanogaster*

Verena Lehmann, Hannah Müller, Bodo M.H. Lange

Current protocols in Cell Biology, 2005. Chapter 3: Unit 3.17, pages 3.17.1-3.17.13,
Publication available online: DOI: 10.1002/0471143030.cb0317s29

Abstract

Classical protocols for the isolation of centrosomes from higher eukaryotic cells are based on enrichment of cell organelles by density gradient centrifugation. Various successful protocols have been described that isolate centrosomes from mammalian tissue culture cells, tissue, clam oocytes, *Drosophila*, and yeast, to mention only some of the more frequently used sources. The material produced is subsequently used in various assays. These include functional tests such as the microtubule nucleation assay, electron microscopic study of centrosome morphology, and antigen localization; the organelles may also be used for the generation of antibodies. Furthermore, centrosomal preparations have been used for the characterization of their protein composition. The method described here focuses on the isolation of centrosomes from the syncytial stages of the early *Drosophila* embryo. This is a particularly attractive system because these organelles are not bounded by cellular membranes. Moreover, the abundance of pericentriolar material of these centrosomes produces excellent total protein yields.

Experimental contributions:

Conception: B.M.H. Lange
Cloning of Cnn, Preparation of *Drosophila* embryo extract: V. Lehmann

Proteome analysis identifies functionally conserved protein components important for centrosome structure and cellular signalling in *Drosophila* and human

Hannah Müller[1,4]; Ekaterina Mirgorodskaya[1,4]; Sandra Steinbrink[2,4]; Verena Lehmann[1]; Karin Habermann[1]; Niklas Gustavsson[1,3]; Hans Lehrach[1]; Johan Gobom[1]; Michael Boutros[2]; Bodo M.H. Lange[1,5]

Manuscript submitted.

[1] Max-Planck Institute for Molecular Genetics, Department of Vertebrate Genomics, 14195 Berlin, Germany

[2] German Cancer Research Center, Division of Signaling and Functional Genomics, 69120 Heidelberg, Germany

[3] current address: Dept. of Biochemistry, Lund University, 22100 Lund, Sweden

[4] these authors contributed equally to this work

[5] author for correspondence:
Max-Planck Institute for Molecular Genetics, Department of Vertebrate Genomics, Ihnestrasse 73, 14195 Berlin, Germany, Tel.: +49-30-8413-1645,
Email: Lange_B@molgen.mpg.de

keywords: centrosome, cell cycle, cytokinesis, proteomics, protein interactions, signal transduction

running title: centrosome proteome analysis in Drosophila

While centrosomal proteins have been implicated in several human diseases (Badano et al. 2005), a comprehensive inventory of the centrosome´s protein components plus knowledge of their function is missing. Here, we identified and analysed the *Drosophila* centrosomal proteome using immunoisolation, mass spectrometry and functional characterisation of 260 identified components through RNA interference. We could assign novel functions to 28 proteins relating to centrosome structure and cellular signalling pathways. Our results provide evidence for the molecular link of the centrosome to major signalling pathways and the functional clustering of the identified proteins in *Drosophila* and in human cells.

The MTOC of eukaryotic cells has evaded a detailed molecular characterisation, mainly due to its low cellular abundance. Several bioinformatic and proteomic studies have identified a number of components of the spindle pole body from yeast (Wigge et al. 1998) and *Dictyostelium* (Reinders et al. 2006) and of the basal body of *Chlamydomonas* (Keller et al. 2005; Li et al. 2004), the structural and functional homologue of the centriole. In *Drosophila,* genetic approaches and genome wide RNAi screening have identified and characterised a series of centrosomal proteins but remained short of a comprehensive molecular characterisation of the centrosome. In higher eukaryotic cells centrosome components have been identified and characterised via bulk isolation methods (Komesli et al. 1989; Lehmann et al. 2005; Lange et al. 2000; Moritz et al. 1995) and by combining mass spectrometry (MS) with protein correlation profiling (Andersen et al. 2003). On a functional level several proteins have been identified to be required for the structural maintenance of the centrosome: Firstly, proteins of the pericentriolar material (PCM) such as cnn are essential for centrosome integrity as they provide a link between the centriole and the PCM in *Drosophila* (Lucas and Raff 2007). Grip84, Grip91 and γ-tubulin, proteins of the small γ-tubulin ring complex (γ-TuSC) are involved in MT nucleation but are also required for structural maintenance of the centrosome (Vérollet et al. 2006). Secondly, centriole proteins are part of the centrosomal core structure, as ablation or depletion of the centriolar proteins Ana1, Ana2, Asl and SPD-2 are resulting in destruction of the mitotic centrosome in *Drosophila* (Goshima et al. 2007; Dix and Raff 2007; Varmark et al. 2007). Thirdly, on the regulatory level, the cell cycle kinases Plk1, CDK1/CDK2 and Aurora A control

PCM recruitment at the beginning of the M-phase and therefore control overall centrosome size and structure (Bettencourt-Dias and Glover, 2007).

The proteins ZYG-1, SAS4, SAS5, SAS6 control distinct steps of daughter centriole formation, structural maturation and mother daughter disengagement. This has been defined on a molecular and electron microscopy level in *C. elegans* (Pelletier et al. 2006). SAK (Plk4 in human and *Drosophila*), CDK1, CDK2, CamKII and the ubiquitin ligase complex SCF are controlling transition steps of centriolar and centrosomal replication and segregation. In addition, DNA damage and DNA replication processes are coupled to centrosome replication and segregation (Sibon et al. 2000; Bettencourt-Dias et al. 2005). Hence, there is a tight coordination of the centrosome with basic physiological cellular functions that control cell cycle regulation, protein expression, DNA replication and DNA damage (Lange 2002). However, on both the biochemical and on the functional level details are lacking of how the centrosome is integrated in different signalling pathways. Here we identified and characterised through a direct biochemical approach centrosome components that play a functional role for centrosome structure maintenance, centrosome replication and segregation. Functional clustering reveals protein networks in the centrosome proteome. We propose that this functional and molecular information is critical for a better understanding of developmental processes, such as asymmetric cell division and for diseases such as cancer in which centrosome morphology and number are frequently dysregulated.

Results and Discussion

Immunoisolation of Drosophila centrosomes from early preblastoderm embryos identified 260 centrosomal candidate proteins

One of the major problems so far in defining the molecules involved in structure maintenance, replication and segregation of the centrosome was the limited quantity and low purity of the available centrosome preparations. This has been partly overcome by a novel MS approaches that applied protein correlation profiling of centrosomes isolated through sucrose gradient centrifugation, thereby identifying over 20 novel human centrosome proteins (Andersen et al. 2003). Here we used immunoisolation in addition to sucrose gradient centrifugation to increase enrichment of centrosome proteins (Lehmann et al. 2005; Lange et al. 2000) (Fig. 1A). The resulting centrosome preparation was analysed by LC-MS and the function of the identified proteins were validated through RNAi in SL2 cells (Bartscherer et al. 2006; Boutros et al. 2004). Centrosome enrichment was confirmed using western blotting against the centrosomal protein markers (γ-tubulin, Grip84) while the cytoplasmic actin was strongly reduced (Fig. 1B). In addition, quantitative immunofluorescence analysis of the immunoisolated centrosomes confirmed an over 600-fold enrichment (Supplemental Methods). MS analysis of the immunoisolated centrosomes identified 260 proteins of which 17 were known from previous studies to be localised to the *Drosophila* centrosome (Supplemental Table 1). The identified proteins and the results from this functional analysis are discussed in the following section and are listed in Supplemental Table 1.

Functional analysis through RNAi in Drosophila SL2 cells assigned novel functions to 28 proteins for maintaining centrosome structure and number

In our functional analysis we used RNAi in *Drosophila* SL2 cells to determine the relevance of the identified components for centrosome structure and cell cycle progression by immunofluorescence microscopy and FACS. 61 proteins (from 260 identified candidate proteins) were found to affect centrosome morphology, separation or replication (Supplemental Table 2). From the total number of abnormal centrosomal phenotypes (61) we identified 33 known and 28 novel centrosome candidate proteins.

Using immunofluorescence microscopy we distinguished three main classes of abnormal centrosome morphology as compared to control cells (Fig. 2): (i) large centrosomes (26/61), (ii) small centrosomes (6/61) and (iii) fuzzy centrosomes (4/61)

(i.e. fragmented or without a clear morphological border). These three classes result from RNAi mediated depletion of proteins involved in centrosome separation, centrosome maturation (recruitment of PCM) and centrosome assembly, respectively.

The accuracy of the functional scoring has been confirmed by the identification of 24 known proteins that have previously been associated with abnormal phenotypes. Examples are Grip75 (Vérollet et al. 2006), Grip84, Grip91 (Barbosa et al. 2003) and cnn, whose depletion resulted in a phenotype of single or no centrosomes. Asp (do Carmo Avides and Glover 1999), ncd (Endow et al. 1994) and aur (Giet et al. 2002) were positive controls of identified proteins relevant to centrosome assembly or splitting confirming the scoring for the morphological class of fuzzy centrosomes. To test the accuracy of the functional scoring on the RNAi level we investigated potential off-target effects both through detailed bioinformatics analysis as well as in a second round of experiments, that positively confirmed 11/13 selected functionally important proteins (Supplemental Table 3). We analysed centrosome localisation of a set of the identified proteins by fluorescence microscopy of expressed N- and C-terminal GFP-fusion or TAP-tag fusion proteins (Fig. 1C-N). We confirmed that our combined biochemical and functional characterisation identified both known and novel centrosome proteins.

Centrosome replication and segregation is depending on proteins that function in nuclear import, receptor tyrosine kinase signalling and contractile ring formation

We identified 14 proteins that upon depletion through RNAi produced a phenotype characterised by a single large centrosome (see Fig. 2D). A group of these proteins (genes fzy, mts, ida, thr, feo, stg) function in cell cycle transition at either the G2/M border or at the exit of mitosis. Hence, their function for centrosome segregation and replication is governed by protein dephosphorylation and protein degradation (Nigg 2001). We identified Pen (Kussel and Frasch 1995), an Importin alpha subunit required for cell proliferation, as a centrosome-associated protein that produced a “large centrosome” phenotype when depleted in SL2 cells. Pen depleted cells also displayed an 8n DNA content as identified through FACS analysis (Supplemental Fig. 1). We suggest therefore that Pen is implicated both in the regulation of cytokinesis and in centrosome segregation. Depletion of the protein mask, an ankyrin and RNA binding domain protein, also resulted in a large centrosome phenotype in SL2 cells and was previously reported to be involved in *Drosophila* receptor tyrosine kinase signalling

(RTS) (Smith et al. 2002). Hence this finding suggests that RTS might be involved in centrosome separation. The feo protein carries a microtubule associated protein domain and is required for the formation of the contractile ring at the central spindle. Removal of feo has previously been described to result in a diffuse localisation of both the pav and asp proteins along spindle microtubules (Verni et al. 2004). Depletion of feo in the RNAi assay resulted in large centrosomes. However, whether this function relates to the effect on the centrosomal fraction of pav or asp remains to be evaluated.

Centrosome and centriole replication is controlled by the origin recognition complex 3 (lat)

Recently it has been suggested that common licensing mechanisms might exist that control both DNA and centrosome replication (Bettencourt-Dias and Glover 2007). The hetero-hexameric origin recognition complex (ORC) is involved in DNA replication and has been proposed to link DNA licensing i.e. the labelling of replicated vs. non replicated DNA to centrosome duplication and cell division (Prasanth et al. 2004). We identified three DNA licensing factors in our centrosomal preparations (ORC1, ORC2, lat) of which lat depletion had an effect on centrosome replication. We investigated if depletion of lat is leading to PCM fragmentation or affects centriolar replication and segregation. Co-labelling of lat-depleted cells for γ-tubulin (a PCM protein) and cp309 (a protein primarily associated with the centriole) (Martinez-Campos et al. 2004) detected multiple centrosome fragments each containing a single centriole as judged by immunofluorescence microscopy labelling (Fig. 3C). Moreover, as we did not detect cells with a significant higher DNA content after lat depletion, the multiple centrosomes/centrioles are not likely to be the result of a cytokinesis failure (Supplemental Table 1). This result suggests that lat provides a functional and molecular link between centrosome replication and DNA replication.

Centrosome structure is maintained through the anillin (ANLN) homologue Scra and the RNA-binding repeat proteins Rae1, CG31716, CG11943

Scra is an anillin homologue causing defects in septin recruitment to the contractile ring and strongly perturbing cellularisation (Field et al. 2005). Our RNAi experiments revealed a centrosome "0" phenotype after scra depletion indicating a role in centrosome structure assembly or maintenance, which can not be explained with the

known role of scra in cytokinesis. This function is not evolutionary conserved, as we could not confirm it for the homologue ANLN in human cells (Supplemental Table 4).

The role of actin related proteins for centrosome structure maintenance however is further corroborated by the depletion of Act57B and the actin binding protein Sop2, which is leading to centrosome disintegration.

We identified in the immunoisolated centrosome samples proteins that are implicated in mRNA transport: Rae1, CG31716, CG11943 and Nup153. Knock-down of these proteins result in a centrosome "0" or "1'" phenotype. The centrosome related function of CG31716 and CG11943 is conserved as siRNA knock-down of their human orthologues CNOT4 and NUP205 leads to centrosome disintegration (Fig. 4; Supplemental Table 4). This suggests a function for centrosome structure of NUP205 (CG11943), RAE1 and NUP153 (Supplemental Fig. 2). This is consistent with the presence of Rae1 at the spindle pole and its translation-independent role in spindle assembly (Blower et al. 2005).

We identified ribosomal proteins in our preparations, which have been previously described as possible contaminants in centrosome preparations (Andersen et al. 2003). The recent discovery of RNA in the centrosome (Alliegro et al. 2006) led us to investigate the function of these proteins for the centrosome. Depletion of ribosomal proteins affects protein translation, is therefore consistent with interfering with centrosomal replication and was reflected by a single centrosome phenotype (Supplemental Table 1). Other, potentially more direct functions of these proteins such as scaffolding remain to be investigated. However, we speculate that a more physical link of ribosomal proteins to the centrosome exists.

Link of the centrosome to cell cycle progression, cell proliferation pathways and cell viability

To elucidate molecular links of centrosomal proteins to cell proliferation pathways, all identified proteins were analysed for their potential role in cell cycle progression (Supplemental Table 1; Supplemental Fig. 1). The depletion of a group of proteins (20/260) resulted in viability defects, represented by an increased cell population with a sub-G1-phase DNA content. An accumulation of cells in G1/G0-phase of the cell cycle occurred after depletion of 9/260 identified proteins. Also a several-fold increase (8n) of DNA content was frequently detected (28/260). Mitotic arrest was another commonly observed phenotype (20/260). We found that a large group of proteins whose depletion

caused mitotic arrest were members of the γ-TuRC. It has been previously described that depletion of γ-TuRC proteins in *Drosophila* (Vérollet et al. 2006; Müller et al. 2006) lead to activation of the spindle checkpoint while a knock-down of centriolar and centrosomal proteins in mammalian cells leads to a p53 and p38 dependent arrest in G1/S phase (Mikule et al. 2007). Taken together, these results suggest that different sets of centrosome proteins are linked to discrete cell cycle transitions.

In summary, the functional characterisation of the centrosome proteome assigned a novel function to 28 proteins that are required for maintaining centrosome morphology and centrosome number control. Moreover, we show that centrosome associated proteins play a role for mitotic progression, cell viability and cytokinesis. Hence, this work provides new insights on how centrosome proteins are clustered into different functional groups and provides evidence for molecular links of the centrosome to cellular signalling pathways.

Material and Methods

Centrosome isolation

Embryo homogenate was prepared from *Drosophila* preblastoderm stage embryos and centrosomes were enriched through sucrose gradients centrifugation according to Moritz et al. (1995). Subsequent immunoisolation of centrosomes was performed as described before (Lehmann et al. 2005) with following modifications: To improve the isolation efficiency, affinity purified antibodies against the centrosomal protein cnn were bound to Protein G coupled magnetic beads (Dynal) and then cross-linked in two consecutive steps using Dimethyl pimelidate dihydrochloride (Sigma).

Nano LC-MALDI MS

Nano LC-MALDI MS was performed as described recently (Mirgorodskaya et al. 2005). In brief, peptide samples were analyzed on an 1100 Series Nanoflow LC system (Agilent Technologies). The mobile phases used for the reversed-phase separation were Buffer A: 1% ACN (v/v), 0.05% TFA (v/v) and Buffer B: 90% ACN (v/v), 0.04% TFA (v/v). The matrix solution was CHCA (100 g/l) in 90% tetrahydrofuran, 0.001% TFA (v/v), 50 mM citric acid, containing the two calibration standards angiotensin I (1 pmol/µl) and ACTH 18-39 (2 pmol/µl).

Mass analysis of positively charged peptide ions was performed on an Ultraflex II LIFT MALDI-TOF/TOF mass spectrometer (Bruker Daltonics).

Protein identification was performed using the Mascot software (Matrixscience), searching the FlyBase sequence database (http://flybase.bio.indiana.edu/).

RNA Interference

SL2 cells were cultured in „Schneider's Drosophila Medium" (Gibco, Invitrogen) with 10% FBS (Foetal bovine serum, Gibco, Invitrogen) at 25°C. DsRNA treatment of cells was performed essentially according to Clemens *et al*. (2000). Differing from this protocol, $1x10^6$ cells were incubated with 10 µg dsRNA for 1 h at 25°C. After 72 h a second dsRNA treatment was carried out to ensure maximum depletion of proteins. The cells were analyzed via immunofluorescence microscopy and FACS.

Immunofluorescence microscopy

SL2 cells were settled on Concanavalin A (Sigma) coated coverslips (Rogers et al. 2002) and fixed with 4% para-formaldehyde (Applichem) for 20 min at room temperature followed by methanol for 1 h at -20°C. Centrosomes were visualised with the mouse monoclonal anti-γ-tubulin GTU-88 (Sigma) or rat cnn (custom-made, Pineda) antibody. Centrioles were visualized with the custom-made rabbit polyclonal anti-cp309 antibody. Images were captured using a Zeiss Imager Z1 or LSM 510 meta microscope with Zeiss MRM CCD camera or a Photometrics Coolsnap HQ slow scan CCD camera and Axiovision image acquisition software. Image processing and annotation was done using the Adobe Photoshop and Adobe Illustrator software.

Data evaluation

For each knockdown a minimum of n = 100 cells were classified by immunofluorescence microscopy regarding these categories: centrosome number (0, 1, 2, 3, >3), centrosome morphology (intact, unequal size, large, small, fuzzy) and chromosome arrangement (normal, abnormal). To verify significant phenotypic deviation from the control, non-parametric two-tailed chi square test of the resulting data was performed using Microsoft Excel. Significance levels < 0.0001 were considered to be statistically significant (list of p-values see Supplemental Table 3).

Flow cytometry

For the flow cytometry experiments, cells were fixed in ice-cold 70% Ethanol overnight and stained with propidium iodide staining solution (50 µg/ml pancreatic RNaseA (Sigma) and 50 µg/ml propidium iodide (Calbiochem) in PBS) for 1.5 h at 37°C. Samples were stored at 4°C in the dark until used for FACS experiments.

The DNA content of the cells was quantified on a flow cytometer (BD FACSArray Bioanalyzer System, BD Biosciences) and analysed using FlowJo software (Tree star). The cell populations were gated and quantified within the different cell cycle phases. The average of both replicates was calculated and the z-scores were assessed for each sample. The z-score signifies the number of standard deviation a specific phase in the cell cycle differs from the mean of the EGFP controls. Specifically, z-scores represent the ratio of the sample value minus the mean of the control divided by the standard deviation of the control.

References

Alliegro, M. C., Alliegro, M. A. and Palazzo, R. E. 2006. Centrosome-associated RNA in surf clam oocytes. *Proc. Natl. Acad. Sci. U S A* **103**: 9034-9038.

Andersen, J. S., Wilkinson, C.J., Mayor ,T., Mortensen, P., Nigg, E.A. and Mann M. 2003. Proteomic characterization of the human centrosome by protein correlation profiling. *Nature* **426**: 570-574.

Badano, J. L., Teslovich, T. M. and Katsanis, N. 2005. The centrosome in human genetic disease. *Nat. Rev. Genet*. **6:** 194-205.

Barbosa, V., Gatt, M., Rebollo, E., Gonzales, C. and Glover, D. M. 2003. *Drosophila* dd4 mutants reveal that gammaTuRC is required to maintain juxtaposed half spindles in spermatocytes. *J Cell Sci.* **116**: 929-941.

Bartscherer, K., Pelte, N., Ingelfinger, D. and Boutros, M. 2006. Secretion of Wnt ligands requires Evi, a conserved transmembrane protein. *Cell* **125**: 523-533.

Bettencourt-Dias, M., Rodrigues-Martins, A., Carpenter, L., Riparbelli, M., Lehmann, L., Gatt, M.K., Carmo, N., Balloux, F., Callaini, G. and Glover, D.M. 2005. SAK/PLK4 is required for centriole duplication and flagella development. *Curr Biol.* **15**: 2199-207.

Bettencourt-Dias, M. and Glover, D.M. 2007. Centrosome biogenesis and function: centrosomics brings new understanding. *Nat Rev Mol Cell Biol.* **8**: 451-63.

Blower, M.D., Nachury, M., Heald, R. and Weis, K. 2005. A Rae1-containing ribonucleoprotein complex is required for mitotic spindle assembly. *Cell* **121**: 223-34.

Boutros, M., Kiger, A.A., Armknecht, S., Kerr, K., Hild, M., Koch, B., Haas, S.A., Paro, R., Perrimon, N. and Heidelberg Fly Array Consortium. Genome-wide RNAi analysis of growth and viability in Drosophila cells. 2004. *Science* **303**: 832.

Clemens, J.C., Worby, C.A., Simonson-Leff, N., Muda, M., Maehama, T., Hemmings, B.A. and Dixon, J.E. 2000. Use of double-stranded RNA interference in *Drosophila* cell lines to dissect signal transduction pathways. *Proc. Natl. Acad. Sci. U.S.A.* **97**, 6499-6503.

Dix, C.I. and Raff, J.W. 2007. Drosophila Spd-2 recruits PCM to the sperm centriole, but is dispensable for centriole duplication. *Curr Biol.* **17**: 1759-64.

do Carmo Avides, M. and Glover, D. M. 1999. Abnormal spindle protein, Asp, and the integrity of mitotic centrosomal microtubule organizing centers. *Science* **283**: 1733-1735.

Endow, S. A., Chandra, R., Komma, D. J., Yamamoto, A. H. & Salmon, E. D. 1994. Mutants of the Drosophila ncd microtubule motor protein cause centrosomal and spindle pole defects in mitosis. *J Cell Sci.* **107**: 859-867.

Field, C. M., Coughlin, M., Doberstein, S., Marty, T. and Sullivan, W. Characterization of anillin mutants reveals essential roles in septin localization and plasma membrane integrity. *Development* **132**: 2849-2860 (2005).

Giet, R., McLean, D., Descamps, S., Lee, M.J., Raff, J.W., Prigent, C. and Glover, D.M. 2002. *Drosophila* Aurora A kinase is required to localize D-TACC to centrosomes and to regulate astral microtubules. *J Cell Biol.* **156**, 437-451.

Goshima, G., Wollman, R., Goodwin, S. S., Zhang, N., Scholey, J. M., Vale, R. D. and Stuurman, N. 2007. Genes required for mitotic spindle assembly in Drosophila S2 cells. *Science* **316**: 417-421.

Keller, L. C., Romijn, E. P., Zamora I., Yates J. R. 3rd and Marshall, W. F. 2005. Proteomic analysis of isolated Chlamydomonas centrioles reveals orthologs of ciliary-disease genes. *Curr. Biol.* **15**: 1090-1098.

Komesli, S., Tournier, F., Paintrand, M., Margolis, R.L., Job, D. and Bornens M. 1989. Mass isolation of calf thymus centrosomes: identification of a specific configuration. *J. Cell Biol.* **109**: 2869-2878.

Kussel, P. and Frasch, M. 1995. Pendulin, a *Drosophila* protein with cell cycle-dependent nuclear localization, is required for normal cell proliferation. *J Cell Biol.* **129**: 1491-1507.

Lange, B. M. H., Bachi, A., Wilm, M. and Gonzales, C. 2000. Hsp90 is a core centrosomal component and is required at different stages of the centrosome cycle in Drosophila and vertebrates. *EMBO J.* **19**: 1252-1262.

Lange, B.M.H. 2002. Integration of the centrosome in cell cycle control, stress response and signal transduction pathways. *Curr Opin Cell Biol.* **14**: 35-43.

Lehmann, V., Müller, H. and Lange, B.M.H. 2005. Immunoisolation of centrosomes from *Drosophila melanogaster. Current Protocols in Cell Biology* (John Wiley & Sons, New York) Supplement 29.

Li, J. B., Gerdes, J.M., Haycraft, C.J., Fan, Y., Teslovich, T.M., May-Simera, H., Li, H., Blacque, O.E., Li, L., Leitch, C.C. et al. 2004. Comparative genomics identifies a flagellar and basal body proteome that includes the BBS5 human disease gene. *Cell* **117**: 541-552.

Lucas, E.P and Raff, J.W. 2007. Maintaining the proper connection between the centrioles and the pericentriolar matrix requires Drosophila centrosomin. *J Cell Biol.* **178**: 725-32.

Martinez-Campos, M., Basto, R., Baker, J., Kernan, M. and Raff, J. W. 2004. The *Drosophila* pericentrin-like protein is essential for cilia/flagella function, but appears to be dispensable for mitosis. *J. Cell Biol.* **165**: 673-683.

Mikule, K., Delaval, B., Kaldis, P., Jurcyzk, A., Hergert, P. and Doxsey S. 2007. Loss of centrosome integrity induces p38-p53-p21-dependent G1-S arrest. *Nat. Cell Biol.* **9**: 160-170.

Mirgorodskaya, E., Braeuer, C., Fucini, P., Lehrach, H. and Gobom, J. 2005. Nanoflow liquid chromatography coupled to matrix-assisted laser desorption/ionization mass spectrometry: Sample preparation, data analysis, and application to the analysis of complex peptide mixtures. *Proteomics* **5**: 399-408.

Moritz, M., Braunfeld, M.B., Fung, J.C., Sedat, J.W., Alberts, B.M. and Agard, D.A. 1995. Three-dimensional structural characterization of centrosomes from early *Drosophila* embryos. *J. Cell Biol.* **130**: 1149-1159.

Müller, H., Fogeron, M. L., Lehmann V., Lehrach, H. and Lange, B.M.H. 2006. A centrosome-independent role for gamma-TuRC proteins in the spindle assembly checkpoint. *Science* **314**: 654-657.

Nigg, E.A. 2001. Mitotic kinases as regulators of cell division and its checkpoints. *Nat Rev Mol Cell Biol.* **2**: 21-32.

Pelletier, L., O'Toole, E., Schwager, A., Hyman, A.A. and Müller-Reichert, T. 2006. Centriole assembly in Caenorhabditis elegans. *Nature **444***: 619-23.

Prasanth, S.G., Prasanth, K.V., Siddiqui, K., Spector, D.L. and Stillman, B. 2004. Human Orc2 localizes to centrosomes, centromeres and heterochromatin during chromosome inheritance. *EMBO J.* **23**: 2651-63.

Reinders, Y., Schulz, I., Graf, R. and Sickmann, A. 2006. Identification of novel centrosomal proteins in Dictyostelium discoideum by comparative proteomic approaches. *J. Proteome Res*. **5**: 589-598.

Rogers, S. L., Rogers, G. C., Sharp, D. J. and Vale, R. D. 2002. *Drosophila* EB1 is important for proper assembly, dynamics, and positioning of the mitotic spindle. *J. Cell Biol.* **158**: 873-884.

Sibon, O.C., Kelkar, A., Lemstra, W. and Theurkauf, W.E. 2000. DNA-replication/DNA-damage-dependent centrosome inactivation in Drosophila embryos. *Nat Cell Biol.* **2**: 90-5.

Smith, R. K., Carroll, P. M., Allard, J. D. and Simon, M. A. 2002. MASK, a large ankyrin repeat and KH domain-containing protein involved in *Drosophila* receptor tyrosine kinase signaling. *Development* **129**: 71-82.

Varmark, H., Llamazares, S., Rebollo, E., Lange, B., Reina, J., Schwarz, H. and Gonzalez, C. 2007. Asterless is a centriolar protein required for centrosome function and embryo development in Drosophila. *Curr Biol.* **17**, 1735-45.

Verni, F., Somma, M.P., Gunsalus, K.C., Bonaccorsi, S., Belloni, G., Goldberg, M.L. and Gatti M. 2004. Feo, the *Drosophila* homolog of PRC1, is required for central-spindle formation and cytokinesis. *Curr. Biol.* **14**: 1569-1575.

Vérollet, C., Colombié, N., Daubon, T., Bourbon, H.M., Wright, M. and Raynaud-Messina B. 2006. *Drosophila melanogaster* gamma-TuRC is dispensable for targeting gamma-tubulin to the centrosome and microtubule nucleation. *J. Cell Biol.* **172**: 517-528.

Wigge, P. A., Jensen, O.N., Holmes, S., Souès, S., Mann, M. and Kilmartin J.V. 1998. Analysis of the Saccharomyces spindle pole by matrix-assisted laser desorption/ionization (MALDI) mass spectrometry. *J. Cell Biol.* **141**: 967-977.

Acknowledgements

We would like to thank T. Kaufman, D. Glover and Y. Zheng for the gift of antibodies and DNA constructs and our colleagues, A. Ploubidou and lab members for comments on the manuscript. The work in BL.s' laboratory is funded by the Berliner Senat für Kultur, Wissenschaft und Forschung, EFRE; BMBF, NGFN2 SMP Protein; EU and the Thyssen Foundation. The work in MBs lab is funded by the German Research Foundation, the European Commission and the Human Frontiers Sciences Program. The work in JGs' lab was funded by the Zukunftsfond of the Technologiestiftung Berlin (TSB) and the Structural Fonds of the European Union within the project 2D/3D-ProteinChips, and NGFN2 SMP Protein. Bruker Daltonics in Bremen is acknowledged for scientific collaboration and support in LC-MALDI MS data analysis.

Figure Description

Fig. 1

Immunoisolation of centrosomes results in highly enriched centrosome preparations. (*A*) Projection of confocal microscopy images of centrosomes (yellow) immunoisolated on magnetic beads (red). (*B*) Western blotting analysis of different isolation stages shows an enrichment of centrosomal proteins (γ-Tub, Grip84). (EH = embryo homogenate, CEF = centrosome enriched fraction, IPC = immunoisolated centrosomes, mock = negative control sample: magnetic beads coupled to preimmune serum incubated with CEF). The cytoplasmic protein actin is strongly reduced in the IPC fraction. (*C-E*) GFP-tagging of the identified centrosomal candidate protein CG17286 verifies its centriolar-like localisation in SL2 cells. CG17286 (red) co-localises with cp309 (green). DNA was labelled with DAPI (blue).

(*F-H*) Transiently expressed fusion protein CG11148 with the N-terminal TAP-tag is localised to the spindle and the centrosome in mitosis. (*I-K*) Centrosome localisation of CG11148 expressed as a fusion protein with an N-terminal TAP-tag is maintained after depolymerisation of microtubules with colchicines. (*L-N*) GFP-tagged cort localises to one centriole in interphase cells. (*C-N*) TAP/GFP-tag localisation in red, γ-Tub in green and superimposition of both images with DNA in blue.

Fig. 2

Depletion of centrosomal candidate proteins by RNAi in SL2 cells resulted in 6 main phenotypic classes, shown by examples of immunofluorescence microscopy images. Centrosomes were labelled with an anti-γ-Tub antibody (green) and mitotic chromosomes with an anti-phospho-histone 3 antibody (red). SL2 cells treated with EGFP-dsRNA were used as a control. Normal centrosome and chromosome arrangement during metaphase (*A, B*) and anaphase (*C*). Examples of centrosome shape phenotypes: (*D*) Abnormally large centrosomes in mitosis after stg depletion. (*E*) Depletion of CG17286 protein caused small centrosomes. (*F*) Aberrant centrosome assembly after ncd-RNAi indicated by fuzzy centrosomes. Examples of centrosome number phenotypes: (*G*) depletion of the CG15524 protein producing a “0” centrosome phenotype. (*H*) Mitotic cells with a single centrosome after ida-RNAi. (*I*) Depletion of the mps1 protein resulted in supernumerary centrosomes.

Fig. 3

Immunofluorescence microscopy of SL2 cells depleted of the proteins feo, lat, cnn and CG17286 shows the centriole number in relationship to centrosome size and number. The PCM marked with an anti-γ-Tub antibody (red), centrioles labelled with an anti-cp309 antibody (green). DNA labelled with DAPI (blue). EGFP was used as negative RNAi control. Below each main image the enlarged insert of one of the centrosomes is shown in the following sequence: γ-Tub, cp309, superimposed image. In the images (*D-F*) phospho-histone 3 was labelled together with γ-Tub in the red channel to visualise three different antibody labels (γ-Tub, H3P, cp309) at the same time in addition to DAPI. (*A, D*) A single centriole can be detected within the PCM in EGFP control cells. (*B*) Large centrosomes after feo depletion contain multiple centrioles demonstrating that centriolar over-replication has occurred. (*C*) Each centrosome fragment co-labels with the anti-cp309 antibody indicating that multiple small centrosomes were generated through over-replication rather than PCM fragmentation after lat-RNAi. (*E*) cnn depletion is causing PCM dispersion and centriole-like structures are still detected. (*F*) CG17286 depletion causes complete PCM dispersion and centriole destruction is marked through the absence of cp309.

Fig. 4

Depletion of the human orthologues of a subset of the centrosomal candidate proteins in U2OS cells influences centrosome shape and number. Immunofluorescence microscopy of mitotic U2OS cells shows examples of the different phenotypes. Centrosomes were labelled with an anti-γ-Tub antibody (green) and mitotic chromosomes with an anti-phospho-histone 3 antibody (red). (*A*) Mock-transfected control cells show normal metaphase chromosome alignment and two centrosomes at the spindle poles. (*B-C*) Depletion of CEP192 and CENPJ affects centrosome structure (small (*B*) or fuzzy (*C*) centrosomes). These phenotypes correlate with the occurrence of defective centrosome number (0 centrosomes (*D*), 1 centrosome (*E*)). ANLN depleted cells exhibit aberrant cytokinesis and supernumerary centrosomes (*F*).

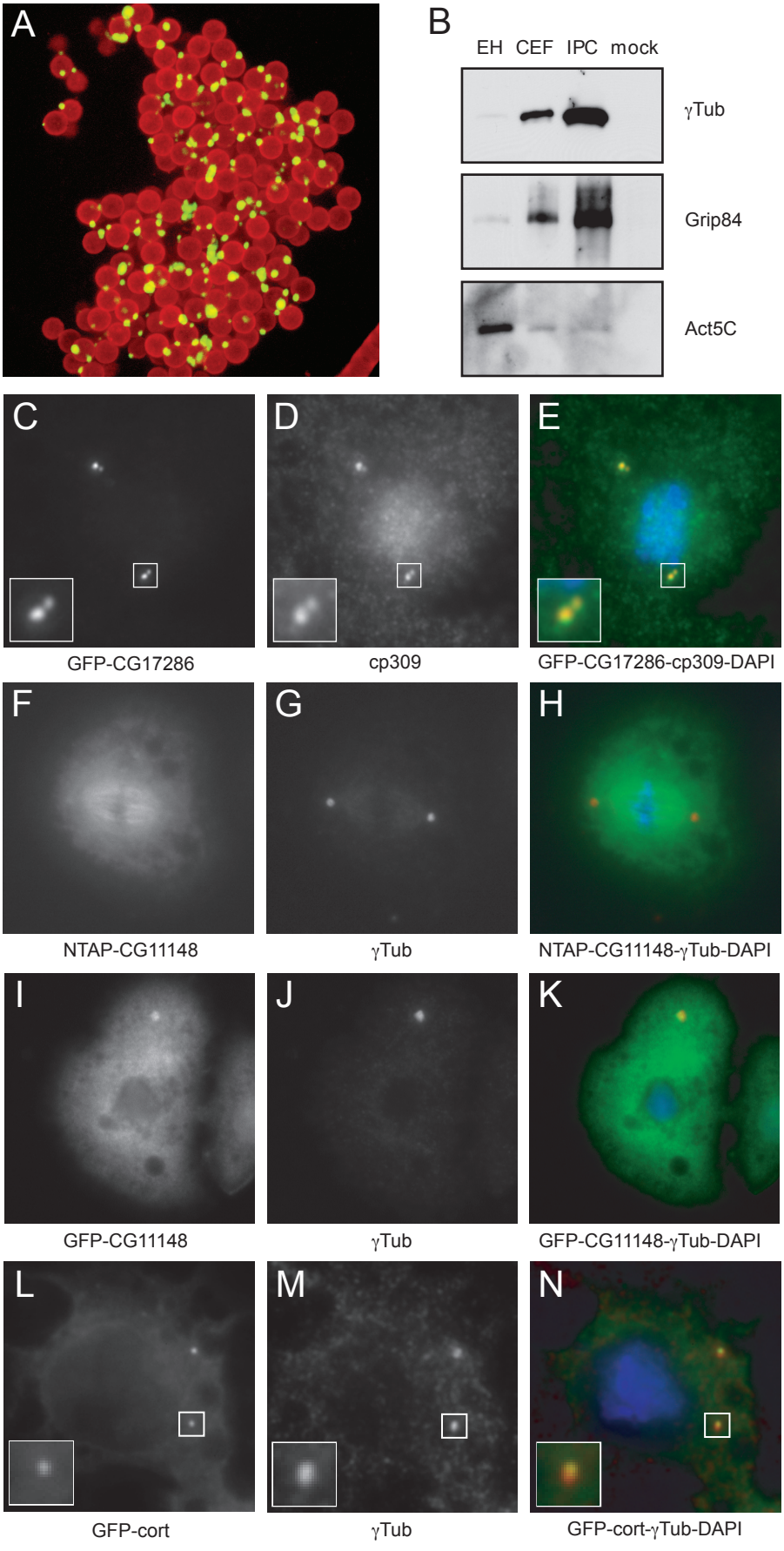
A
B
EH CEF IPC mock
γTub
Grip84
Act5C
C
D
E
GFP-CG17286
cp309
GFP-CG17286-cp309-DAPI
F
G
H
NTAP-CG11148
γTub
NTAP-CG11148-γTub-DAPI
I
J
K
GFP-CG11148
γTub
GFP-CG11148-γTub-DAPI
L
M
N
GFP-cort
γTub
GFP-cort-γTub-DAPI

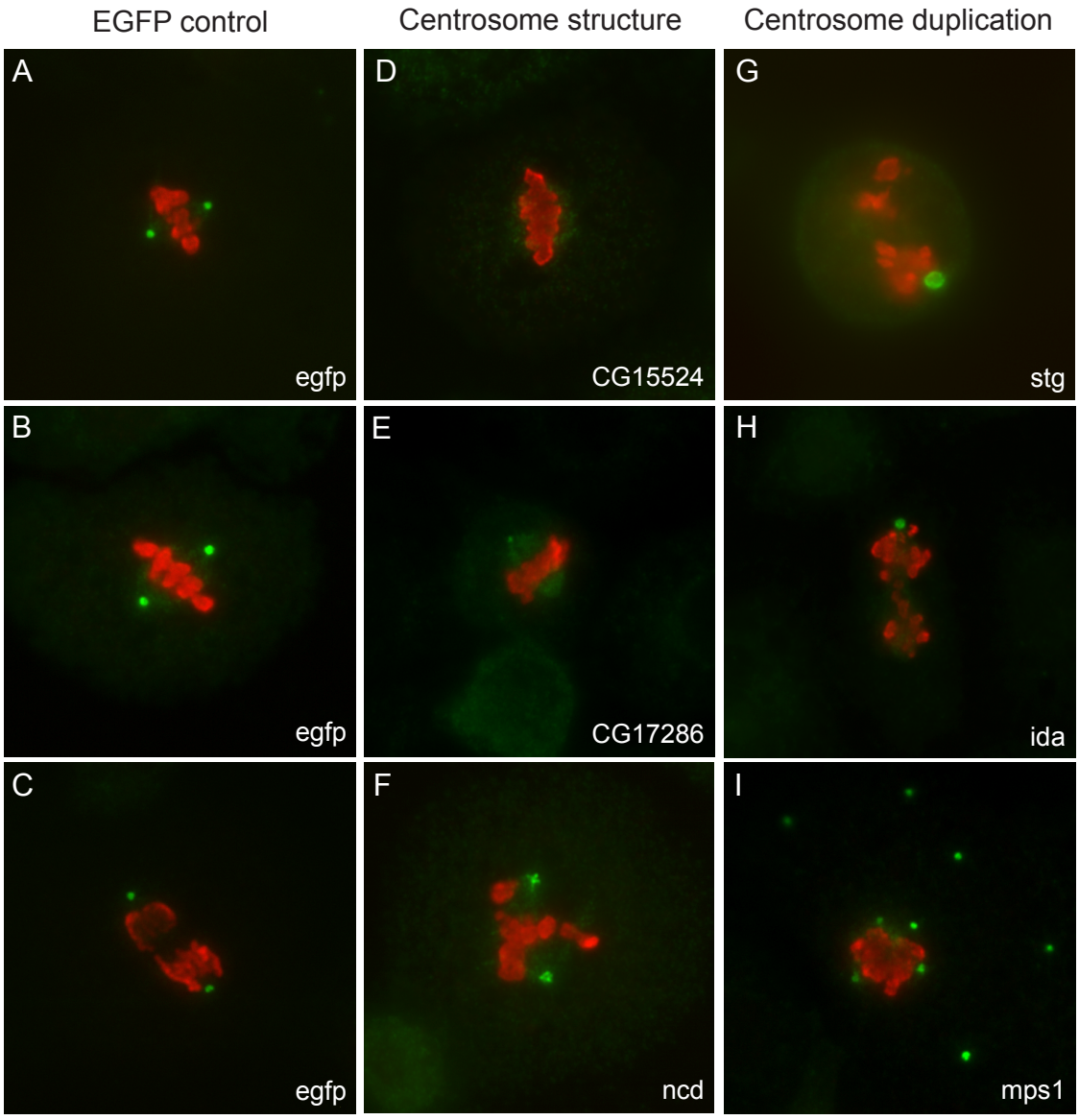
EGFP control
Centrosome structure
Centrosome duplication
A
egfp
D
CG15524
G
stg
B
egfp
E
CG17286
H
ida
C
egfp
F
ncd
I
mps1

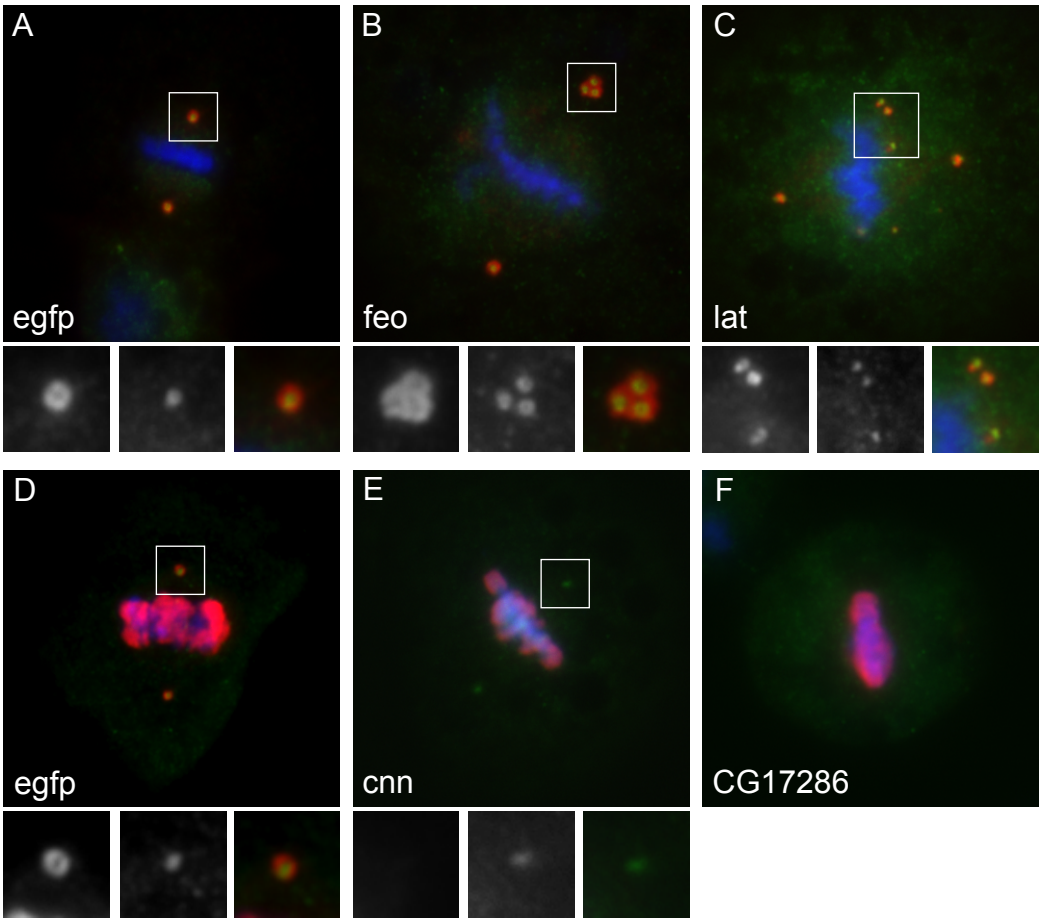
A
egfp
B
feo
C
lat
D
egfp
E
cnn
F
CG17286

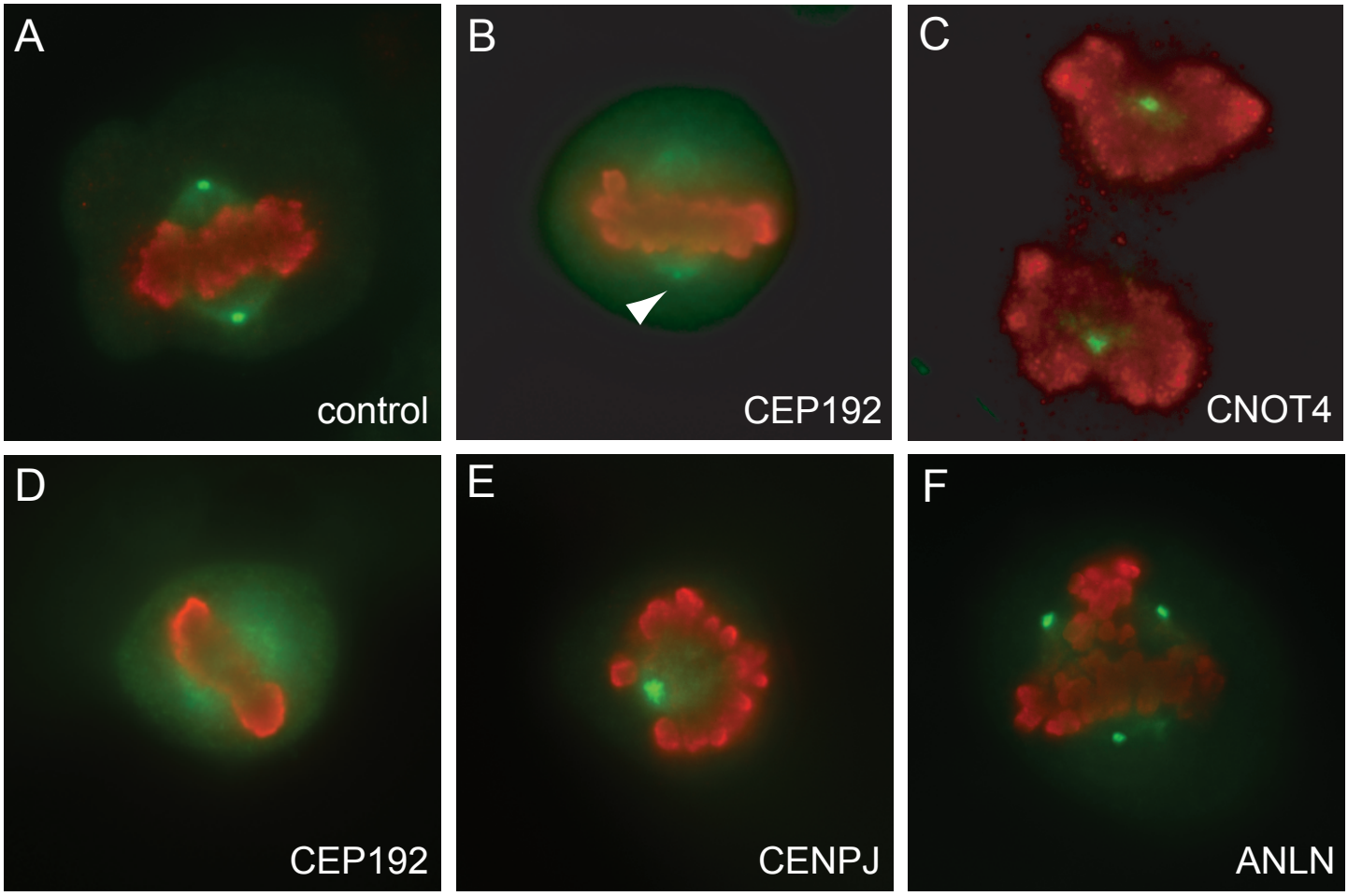
A
control
B
CEP192
C
CNOT4
D
CEP192
E
CENPJ
F
ANLN

Supplemental Methods

Cloning and Molecular Biology

Exon 6 of the cnn gene was amplified by PCR from genomic DNA from the *Drosophila* W118 strain. The amplified DNA sequence was first cloned into the entry vector pENTR/D-Topo (Invitrogen) and then recombined with the destination vector pDest 17 (Invitrogen) for His-tagged protein expression. CG17286 and cort were amplified by PCR from the DGRC cDNA gold collection and afterwards cloned into the entry vector pENTR/D-Topo (Invitrogen). Recombination was done with the Gateway vectors pAGW (N-terminal EGFP Tag) and pAWG (C-terminal EGFP Tag) from the *Drosophila* Gateway vector collection from the DGRC. CG11148 was PCR-amplified using clone GH25014 from the DGRC release 1 collection as template. The attB-flanked PCR product was then recombined with the Gateway donor vector pDONR201 (Invitrogen) and subsequently shuttled into expression vectors pMK33-CTAP and pMK33-NTAP, respectively.

Cloning Primer Pairs

Gene Symbol	Gene ID	Primer Sequence
cnn	CG4832	5’CACCAGTGACAACGAGGCCAGCTCCCAGG 3’CTACTCTGACTTTGCCTTTGGACTCGCT
CG17286	CG17286	5’CACCGACAGTAGCAGTGGAAGCCAA (N-term.) 3’TTAAAATTTAAAACTAATCGGGACA (N-term.)
		5’CACCATGGACAGTAGCAGTGGAAGC (C-term.) 3’AAATTTAAAACTAATCGGGACACTG (C-term.)
cort	CG11330	5’GGGGACAAGTTTGTACAAAAAAGCAGGCTT CCCTGGCATATGCAGTCCCGT (N-term.) 3’GGGGACCACTTTGTACAAGAAAGCTGGGTCTC ACCGTATGCCTTTGTACA (N-term.)
		5’GGGGACAAGTTTGTACAAAAAAGCAGGCTACCATG GGTCCTGGCATATGCAGTCC (C-term.) 3’GGGGACCACTTTGTACAAGAAAGCTGGGTCCCGTA TGCCTTTGTACAGGC (C-term.)

CG11148	CG11148	5’ GGGGACAAGTTTGTACAAAAAAGCAGGCTTCAG ATCGGCGCCTGGTCTGGC (N-term) 3’GGGGACCACTTTGTACAAGAAAGCTGGGTCTTAT GGTCCTTCGACGTAGT (N-term)
		5’GGGGACAAGTTTGTACAAAAAAGCAGGCTACCA TGGGTAGATCGGCGCCTGGTCTGGC (C-term) 3’GGGGACCACTTTGTACAAGAAAGCTGGGTCTGGT CCTTCGACGTAGTCTC (C-term)

Transfection of SL2 cells

The N- and C-terminal EGFP-tagged Gateway constructs were transiently transfected in *Drosophila* cells with Cellfectin (Invitrogen) and analysed by immunofluorescence microscopy. The N-terminal EGFP Gateway vectors carrying the CG17286 gene was stably co-transfected with the pCoBlast vector (carrying a Blasticidin resistance marker) in *Drosophila* SL2 cells by calcium phosphate transfection (Invitrogen) for 24 h using 3x 10^6 cells per well. Selection for the plasmid resistancy marker was started seven days after transfection with 75 µg/ml Blasticidin. After two weeks, resistant cells were maintained in medium containing 10 µg/ml Blasticidin.

Antibodies

His-tagged fusion protein corresponding to cnn exon 6 was used to raise and affinity purify rabbit and rat polyclonal antibody (Pineda). Anti-peptide antibodies were custom-made and affinity purified (Eurogentec) against the peptides from the cp309 protein AA: C+2447-246: C+KSPGDSPRKSPRADF--conh2; C+1014-1028: C+KFYERQQGDDDYKPA--conh2). For Western blotting and immunofluorescence staining following antibodies were used: Mouse monoclonal anti-γ-Tubulin (clone GTU-88) (Sigma), rabbit polyclonal anti-Grip84, rat monoclonal anti-Actin (Babraham), rabbit polyclonal anti-phospho-histone H3 (Upstate).

Primary antibodies were detected with the secondary antibodies Alexa Fluor 488-conjugated anti-mouse, Alexa Fluor 594-conjugated anti-rabbit (Molecular Probes) and FITC-conjugated anti-rat (Jackson ImmunoResearch).

Centrosome Isolation

Cnn protein expression and purification

Cnn protein was expressed as a His-tagged fusion protein in Isopropyl-ß-D-thiogalactopyranoside (IPTG) induced BL 21 cells for 6 h at 30°C. The cell extract was prepared by resuspending the cell pellet in lysis buffer (10 mM ß-Mercaptoethanol, 10% Sucrose, 1x PBS, 0.8 M NaCl, 1 mM Imidazole ph 7.0, 1mg/ml Lysozym) supplemented with a proteinase inhibitor mix (100 mg/ml Pefabloc SC Roche, 2.5 mM Phenylmethanesulfonyl fluoride (PMSF) and 1 mg/ml of Aprotinine, Leupeptine, Pepstatine A) sonicated and further incubated after adding 1% Triton X-100, 10 µg/ml Dnase I, 10 mM $MgCl_2$ and 1 mM MnCl for 30 min. The inclusion bodies were recovered and solubilised by a protocol adapted from Sambrook and Russel (2001) and purified using TALON Metal Affinity Beads (BD) according to the manufacturers instructions. The eluted protein was precipitated with trichloracetic acid.

Drosophila embryo extract

An average of 30-50 g of 0-3 h old *Drosophila* (strain W118) embryos were collected per day on apple juice/molasses agar trays from large fly populations (>200 000 flies) (Bonte and Becker, 1999). Embryo extract was prepared as described previously (Moritz et al. 1995).

Centrosome isolation

Centrosomes were enriched through sucrose gradients centrifugation according to Moritz et al. (1995). Subsequent immunoisolation of centrosomes was performed as described before (Lehmann et al. 2005) with following modifications: To increase the concentration of centrosomes, several preparations were combined (in total from more than 200 ml of embryo homogenate starting material) in an additionally third centrifugation step through a 1.5 ml 55% (w/v) onto a 70% (w/v) sucrose cushion. To improve the isolation efficiency, affinity purified antibodies against the centrosomal protein cnn were bound to Protein G coupled magnetic beads (Dynal) and then cross-linked in two consecutive steps using Dimethyl pimelidate dihydrochloride (DMP) (Sigma). Antibody to bead coupling efficiency was monitored by SDS-PAGE.

Purification Step	Total Protein [mg/ml]	Centrosomes/ ml	Centrosomes/ mg Total Protein
Embryo Homogenate	140	5 E6	0.03
Centrosome Enriched Fraction	6	50 E6	8.3
Immunopurified Centrosomes	28	500 E6	17.9

Protein concentration of the embryo homogenate (EH) was determined by measuring the absorbance at 280 nm in a spectrophotometer. Protein concentrations of the centrosome enriched fraction (CEF) and the immunopurified fraction (IPC) were calibrated using SDS-PAGE gels, based on comparison to the known concentration of EH. Immunofluorescence microscopy was used to determine the number of centrosomes/ml. Equal volumes of sample from each purification step were centrifuged onto coverslips, labelled with the anti-g-Tubulin antibody and centrosomes in ten fields of view (using the 63x PlanApo objective) per sample were quantified using the ImageJ software. The following equation was then used to calculate the concentration of centrosomes during the different purification steps:

$$\text{centrosomes/ml} = \frac{\frac{A^{\text{coverslip}}}{A^{\text{field of view}}} \times \text{average counts per field of view}}{\text{test volume}[\text{ml}]}$$

Centrosomes/mg total protein was calculated as a ratio of centrosomes/ml to total protein concentration of the respective sample. N-fold change in this quantity during a purification step should be equal to the n-fold enrichment of centrosomes relative to total protein. Calculation of total enrichment during the isolation procedure is found to be at least 600-fold, based on comparison of data for embryo homogenate and the immunopurified fraction.

Mass spectrometry

Chemicals

The peptide calibration standards, angiotensin I and ACTH 18-39 were purchased from Bachem (Heidelberg, Germany). Acetonitrile (HPLC Gradient Grade, Carl Roth GmbH (Karlsruhe, Germany). Trifloroacetic acid (TFA), tetrahydrofuran (THF), n-octylglucopyranoside (nOGP), α-cyano-4-hydroxycinnamic acid (CHCA), and water used for HPLC solvents and MALDI matrix solutions were purchased from Fluka Chemie (Buchs, Switzerland). Porcine trypsin was purchased from Promega

(Mannheim, Germany), dithiotreitol (DTT), iodoacetamide (IAA), from Sigma (Sigma-Aldrich, St. Louis, MO), citric acid and 2,2'-thiodiethanol from Aldrich (Sigma-Aldrich, St. Louis, MO)

In-solution trypsinolysis of protein samples

Samples from the affinity pull-down experiment (3.3 µg) and the control experiment were subjected to trypsinolysis. Lyophylised samples were dissolved in 10 µl 100 mM NH_4HCO_3, 20 mM n-OGP. For reduction of cysteines, a 2 µl aliquot of 20 mM DTT was added and samples were incubated at 37°C for 30 min. Cysteine carbamidomethylation was performed by adding a 2 µl aliquot of 50 mM IAA and incubating the samples at room temperature for 30 min. 26 µl of 100 mM NH_4HCO_3 were added followed by 1 µl of trypsin solution (0.05 µg/µL, in 1 mM HCl) and the samples were incubated at 37°C over night. To terminate trypsinolysis, the samples were acidified by addition of 1 µl 10% TFA (v/v).

SDS-PAGE

Due to the high complexity of the samples, the proteins were separated by SDS-PAGE prior to trypsinolysis. Proteins from the centrosome purification and from the control experiment (4 times larger volume) were separated by SDS-PAGE on a 10 cm gel (vertical SDS-PAGE chamber, EMBL workshop, Heidelberg). The proteins were stained with colloidal Coomassie Blue G250 (Serva) and each lane was cut into 25 slices of different width, with smaller sizes at the high MW region (3 mm for the first 10 slices, 4 mm for the next ten slices, and 5 mm for the last 5 slices). Each gel sample was further cut into smaller pieces and washed by incubation with 800 µl 50% ethanol (v/v), 50 mM NH_4HCO_3 (wash solution) for 30 min. The wash solution was removed and the gel samples were dehydrated by incubation with 800 µl ethanol for 5 min. The ethanol was aspirated and the samples were stored at –20°C prior to *in-situ* trypsinolysis.

***In-situ* trypsinolysis**

The samples were washed twice by addition of 800 µl wash solution and incubation for 30 min while shaking. The Wash solution was removed and the gel samples were dehydrated by incubation with 800 µl ethanol for 5 min, after which the ethanol was

removed. For reduction of cysteine disulfides, 400 µl 10 mM DTT, 50 mM NH_4HCO_3 were added and the samples were incubated for 30 minutes at 37 °C. The supernatants were removed and the samples were dehydrated by incubation with 800 µl ethanol for 5 min, after which the ethanol was removed. For alkylation of cysteines, 400 µl 20 mM IAA, 50 mM NH_4HCO_3 were added and the samples were incubated for 30 min at room temperature in the dark. The supernatants were aspirated and excess IAA was inactivated by incubating the gel samples in 400 µl 20 mM 2,2'-thiodiethanol for 10 min at room temperature. The liquid was removed and the samples washed by incubation with 800 µl wash solution for 5 min. The wash solution was removed and the washing procedure was repeated once followed by incubation with 800 µl ethanol (100%) for 10 minutes. After removing the liquid, the samples were dried in a vacuum centrifuge for 60 min. For trypsinolysis, 20 µl trypsin (2.5 ng/µl in 50 mM NH_4HCO_3, pH7.8) were added to the dry gel pieces. After 30 min incubation on ice, additional volumes of 50 mM NH_4HCO_3 (pH 7.8), necessary to just cover the gel pieces, were added to the gel followed by incubation over night at 37°C. For peptide extraction, 100 µl of 0.1% TFA, 0.2 mM n-OGP were added and the gel samples were placed on a shaker for 10 min. The supernatants were collected into fresh vials and the extraction procedure was repeated twice using 100 µl 0.1 % TFA, 50 % ACN. The pooled extracts were dried in a vacuum centrifuge and stored at -20°C prior to further analysis.

Nano LC-MALDI MS

Nano LC-MALDI MS was performed as described recently (Mirgorodskaya et al. 2005). In brief, peptide samples were analyzed on an 1100 Series Nanoflow LC system (Agilent Technologies). The mobile phases used for the reversed-phase separation were Buffer A: 1% ACN (v/v), 0.05% TFA (v/v) and Buffer B: 90% ACN (v/v), 0.04% TFA (v/v). The samples were first loaded onto a trapping column (ZORBAX 300 SB C18, 0.3 mm × 5 mm, Agilent Technologies), using Buffer A, delivered by the loading pump with a flow-gradient according to the manufacturer's recommendation. After 5 min, the trapping column was connected to the nanoflow path and the samples were eluted onto the analytical separation column (ZORBAX 300 SB C18, 75 µm × 150 mm, Agilent Technologies), using a binary pump operated at 300 nl/min. For fractionation, the LC effluent was deposited onto pre-formed microcrystalline layers of CHCA prepared on prestructured MALDI sample supports (AnchorChip 600/384, Bruker Daltonics). The

matrix solution was CHCA (100 g/l) in 90% tetrahydrofuran, 0.001% TFA (v/v), 50 mM citric acid, containing the two calibration standards angiotensin I (1 pmol/µl) and ACTH 18-39 (2 pmol/µl). Thin layers of CHCA were prepared by spreading 200 µl of matrix solution over the target surface with a Teflon rod (Gobom et al. 2005).

Mass analysis of positively charged peptide ions was performed on an Ultraflex II LIFT MALDI-TOF/TOF mass spectrometer (Bruker Daltonics). Positively charged ions in the *m/z* range 500 – 4,500 Da were analyzed automatically in the reflector mode. Sums of 50 single-shot spectra were acquired from 14 different sample spot positions (700 in total from each sample). Fixed laser attenuation was used, the optimal value of which was determined prior to analysis by evaluation of a few fractions. MALDI-TOF/TOF analysis was performed on the Ultraflex II instrument operated in the LIFT mode. MS/MS spectra were acquired automatically with fixed laser attenuation and fixed laser power boost. Up to 15 MS/MS spectra, each consisting of a total sum of 4,100 laser single-shot spectra, were acquired from a single MALDI sample. Additionally, manual spectra acquisition of signals for which parent ion isolation failed in the automatic mode were performed when sample availability permitted.

Data processing

Automatic detection of the peptide monoisotopic signals was performed using the algorithm SNAP, implemented in the FlexAnalysis software (Bruker Daltonics). Internal mass correction was performed using the signals of two peptides (Angiotensin I, MH^+ 1,296.6853 (monoisotopic mass), and ACTH (18-39), MH^+ 2,465.1989) included in the MALDI matrix solution, as reference masses.

Selection of precursor ions was performed based on the entire MS data set using a beta-version of the WARPLC software (collaboration with Bruker Daltonics), with manual corrections when necessary. Protein identification was performed using the Mascot software (Matrixscience), searching the FlyBase sequence database (http://flybase.bio.indiana.edu/). The following settings were used for the searches: mass error tolerance for the precursor ions: 30 ppm; mass error tolerance for the fragment ions: 0.8 Da; fixed modification: carbamidomethylation; variable modification: methionine oxidation; number of missed cleavage sites: 1; type of instrument: MALDI-TOF-PSD.

Phenotypic and microscopy assays

Production of double-stranded RNA (dsRNA)

Long dsRNA for RNAi experiments were generated by using ~500bp long PCR fragments from a genome-covering *Drosophila* library as templates (Hild et al. 2003). The amplicons contain T7 promoter sites flanked by unique tag sequences and are amplified using tag-specific primers (Boutros et al. 2004). The resulting T7-PCR fragments are used as templates for in vitro transcription reactions, followed by DNaseI digestion and ethanol precipitation to purify the RNA (Boutros et al. 2004). Primer and amplicon sequence information are shown in Supplemental Table 2 and are available from http://rnai.dkfz.de/.

Mitotic index

To determine the mitotic index, SL2 cells were processed for immunofluorescence microscopy as described above. The cells were labelled with an antibody against phosphorylated histone 3 (Upstate), as a marker of mitotic cells and with diamidino-2-phenylindoldihydrochloride (DAPI) to visualise the DNA. The percentage of mitotic cells was determined using the image processing software ImageJ (http://rsb.info.nih.gov/ij/) and custom-made macros available for downloading from our webpage: http://www.molgen.mpg.de/~ag_lange/links.html. A minimum of n = 2000 cells per experiment was counted. Evaluation of significant deviation of mitotic index: arithmetic mean of mitotic indices of all control samples were subtracted from arithmetic mean of mitotic index of each sample. An arithmetic mean whose standard deviation was out of the range of two times the standard deviation of the control was accepted to be statistically significant.

Mitotic arrest of SL2 cells

To enrich mitotic SL2 cells, cultures were treated with 25µM Colchizine (Calbiochem) for 16 h at 25°C in “Schneider’s Drosophila Medium“ (Gibco, Invitrogen).

Supplemental references

Bettencourt-Dias, M., Giet, R., Sinka, R., Mazumdar, A., Lock, W.G., Balloux, F., Zafiropoulos, P.J., Yamaguchi, S., Winter, S. et al. 2004. Genome-wide survey of protein kinases required for cell cycle progression. *Nature* **432**: 980-987.

Bjoerklund, M., Taipale, M., Varjosalo, M., Saharinen, J., Lahdenperä, J. and Taipale, J. 2005. Identification of pathways regulating cell size and cell-cycle progression by RNAi. *Nature* **439**: 1009-1013.

Bonte, E. and Becker, P.B. 1999. Preparation of chromatin assembly extracts from preblastoderm *Drosophila* embryos. *Methods Mol. Biol.* **119**: 187-194.

Gobom, J., Schuerenberg, M., Mueller, M., Theiss, D., Lehrach, H. and Nordhoff, E. 2001. Alpha-cyano-4-hydroxycinnamic acid affinity sample preparation. A protocol for MALDI-MS peptide analysis in proteomics. *Anal Chem.* **73**: 434-438.

Hild, M., Beckmann, B., Haas, S.A., Koch, B., Solovyev, V., Busold, C., Fellenberg, K., Boutros, M., Vingron, M., Sauer, F. et al. 2003. An integrated gene annotation and transcriptional profiling approach towards the full gene content of the Drosophila genome. *Genome Biol*. **5**: R3.

Sambrook, J. and Russell, D. W. 2001. *Molecular Cloning: A Laboratory Manual.* (Cold Spring Harbor Laboratory Press, Cold Spring Harbor).

Supplemental Figure Descriptions

Supplemental Fig. 1

FACS analysis of the dsRNA treated cells shows accumulation of cells in different phases of the cell cycle. Compared to control cells (*A*), a large group of proteins produced an accumulation in sub-G1 (*B*, 20 proteins) and G1/G0 when depleted (9 proteins, *C*). Protein level reduction resulted in arrest in S-phase (*D,* 6 proteins) or G2/M-phase (*E,* 7 proteins). The major group (*F*, 28 proteins) displayed 8n-DNA content, indicating that these proteins influence cytokinesis. The mitotic index of the SL2 cells after RNAi was analysed by labelling with an anti-phospho-histone 3 antibody (red) and DNA staining with DAPI (blue) (*G,H*). An example for cells displaying a phenotype with a low mitotic index and a list of the relevant proteins are shown in (*G*, 14 proteins). An example of cells with a high mitotic index together with the corresponding list of proteins is shown in (*H,* 20 proteins). Aberrant chromosome segregation occurred frequently (36/260) of which 8/36 were consistent with cytokinesis defects (*I*).

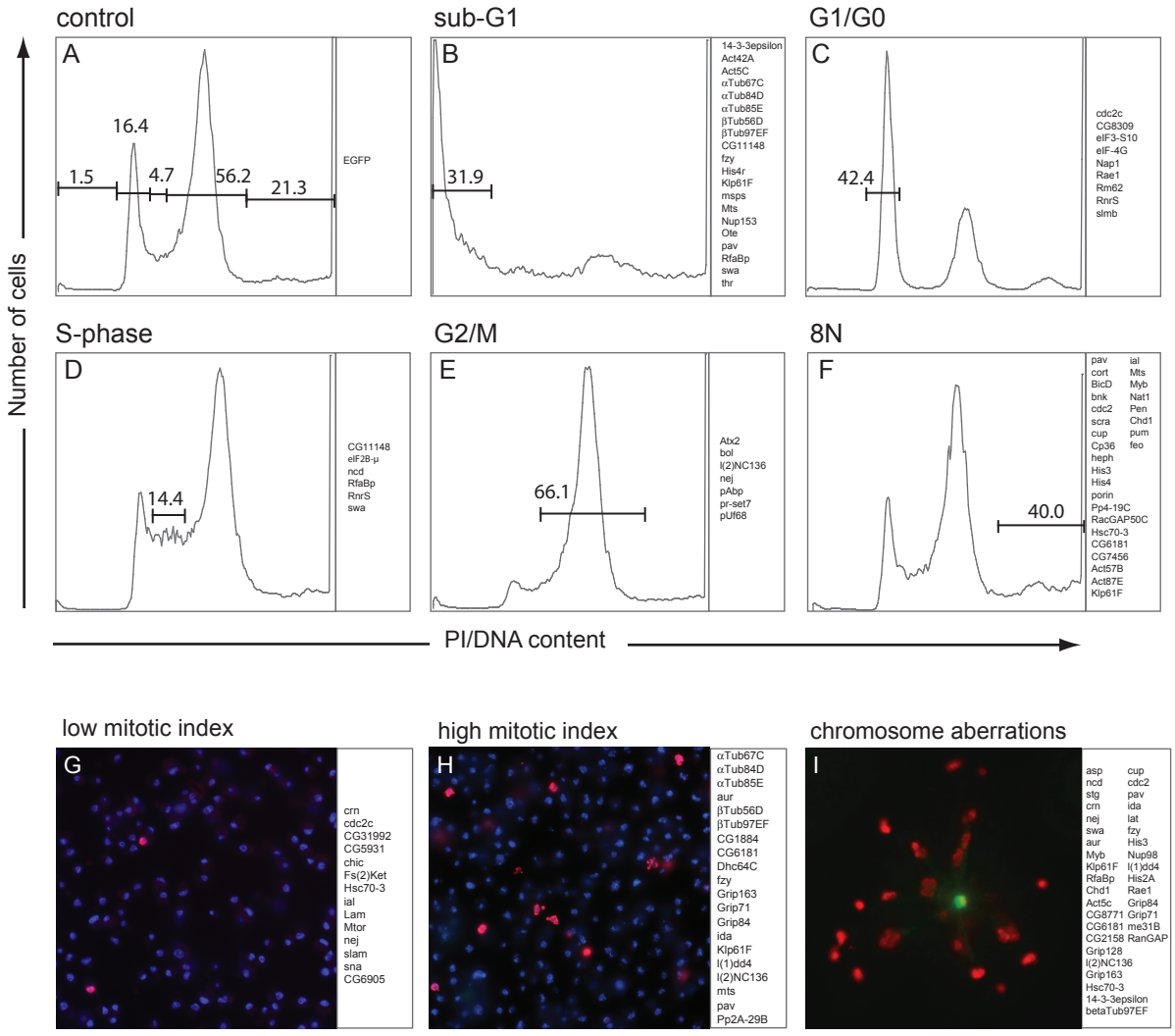
control
sub-G1
G1/G0
A
16.4
1.5
4.7
56.2
21.3
EGFP
B
31.9
14-3-3epsilon
Act42A
Act5C
αTub67C
αTub84D
αTub85E
βTub56D
βTub97EF
CG11148
fzy
His4r
Klp61F
msps
Mts
Nup153
Ote
pav
RfaBp
swa
thr
C
42.4
cdc2c
CG8309
eIF3-S10
eIF-4G
Nap1
Rae1
Rm62
RnrS
slmb
Number of cells
S-phase
G2/M
8N
D
14.4
CG11148
eIF2B-μ
ncd
RfaBp
RnrS
swa
E
66.1
Atx2
bol
l(2)NC136
nej
pAbp
pr-set7
pUf68
F
40.0
pav
cort
BicD
bnk
cdc2
scra
cup
Cp36
heph
His3
His4
porin
Pp4-19C
RacGAP50C
Hsc70-3
CG6181
CG7456
Act57B
Act87E
Klp61F
ial
Mts
Myb
Nat1
Pen
Chd1
pum
feo
PI/DNA content
low mitotic index
high mitotic index
chromosome aberrations
G
crn
cdc2c
CG31992
CG5931
chic
Fs(2)Ket
Hsc70-3
ial
Lam
Mtor
nej
slam
sna
CG6905
H
αTub67C
αTub84D
αTub85E
aur
βTub56D
βTub97EF
CG1884
CG6181
Dhc64C
fzy
Grip163
Grip71
Grip84
ida
Klp61F
l(1)dd4
l(2)NC136
mts
pav
Pp2A-29B
I
asp
ncd
stg
crn
nej
swa
aur
Myb
Klp61F
RfaBp
Chd1
Act5c
CG8771
CG6181
CG2158
Grip128
l(2)NC136
Grip163
Hsc70-3
14-3-3epsilon
betaTub97EF
cup
cdc2
pav
ida
lat
fzy
His3
Nup98
l(1)dd4
His2A
Rae1
Grip84
Grip71
me31B
RanGAP

Supplemental Table 1

geneID	name	cg	flybase	ms control	control: centrosomal location (flybase)	control: centrosome-related (UniProt)	ms identified	centrosome number	centrosome shape	chromosome aberrations	mitotic index	FACS phenotype					Goshima et al., Science 2007	Keller et al., Curr Biol, 2005	Li et al., Cell 2004	Andersen et al., Nature 2003	Bettencourt et al., Nature 2004	protein domains (Ensemble)	Orthologs flybase/ inparanoid	OMIM
												sub-G1	G1/G0	S-phase	G2/M	8N								
42186	14-3-3epsilon	CG31196	FBgn0020238																			14-3-3, 1 CC	YWHAE	MILLER-DIEKER LISSENCEPHALY SYNDROME; MDLS
39547	26-29-p	CG8947	FBgn0028967																			Pept_cys_AS, Peptidase_C1A_C, Propeptide_I29, LC, Signal peptide	-	
35526	Act42A	CG12051	FBgn0000043																			Actin, Actin-like	ACTB	DYSTONIA, JUVENILE-ONSET [ACTB, ARG183TRP]
37368	Act57B	CG10067	FBgn0000044																			Actin, Actin_like	-	
31521	Act5C	CG4027	FBgn0000042																			Actin, Actin_like	ACTB	
40444	Act79B	CG7478	FBgn0000045																			Actin, Actin_like	-	
48632	Act87E	CG18290	FBgn0000046																			Actin, Actin_like	-	
41885	Act88F	CG5178	FBgn0000047																			Actin, Actin_like	-	
42126	ald	CG7643	FBgn0000063																			CaMKII_AD, Prot_kinase, Ser_thr_pkin_AS, WAK, LC	-	
38231	alpha-Spec	CG1977	FBgn0003470																			EF_hand_Ca_bd, EF_hand_assoc_2, Miro-like, NADPH_Ox, Neu_cyt_fact_2, SH3, SH3_2, Spectrin, LC, 15 CC	SPTAN1	-
39130	alphaTub67C	CG8308	FBgn0004236																			Tubulin, Tub_FtsZ, Alpha_tubulin, Epsilon_tubulin, Delta_tubulin, Beta_tubulin, Gamma_tubulin, FtsZ, Tubulin_FtsZ, LC	-	
40848	alphaTub84B	CG1913	FBgn0003884																			Alpha_tubulin, Beta_tubulin, Delta_tubulin, Epsilon_tubulin, FtsZ_Gamma_tubulin, Tub_FtsZ_C, Tubulin, Tubulin_FtsZ, LC, 1 CC	TUBA1A	-
40904	alphaTub84D	CG2512	FBgn0003885																			Alpha_tubulin, Beta_tubulin, Delta_tubulin, Epsilon_tubulin, FtsZ_Gamma_tubulin, Tub_FtsZ_C, Tubulin, Tubulin_FtsZ, LC, 1 CC	-	
41183	alphaTub85E	CG9476	FBgn0003886																			Alpha_tubulin, Beta_tubulin, Delta_tubulin, Epsilon_tubulin, FtsZ_Gamma_tubulin, Tub_FtsZ_C, Tubulin, Tubulin_FtsZ, LC, 1 CC	-	
42127	alt	CG18212	FBgn0038535																			LC, Signal peptide, Transmembrane, 9 CC	-	
44642	Apc	CG1451	FBgn0015589																			APC_15aa, APC_crr, Armadillo, HEAT, LC	APC	ADENOMATOUS POLYPOSIS OF THE COLON; APC
42871	Apc2	CG6193	FBgn0026598																			APC_15aa, APC_crr, Armadillo, LC	-	
43616	aralar1	CG2139	FBgn0028646																			Aden_trnslctor, EF_hand_Ca_bd, EF_hand_assoc_2, Miro-like, Mit_carrier, Mitoch_carrier, NADPH_Ox, LC	SLC25A12	Mohr-Tranebjaerg syndrome
31151	arm	CG11579	FBgn0000117																			Armadillo, HEAT, LC	CTNNB1	implicated in many types of CANCER
42946	asp	CG6875	FBgn0000140																			Calponin_act_bd, IQ_CaM_bd_region, LC, 3 CC	ASPM	MICROCEPHALY, PRIMARY AUTOSOMAL RECESSIVE
43829	ATPsyn-beta	CG11154	FBgn0010217																			ATPase_a_b_C, ATPase_a_b_N, ATPase_a_b_nl-bd, LC	ATP5B	
41883	Atx2	CG5166	FBgn0041188																			Ataxin-2_C, Ataxin-2_N, PRO_rich, Involucrin_rpt, LC, 1 CC	-	
41446	aur	CG3068	FBgn0000147																			CaMKII_AD, Prot_kinase, Ser_thr_pkin_AS, Tyr_pkinase, WAK, LC	AURKA	COLON CANCER, SUSCEPTIBILITY TO
32703	baz	CG5055	FBgn0000163																			Atrophin, PDZ, LC	PARD3B	-
45826	bel	CG9748	FBgn0000171																			DEAD, DEAD/DEAH_N, DEAD/DEAH_assoc, DEAD_box, Eggshell, Helicase_C, NPHI_C, SNF2_assoc_bac, LC	DDX3X	
37238	betaTub56D	CG9277	FBgn0003887																			Alpha_tubulin, Beta_tubulin, Delta_tubulin, Epsilon_tubulin, FtsZ_Gamma_tubulin, Tub_FtsZ_C, Tubulin, Tubulin_FtsZ, LC, 1 CC	-	
43359	betaTub97EF	CG4869	FBgn0003892																			Alpha_tubulin, Beta_tubulin, Delta_tubulin, Epsilon_tubulin, Gamma_tubulin, Tub_FtsZ_C, Tubulin, Tubulin_FtsZ, LC, 1 CC	-	
34946	BicC	CG4824	FBgn0000182																			KH_type_1, SAM, SAM_2, LC	ANKS6	-
35051	BicD	CG6605	FBgn0000183																			LC, 8 CC	BICD1	-
37617	blw	CG3612	FBgn0011211																			ATPase_a_b_C, ATPase_a_b_N, ATPase_a_b_nl-bd	ATP5A1	-
43687	bnk	CG1480	FBgn0004389																			LC	-	
39049	bol	CG4760	FBgn0011206																			Hud_Sxl_RNA, RNP1_RNA_bd, LC	BOLL	-
53565	bor	CG6815	FBgn0040237																			AAA_ATPase_centr, LC, 2 CC	ATAD3A	-
35197	brat	CG10719	FBgn0010300																			NHL, Pept_M_Zn_BS, Znf_Bbox, Znf_C2H2, LC	-	
39744	brm	CG5942	FBgn0000212																			BRK, Bromodomain, DEAD/DEAH_assoc, Helicase_C, NLS_BP, NPHI_C, PRO_rich, SNF2_N, SNF2_assoc_bac, LC, 4 CC	SMARCA2	-
35016	Cas	CG13281	FBgn0022213																			CAS_CSE1_C, Cse1, Importinb_N, Xpo1	CSE1L	CANCER
42029	Cctgamma	CG8977	FBgn0015019																			Chaperonin_TCP-1, Chaprnin_Cpn60, Cpn60/TCP-1, LC, 1 CC	CCT3	
34411	cdc2	CG5363	FBgn0004106																			CaMKII_AD, Prot_kinase, Ser_thr_pkin_AS, Tyr_pkinase, WAK	CDC2	
42453	cdc2c	CG10498	FBgn0004107																			CaMKII_AD, Prot_kinase, Ser_thr_pkin_AS, Tyr_pkinase, WAK, LC	CDK2	
38756	CG10077	CG10077	FBgn0035720																			DEAD, DEAD/DEAH_N, DEAD/DEAH_assoc, DEAD_box, Eggshell, Helicase_C, NPHI_C, SNF2_assoc_bac, LC	DDX5	
42017	CG10345	CG10345	FBgn0027562																			CD36, CD36_antigen, Signal peptide, Transmembrane, LC	-	
39513	CG10732	CG10732	FBgn0036365																			PRO_rich, LC, 8 CC	-	
31707	CG10777	CG10777	FBgn0029979																			Antifreeze_1, DEAD, DEAD/DEAH_N, DEAD/DEAH_assoc, DEAD_box, Eggshell, Helicase_C, NPHI_C, SNF2_assoc_bac, LC	-	
32350	CG11092	CG11092	FBgn0027537																			NIC, LC	-	
43842	CG11148	CG11148	FBgn0039936																			GYF, LC, 3 CC	PERQ1	-
33002	CG11943	CG11943	FBgn0031078																			LC	NUP205	-
43372	CG14065	CG14065	FBgn0039579																			LC	-	
32971	CG14215	CG14215	FBgn0031052																			Aminotrans_II, LC, 1 CC	AHCTF1	
32989	CG14235	CG14235	FBgn0031066																			Cyt_c_ox6B, LC	COX6B1	-
42212	CG14309	CG14309	FBgn0038611																			LC, Signal peptide	-	
41567	CG14391	CG14391	FBgn0038078																			-	-	
37164	CG15092	CG15092	FBgn0034388																			LC, Transmembrane	-	
43555	CG15524	CG15524	FBgn0039731																			LC, 6 CC	SASS6	
31976	CG17255	CG17255	FBgn0030205																			BAT2_N, Chaprnin_Cpn60, Eggshell, Galnin2_receptor, Involucrin_rpt, LC, 5 CC	-	
39850	CG17286	CG17286	FBgn0027500																			LC	-	
35149	CG18397	CG18397	FBgn0032723																			AMP-bind, DopaD4_receptor, LC, 8 CC	SCAPER	
59172	CG18811	CG18811	FBgn0042134																			Eggshell, PRO_rich, LC, 3 CC	CAPRIN1	
35330	CG1962	CG1962	FBgn0032876																			Disease_resist, LC, 2 CC	-	
35784	CG2158	CG2158	FBgn0033264																			EVH1, Ran_BP1, LC	NUP50	
37146	CG30122	CG30122	FBgn0050122																			Eggshell, SAP_DNA_bd, SPRY_rcpt, LC	HNRPUL1	
35611	CG30159	CG30159	FBgn0050159																			-	-	
34416	CG31716	CG31716	FBgn0051716																			RNP1_RNA_bd, Znf_CCCH, Znf_RIN, LC, 2 CC	CNOT4	
37840	CG3173	CG3173	FBgn0034964																			LC	INTS1	
318949	CG31802	CG31802	FBgn0051802																			EF_hand_Ca_bd, EF_hand_assoc_2, Miro-like, NADPH_Ox, LC	CETN2	
39537	CG32137	CG32137	FBgn0052137																			Tropomyosin, LC, 5 CC	CCDC64	
37707	CG3530	CG3530	FBgn0028497																			DZC, EGF_like, Myotub-related, TYR_phosphatase, Znf_FYVE, 1 CC	MTMR6	Mutations in the myotubularin, dual-specific phosphatase gene cause X-linked myotubular myopathy
39846	CG4169	CG4169	FBgn0036642																			M16C_assoc, Pept_M16_N, Peptidase_M16_C, TFIIB_euk_relate, LC	UQCRC2	
36838	CG4398	CG4389	FBgn0028479																			3HCDH_NAD_bd, 3HC_DH_C, EnCoA_hydratase, LC	-	
38612	CG4769	CG4769	FBgn0035600																			Cyt_C1, LC	CYC1	
31363	CG4857	CG4857	FBgn0026083																			POA_allergen_C, LC	-	
32441	CG5599	CG5599	FBgn0030612																			2Oxoacid_DH, Biotin_lipoyl, E3_bd, Lipoyl_BS, LC	DBT	MAPLE SYRUP URINE DISEASE
37082	CG5726	CG5726	FBgn0034313																			LC	-	
39737	CG5931	CG5931	FBgn0036548																			DEAD, DEAD/DEAH_N, DEAD/DEAH_assoc, EF_hand_Ca_bd, Helicase_C, NPHI_C, SNF2_assoc_bac, Sec63, LC	ASCC3L1	
34541	CG6181	CG6181	FBgn0032340																			WD40, LC, 5 CC	EDC4	
39957	CG6311	CG6311	FBgn0036735																			LC, 1 CC	EDC3	
42587	CG6455	CG6455	FBgn0019960																			Antifreeze_1, WD40, LC, 2 CC	IMMT	
39930	CG6479	CG6479	FBgn0036710																			LC, Transmembrane	NP_116231.2	
32851	CG6540	CG6540	FBgn0030943																			MPPN	NUP35	
3772232	CG6783	CG6783	FBgn0037913																			Fatty_acid_bd, Lipocln_cytFABP, LC	-	
38062	CG6905	CG6905	FBgn0035136																			Myb_DNA_bd, LC, 5 CC	CDC5L	
31838	CG7033	CG7033	FBgn0030086																			Chaperonin_TCP-1, Chaprnin_Cpn60, Cpn60/TCP-1, DEAD_box, LC	CCT2	
41804	CG7262	CG7262	FBgn0038274																			NIC	NUP93	
34442	CG7456	CG7456	FBgn0032258																			COG4, LC, 2 CC	COG4	
41599	CG7518	CG7518	FBgn0038108																			Antifreeze_1, Myb_DNA_bd, NLS_BP, PRO_rich, LC, 6 CC	-	

42209	CG7671	CG7671	FBgn0038609	LLGL2, WD40	NUP43	
38852	CG7716	CG7716	FBgn0035800	Spc97_Spc98, LC, 3 CC	-	
38178	CG7852	CG7852	FBgn0035229	DENN, LipOase_LH2, dDENN, uDENN, LC	RAB6IP1	
42173	CG7940	CG7940	FBgn0038576	Actin_like, LC, 2 CC	ACTR5	
32763	CG8142	CG8142	FBgn0030871	AAA_ATPase_centr, RFC, Rep_fac_C	RFC4	
36793	CG8443	CG8443	FBgn0034087	LC	KIAA0664	
36397	CG8771	CG8771	FBgn0033766	LC	NUP188	
41646	CG8863	CG8863	FBgn0038145	DnaJ_C, DnaJ_CXXCXGXG, DnaJ_N, Hsp_DnaJ, LC	DNAJA4	
32508	CG9281	CG9281	FBgn0030672	ABC_transp_like, ATP_GTP_BS_A, Oligopep_ABC_C, LC, 1 CC	ABCF2	
39613	CG9425	CG9425	FBgn0036451	Ataxin-2_C, Involucrin_rpt, PRO_rich, ResIII, Znf_C2H2, Znf_CCCH, tRNA-synt_I, LC, 1 CC	HELZ	
43901	chb	CG32435	FBgn0021760	HEAT, LC	CLASP1	
33505	Chd1	CG3733	FBgn0016132	Chromo, DEAD/DEAH_assoc, DEAH_box, Helicase_C, NPHI_C, SNF2_N, SNF2_assoc_bac, LC	CHD2	
33834	chic	CG9553	FBgn0000308	Profilin, Profilin_plant	-	
40508	Chro	CG10712	FBgn0044324	Chromo, LC, 2 CC	-	
34096	Cka	CG7392	FBgn0044323	LLGL2, Striatin_N, WD40, LC, 1 CC	STRN4	
48448	CkIIalpha	CG17520	FBgn0000258	CaMKII_AD, Prot_kinase, Ser_thr_pkin_AS, Tyr_pkinase, WAK, LC	CSNK2A1	
53561	cmet	CG6392	FBgn0040232	kinesin_motor, Tropomyosin, 26 CC	CENPE	
36491	cnn	CG4832	FBgn0013765	Spindle_assoc, Tropomyosin, LC, 13 CC	CDK5RAP2	MICROCEPHALY, PRIMARY AUTOSOMAL RECESSIVE
35596	coro	CG9446	FBgn0033109	Arg_agm_form, LLGL2, WD40, LC, 1 CC	CORO1B	
33937	cort	CG11330	FBgn0000351	WD40, LLGL2	-	
40616	corto	CG2530	FBgn0010313	Antifreeze_1, NOR1_rcpt, Tubby_N, LC, 3 CC	-	
41432	CoVa	CG14724	FBgn0019624	Cyt_c_ox5A	COX5A	
41848	Cp190	CG6384	FBgn0000283	BTB, BTB_POZ, ER_target_S, Znf_C2H2, LC	-	
39639	cp309	CG6735	FBgn0036472	LC, 20 CC	-	
31787	Cp36	CG1478	FBgn0000359	Chorion_3, LC, Signal peptide	-	
31785	Cp7Fb	CG15350	FBgn0030044	Ald_DH, LC, Transmembrane, Signal peptide	-	
31208	crn	CG3193	FBgn0000377	HAT, TPR_region, LC	-	
41602	CtBP	CG7583	FBgn0020496	2_Hacid_DH, 2hydac_DH_NAD_bd	CTBP2	
33934	cup	CG11181	FBgn0000392	PRO_rich, LC, 2 CC	-	
37790	Dcp1	CG11183	FBgn0034921	DCP1, tRNA-synt_I, LC	DCP1B	
38580	Dhc64C	CG7507	FBgn0010349	AAA_5, CbbQ_C, DHC_N1, DHC_N2, Dynein_heavy, Pept_cys_AS, Peptidase_S16, LC, 6 CC	DYNC1H1	
35340	dia	CG1768	FBgn0011202	Drf_DAD, Drf_FH3, Drf_GTPase_bd, FH2_actin_bd, Glutelin, PRO_rich, LC, 3 CC	DIAPH2	PREMATURE OVARIAN FAILURE 2A [DIAPH2, INTRONIC BREAKPOINT]
44653	dpld	CG1624	FBgn0015930	NHL, Znf_Bbox, LC, 1 CC	-	
36271	Ef1alpha48D	CG8280	FBgn0000556	EFTU_C, EFTU_D2, ProtSyn_GTP_bd, LC	-	
44791	Ef1gamma	CG11901	FBgn0029176	EF1_G, GST_C, GST_N, LC, 1 CC	EEF1G	
35422	Ef2b	CG2238	FBgn0000559	EFG_C, EFG_IV, EFTU_D2, EFG_IV, ProtSyn_GTP_bd, LC, 1 CC	EEF2	
37757	egl	CG4051	FBgn0000562	3_5_exonuclease, LC	-	
31156	eIF2B-ε	CG3806	FBgn0023512	Hexapep_transf, eIF5C, LC	EIF2B5	LEUKOENCEPHALOPATHY WITH VANISHING WHITE MATTER
40563	eIF3-S10	CG9805	FBgn0037249	PCI, LC, 4 CC	EIF3A	
33835	eIF-4a	CG9075	FBgn0001942	DEAD, DEAD/DEAH_N, DEAD/DEAH_assoc, DEAD_box, Helicase_C, NPHI_C, SNF2_assoc_bac, LC	EIF4A2	
43839	eIF-4G	CG10811	FBgn0023213	IF_eIF4G, IF_eIF4G_MA3, eIF5C, LC	EIF4G1	
34903	esg	CG3758	FBgn0001981	Antifreeze_1, Znf_C2H2, Znf_C2H2_sub, LC	SNAI2	WAARDENBURG SYNDROME
46234	fbl	CG5725	FBgn0011205	Fumble, LC	PANK1	
32015	feo	CG11207	FBgn0030241	MAP65_ASE1, LC, 3 CC	PRC1	
37662	Fib	CG9888	FBgn0003062	Eggshell, Fibrillarin, Prion, LC	FBL	
37528	Fmr1	CG6203	FBgn0028734	EDG6_rcpt, KH_type_1, RtxD_bac, TONB_Box_N, LC, 1 CC	FXR1	
35211	fon	CG15825	FBgn0032773	LC, Signal peptide	-	
45973	fs(1)N	CG11411	FBgn0004650	Signal peptide, LC, 4 CC	-	
35336	Fs(2)Ket	CG2637	FBgn0000986	HEAT, Importinb_N, Xpo1	KPNB1	
45307	fz	CG3646	FBgn0001085	Frizzled, Fz_domain, GPCR_secretin, Signal peptide, Transmembrane, LC	FZD1	
34968	fzy	CG4274	FBgn0001086	Fizzy, LLGL2, WD40, LC	CDC20	
33501	gammaTub23C	CG3157	FBgn0004176	Alpha_tubulin, Beta_tubulin, Delta_tubulin, Epsilon_tubulin, Gamma_tubulin, Tub_FtsZ_C, Tubulin, Tubulin_FtsZ, 1 CC	TUBG1	
35199	gammaTub37C	CG17566	FBgn0010097	Alpha_tubulin, Beta_tubulin, Delta_tubulin, Epsilon_tubulin, FtsZ, Gamma_tubulin, Tub_FtsZ_C, Tubulin, Tubulin_FtsZ	-	
39615	gnu	CG5272	FBgn0001120	SAM_2, LC	-	
35512	gp210	CG7897	FBgn0033039	Transmembrane, Signal peptide, LC	NUP210	
40559	growl	CG14648	FBgn0037245	FTHF_cligase, LC	MTHFSD	
32478	Grip128	CG9201	FBgn0026433	S_T_dehydrtse_BS, Thiored, LC, 1 CC	TUBGCP5	
39365	Grip163	CG5688	FBgn0026432	Spc97_Spc98, 2 CC	-	
35130	Grip71	CG10346	FBgn0032705	LLGL2, WD40, LC, 1 CC	-	
34441	Grip75	CG6176	FBgn0026431	AP_endnuclease2, Spc97_Spc98	TUBGCP4	
32946	Grip84	CG3917	FBgn0026430	Spc97_Spc98, LC	TUBGCP2, DOCK1	
43808	gw	CG31992	FBgn0051992	UBA, LC, 1 CC	TNRC6C	
34993	grp	CG17161	FBgn0011598	CaMKII_AD, Prot_kinase, Ser_thr_pkin_AS, Tyr_pkinase, WAK, LC	CHEK1	
48571	heph	CG31000	FBgn0011224	RNP1_RNA_bd, LC	PTBP1	
318855	His2A:CG31618	CG31618	FBgn0051618	CBFA_NFYB_domain, Hist_TAF, Histone_core_D, LC	HIST2H2AB	
43229	His2Av	CG5499	FBgn0001197	Hist_TAF, Histone_H2A, Histone_core_D, LC	H2AFV	
326273	His2B:CG17949	CG17949	FBgn0061209	Hist_TAF, Histone_H2A, Histone_core_D, LC	HIST3H2BB	
31848	His3.3B	CG8989	FBgn0004828	Hist_TAF, Histone_H3, Histone_core_D	H3F3B	
318847	His3:CG31613	CG31613	FBgn0051613	Hist_TAF, Histone_H3, Histone_core_D	HIST2H3D, HIST2H3P	-
318846	His4:CG31611	CG31611	FBgn0051611	Hist_TAF, Histone_H4, Histone_core_D, LC	H4_HUMAN	
41773	His4r	CG3379	FBgn0013981	Hist_TAF, Histone_H4, Histone_core_D, LC	H4_HUMAN	
39542	Hsc70-1	CG8937	FBgn0001216	Hsp70, Hsp_70, LC	-	
32133	Hsc70-3	CG4147	FBgn0001218	ER_target_S, Hsp70, Hsp_70, LC, Signal peptide, LC, 1 CC	HSPA5	MARINESCO-SJOGREN SYNDROME; MSS (indirekt)
41840	Hsc70-4	CG4264	FBgn0001219	Hsp70, Hsp_70, LC, 1 CC	HSPA8	
39557	Hsc70Cb	CG6603	FBgn0026418	Hsp70, Hsp_70, LC, 2 CC	HSPA4L	
39075	Hsp26	CG4183	FBgn0001225	Crystallin_alpha, Hsp20, TONB_Box_N, LC	-	
39078	Hsp27	CG4466	FBgn0001226	Crystallin_alpha, Hsp20, TONB_Box_N, LC	-	
44921	Hsp70Ba	CG31449	FBgn0013277	Hsp70, Hsp_70, LC, 2 CC	-	
38389	Hsp83	CG1242	FBgn0001233	ATP_bd_ATPase, Hsp90, LC, 2 CC	HSP90AA2	
34504	ial	CG6620	FBgn0024227	CaMKII_AD, Prot_kinase, Ser_thr_pkin_AS, Tyr_pkinase, WAK	-	
45574	ida	CG10850	FBgn0041147	LC	ANAPC5	
32009	Imp	CG1691	FBgn0030235	KH_TYPE_2, KH_type_1, LC, 1 CC	IGF2BP1	
37355	insc	CG11312	FBgn0011674	LC	INSC	
53578	Jafrac1	CG1633	FBgn0040309	AhpC-TSA, Redoxin	PRDX2	candidate gene for cancer, muscular dystrophy
43093	jigr1	CG17383	FBgn0039350	LC	-	
32049	Klp10A	CG1453	FBgn0030268	kinesin_motor, LC, 1 CC	KIF2A	
38135	Klp61F	CG9191	FBgn0004378	kinesin_motor, LC, 9 CC	KIF11	
38418	kst	CG12008	FBgn0004167	Actnin_actin_bd, Calponin_act_bd, Rib_bd_factA, SH3, SH3_2, Spectrin, Spectrin_PH, LC, 19 CC	SPTBN5	
48481	l(1)dd4	CG10988	FBgn0001612	S_T_dehydrtse_BS, Spc97_Spc98, LC, 1 CC	TUBGCP3	
49168	l(2)37Cc	CG10691	FBgn0002031	Band_7, Prohibitin, LC, 1 CC	PHB	BREAST CANCER, SPORADIC [PHB, ARG105HIS]
35501	l(2)NC136	CG8426	FBgn0033029	NOT, Not_N, LC, 2 CC	CNOT3	
33782	Lam	CG6944	FBgn0002525	IF, IF_tail, LC, 4 CC	LMNB1	LEUKODYSTROPHY, ADULT-ONSET, AUTOSOMAL DOMINANT [LMNB1, DUP]
38811	lark	CG8597	FBgn0011640	Hud_Sxl_RNA, PRO_rich, RNP1_RNA_bd, Znf_CCHC, LC	RBM4B	
36454	lat	CG4088	FBgn0005654	ORC3_N, LC, 1 CC	ORC3L	
37482	LBR	CG17952	FBgn0034657	ERG4_ERG24, LC, Transmembrane	LBR	PELGER-HUET ANOMALY, GREENBERG DYSPLASIA
45894	lds	CG2684	FBgn0002542	DEAD/DEAH, Helicase_C, NPHI_C, SNF2_N, SNF2_assoc_bac, LC, 1 CC	TTF2	BAMFORTH-LAZARUS SYNDROME [FOXE1, ALA65VAL], HYPOTHYROIDISM, ATHYROIDAL
32257	lic	CG12244	FBgn0015763	CaMKII_AD, Prot_kinase, Ser_thr_pkin_AS, Tyr_pkinase, WAK	MAP2K3	
35771	lig	CG8715	FBgn0020279	Antifreeze_1, UBA, LC	-	
44672	Lk6	CG17342	FBgn0017581	CaMKII_AD, Prot_kinase, Ser_thr_pkin_AS, WAK, LC, 2 CC	MKNK2	

35288	Lok	CG10895	FBgn0019686		CaMKII_AD, FHA, Prot_kinase, Ser_thr_pkin_AS, Tyr_pkinase, WAK, LC	CHEK2	LI-FRAUMENI SYNDROME 2, OSTEOSARCOMA, PROSTATE CANCER, BREAST CANCER
31350	lva	CG6450	FBgn0029688		Involucrin_rpt, Tropomyosin, LC, 37 CC	-	
35991	Map60	CG1825	FBgn0010342		LC	-	
50070	mask	CG33106	FBgn0043884		ANK, Antifreeze_1, Gliadin, Involucrin_rpt, KH_type_1, TRP_2, LC, 3 CC	ANKHD1-EIF4EBP3	
41562	mbo	CG6819	FBgn0026207		LC, 1 CC	NUP88	
34364	me31B	CG4916	FBgn0004419		DEAD, DEAD/DEAH_N, DEAD/DEAH_assoc, DEAD_box, Helicase_C, NPHI_C, SNF2_assoc_bac	DDX6	
32979	Mer	CG14228	FBgn0013951		Band_4.1, ERM_C, Ez/rad/moesin, LC, 4 CC	-	
36102	micr	CG11763	FBgn0033522		CTLH_C, LisH, LisH-PF08513, PRO_rich, SPRY_rcpt, LC, 1 CC	RANBP9	
43764	mod	CG2050	FBgn0002780		RNP1_RNA_bd, LC	-	
38028	mri	CG1216	FBgn0035107		K_tetra, LC, 1 CC	BTBD10	
36797	mrj	CG8448	FBgn0034091		DnaJ_N, LC, 1 CC	DNAJB6	
41952	msps	CG5000	FBgn0027948		HEAT, LC	CKAP5	
36264	Mtor	CG8274	FBgn0013756		TPR_MLP1_2, LC, 22 CC	TPR	
45959	mts	CG7109	FBgn0004177		M-pesterase, Metallophos_C, T_phtase_apaH	PPP2CB	
41968	mtSSB	CG4337	FBgn0010438		SSB_primosomal_n, ssDNA_bd, LC	SSBP1	
32543	Myb	CG9045	FBgn0002914		Myb_DNA_bd, LC	MYB	cancer
37798	Nap1	CG5330	FBgn0015268		NAP_familyS, LC	NAP1L1	
32934	Nat1	CG12202	FBgn0031020		TPR_1, TPR_2, TPR_region, LC, 2 CC	NARG1	high expression in tumor cells
43517	ncd	CG7831	FBgn0002924		kinesin_motor, LC, 1 CC	KIFC1_HUMAN	
31762	ND75	CG2286	FBgn0017566		Aminotrans_II, Complex1_75K, Ferredoxin, Molybdopterin, LC	NDUFS1	MITOCHONDRIAL COMPLEX I DEFICIENCY
35293	neb	CG10718	FBgn0004374		FHA, kinesin_motor, LC, 4 CC	PAPD1, KIF14	
43856	nej	CG15319	FBgn0015624		Antifreeze_1, Bromodomain, DUF902_CREBbp, GGT_peptidase, Involucrin_rpt, KIX, Trans_coact , Znf_PHD, Znf_TAZ, Znf_ZZ, LC, 2 CC	EP300	COLORECTAL CANCER, RUBINSTEIN-TAYBI SYNDROME
31696	Nek2	CG17256	FBgn0029970		CaMKII_AD, Prot_kinase, Ser_thr_pkin_AS, Tropomyosin, Tyr_pkinase, WAK, LC, 2 CC	NEK2	
35982	Not1	CG1884	FBgn0033424		FGGY_kin, Ig_MHC, Lectin_legB, Not1, PRO_rich, LC	-	
39572	nuf	CG7867	FBgn0013718		Tropomyosin, LC, 5 CC	RAB11FIP4	
32630	Nup153	CG4453	FBgn0061200		PLD_envelope, Znf_RanBP2, LC	NUP153	
34527	Nup154	CG4579	FBgn0021761		Nup_nucleoporin, LC, 1 CC	NUP155	
34481	Nup170	CG6743	FBgn0027868		Nup84_Nup100	NUP107	
43041	Nup358	CG11856	FBgn0035520		EVH1, PLD_envelope, PRO_rich, Ran_BP1, TPR_region, Znf_RanBP2, LC, 3 CC	RANBP2	
37078	Nup75	CG5733	FBgn0034310		Nucleopor_Nup85, LC	NUP85	
42816	Nup98	CG10198	FBgn0039120		Peptidase_S59, LC	NUP98	human myeloid leukemia
35686	Orc1	CG10667	FBgn0022772		AAA_ATPase_centr, BAH, kinesin_motor, LC	ORC1L	
41703	Orc2	CG3041	FBgn0015270		Aldo/ket_red, ORC2, Pept_S8_S53, LC	ORC2L	
37090	Ote	CG5581	FBgn0003022		LC, Transmembrane, 1 CC	-	
3355143	p120ctn	CG17484	FBgn0015587		Armadillo, HEAT, LC	-	
37070	pAbp	CG5119	FBgn0003031		Hud_Sxl_RNA, PABP_HYD, RNP1_RNA_bd, LC, 1 CC	PABPC4	
2768852	par-1	CG11960	FBgn0026193		Antifreeze_1, CaMKII_AD, Kinase_C, Prot_kinase, Ser_thr_pkin_AS, Tyr_pkinase, UBA, WAK, LC	-	
42058	Patr-1	CG5208	FBgn0028470		PRO_rich, LC, 1 CC	NP_689929.1	
38515	pav	CG1258	FBgn0011692		kinesin_motor, LC, 2 CC	KIF23	
34338	Pen	CG4799	FBgn0011823		Armadillo, HEAT, IMPDh/GMPRtase, ImportinA_B_bd, LC	KPNA2	candidate gene for Russell-Silver syndrome
44848	plu	CG9183	FBgn0003114		ANK, TRP_2	-	
40232	polo	CG12306	FBgn0003124		CaMKII_AD, POLO_box, Prot_kinase, Ser_thr_pkin_AS, Tyr_pkinase, WAK, LC	PLK1	
34500	porin	CG6647	FBgn0004363		Porin_Euk	VDAC2	
42922	Pp1α-96A	CG6593	FBgn0003134		M-pesterase, Metallophos_C, T_phtase_apaH, LC	PPP1CA	
2768940	Pp2A-29B	CG33297	FBgn0005776		HEAT, Peptidase_M20C, LC	PPP2R1A	
45031	Pp4-19C	CG1459	FBgn0023177		M-pesterase, Metallophos_C, T_phtase_apaH	PPP4C	
41743	pr-set7	CG3307	FBgn0011474		SET, LC	-	
38173	pUf68	CG12085	FBgn0028577		Antifreeze_1, RNP1_RNA_bd, LC, 1 CC	PUF60	
41094	pum	CG9755	FBgn0003165		Antifreeze_1, POA_allergen_C, Pum_puf_RNA_bd, LC	PUM1	
42131	pxt	CG7660	FBgn0038538		Anim_peroxidase, LC, Signal peptide	-	
42620	PyK	CG7070	FBgn0003178		Antifreeze_1, Pyruvate_kinase, LC	PKM2	
43864	Qm	CG17521	FBgn0024733		Ribosomal_L10E, LC	RPL10	
32640	r	CG18572	FBgn0003189		ATP-grasp, Amidohydro_1, Anth_synthII, Asp/Orn_COtranf , Asp_Orn_bd, Asp_carbmltransf, CPSase_D2_ATP_bd, CP_synthGATase, CP_synthsmall, CPase_L, CPase_L_D3, CPase_L_N, Dihydroorotase, GATASE, GATase_1, GATase_1_AS, MGS, OCTace_P_bd, Orn_carbamltrans, LC	CAD	
37467	Rae1	CG9862	FBgn0034646	*	LLGL2, WD40	RAE1	
35223	RanGap	CG9999	FBgn0003346		LRR_RNinh, LRR, LC, 1 CC	RANGAP1	
31027	Rbf	CG7413	FBgn0015799		RB_A, RB_B, LC	RBL1	
43827	RfaBp	CG11064	FBgn0016724		DUF1081,Lipid_transprt_N, VWF_D, LC, Signal peptide, Transmembrane, LC, 1 CC	DHDDS	
47998	rin	CG9412	FBgn0015778		Hud_Sxl_RNA, NTF2, PRO_rich, RNP1_RNA_bd	G3BP1	
40739	Rm62	CG10279	FBgn0003261		DEAD, DEAD/DEAH_N, DEAD/DEAH_assoc, DEAD_box, Helicase_C, NPHI_C, SNF2_assoc_bac	-	
36280	RnrS	CG8975	FBgn0011704		Ribonucl_redctse, LC, Transmembrane	RRM2	
39338	RpL10Ab	CG7283	FBgn0036213		Ribosomal_L1, LC	RPL10A	
37235	RpL11	CG7726	FBgn0013325		Ribosomal_L5	RPL11	
45329	RpL12	CG3195	FBgn0002611		Ribosomal_L11	RPL12	
34329	RpL13	CG4651	FBgn0011272		Ribosomal_L13E, LC	RPL13	
40687	RpL13A	CG1475	FBgn0037351		Ribosomal_L13	Q5VY36_HUMAN	
38983	RpL14	CG6253	FBgn0017579		Ribosomal_L14e, LC	RPL14	
31613	RpL17	CG3203	FBgn0029897		Ribosomal_L22, LC	RPL17	
38794	RpL18	CG8615	FBgn0035753		Ribosomal_L18e	RPL18	
36985	RpL18A	CG6510	FBgn0010409		Ribosomal_L18ae	RPL18A	
37995	RpL19	CG2746	FBgn0002607		Ribosomal_L19e, LC, 1 CC	RPL19	
35453	RpL21	CG12775	FBgn0032987		Ribosomal_L21e, 1 CC	RPL21	
31022	RpL22	CG7434	FBgn0015288		Antifreeze_1, Histone_H5, POA_allergen_C, Ribosomal_L22e, Ribosomal_P2, SibA, Tubby_N, treacle, LC	RPL22	acute and chronic myeloid leukemia
37628	RpL23	CG3661	FBgn0010078		Ribosomal_L14	RPL23	
38208	RpL23A	CG7977	FBgn0026372		Antifreeze_1, Histone_H3, Histone_H5, POA_allergen_C, Ribosomal_L23, Ribosomal_L23eN, Ribosome_L25_23, treacle, LC	RPL23A	
34754	RpL24	CG9282	FBgn0032518		Ribosomal_L24E, LC	RPL24	
43103	RpL27	CG4759	FBgn0039359		KOW, Ribosomal_L27e, LC	RPL27	
33654	RpL27A	CG15442	FBgn0010410		Ribosomal_L15, LC	RPL27A	
38397	RpL28	CG12740	FBgn0035422		Ribosomal_L28e, LC	RPL28	
41347	RpL3	CG4863	FBgn0020910		Ribosomal_L3, LC	RPL3	
44059	RpL30	CG10652	FBgn0015745		Ribosomal_L30e, Ribosomal_L7A	-	
31483	RpL35	CG4111	FBgn0029785		Ribosomal_L29, LC, 1 CC	RPL35	
31009	RpL36	CG7622	FBgn0002579		Ribosomal_L36e, 1 CC	RPL36	
43349	RpL4	CG5502	FBgn0003279		Ribos_L4_L1E_arc, Ribosomal_L4/L1E, LC	RPL4	
43723	RpL6	CG11522	FBgn0039857		Ribosomal_L6E, Ribosomal_L6e_N, LC	RPL6	
34352	RpL7	CG4897	FBgn0005593		Pept_cys_AS, Ribosomal_L30, Ribosomal_L30_N, LC, 1 CC	O95036_HUMAN	
31588	RpL7A	CG3314	FBgn0014026		Ribosomal_7A, Ribosomal_HS6, Ribosomal_L7A, Ribosomal_L7Ae, LC	RPL7A	
44251	RpL8	CG1263	FBgn0024939		Ribosomal_L2, LC	RPL8	
34526	RpL9	CG6141	FBgn0015756		Adhesion, Ribosomal_L6, Ribosomal_L6_2	RPL9	
40451	RpLP0	CG7490	FBgn0000100		Ribosomal_60S, Ribosomal_L10, Ribosomal_P2, LC	RPLP0	
36321	RpS11	CG8857	FBgn0033699		Ribosomal_S17	RPS11	
34149	RpS13	CG13389	FBgn0010265		Ribosomal_S13_N, Ribosomal_S15	RPS13	
39088	RpS17	CG3922	FBgn0005533		Ribosomal_S17E, LC	RPS17	
32635	RpS19a	CG4464	FBgn0010412		Ribosomal_S19E	RPS19	DIAMOND-BLACKFAN ANEMIA
36576	RpS23	CG8415	FBgn0033912		Ribosom_S12_bac, Ribosomal_S12_23	RPS23	
37589	RpS24	CG3751	FBgn0034751		Ribosomal_S24E, LC	RPS24	DIAMOND-BLACKFAN ANEMIA 3
42761	RpS3	CG6779	FBgn0002622		KH_TYPE_2, Ribosomal_S3_C	RPS3	more abundant in 8 of 8 colon adenocarcinomas and 7 of 10 adenomatous polyps

43768	RpS3A	CG2168	FBgn0017545	Ribosomal_S3AE, LC	RPS3A	
39484	RpS4	CG11276	FBgn0011284	KOW, Ribosomal_S4E, S4_RNA_bd	RPS4X	
41807	RpS5b	CG7014	FBgn0038277	Ribosomal_S7, LC	-	
31700	RpS6	CG10944	FBgn0004922	Ribosomal_S6E, LC, 1 CC	RPS6	
43594	RpS7	CG1883	FBgn0039757	Ribosomal_S7E	RPS7	
43532	RpS8	CG7808	FBgn0039713	NLS_BP, Ribosomal_S8E, LC	RPS8	increased levels of RPS8 mRNA in all 3 human colorectal tumors and all 3 human colon polyps examined
39108	RpS9	CG3395	FBgn0010408	Ribosomal_S4, S4_RNA_bd, LC	RPS9	
40859	sas-4	CG10061	FBgn0011020	Tcp10_C, LC, 2 CC	-	
38457	Sc2	CG10849	FBgn0035471	Strd5A_DH_C, Ubiquitin, LC, Transmembrane	GPSN2	
35564	sced	CG3273	FBgn0013732	LC	-	
35696	scra	CG2092	FBgn0004243	PH, PRO_rich, LC, 1 CC	ANLN	
32007	sesB	CG16944	FBgn0003360	Aden_trnslctor, Mit_carrier, Mitoch_carrier, LC, Transmembrane	SLC25A5	
36542	shot	CG18076	FBgn0013733	Actnin_actin_bd, Calponin_act_bd, EF_hand_Ca_bd, EF_hand_assoc_2, GAS2, Miro-like, NADPH_Ox, SH3, SH3_2, Spectrin, LC, 32 CC	DST	autoantigen in the blistering disease bullous pemphigoid
3771796	Skeletor	CG33676	FBgn0020517	PRO_rich, Vprs_rcpt_V1B, LC	-	
33890	slam	CG9506	FBgn0043854	LC, 1 CC	-	
37893	slik	CG4527	FBgn0035001	CaMKII_AD, Glutelin, NOR1_rcpt, PRO_rich, Prot_kinase, Ser_thr_pkin_AS, Tyr_pkinase, WAK, LC, 6 CC	STK10	
42504	slmb	CG3412	FBgn0023423	F-box, FBD, LLGL2, WD40	BTRC	split-hand/split-foot malformation (SHFM3; 600095)
39034	smg	CG5263	FBgn0016070	SAM, SAM_2, LC	SAMD4B	
34908	sna	CG3956	FBgn0003448	Ig_MHC, Znf_C2H2, Znf_C2H2_sub, LC	-	
34309	sop	CG5920	FBgn0004867	Ribosomal_S5, Ribosomal_S5_C, LC	RPS2	
34793	Sop2	CG8978	FBgn0001961	LLGL2, WD40	ARPC1A	
46059	Sply	CG8946	FBgn0010591	Pyridoxal_deC, 1 CC	SGPL1	
46194	Spn	CG16757	FBgn0010905	PDZ, PRO_rich, Ppantne_S, SAM, SAM_2, LC, 4 CC	PPP1R9A	
39768	SsRβ	CG5474	FBgn0011016	TRAP_beta, Signal peptide, Transmembrane	SSR2	
31106	sta	CG14792	FBgn0003517	Ribosomal_S2, LC	CHECK	
43466	stg	CG1395	FBgn0003525	MPI_Phosphatase, Rhodanese-like, LC	CDC25C	
31580	swa	CG3429	FBgn0003655	LC, 2 CC	-	
39485	Syx13	CG11278	FBgn0036341	Synaptobrevin, Syntaxin_N, T_SNARE, LC, Transmembrane, 2 CC	-	
40589	tacc	CG9765	FBgn0026620	TACC, LC, 3 CC	NXT2	
35297	Taf13	CG10756	FBgn0032847	TFIID-18, LC	TAF13	
36565	Tango7	CG8309	FBgn0033902	26S_Psome_reg_C, PCI	EIF3M	HSV, acts as a receptor or coreceptor for entry of herpes simplex virus (HSV)
43095	tankyrase	CG4719	FBgn0027508	ANK, PARP, SAM, SAM_2, LC	TNKS2	
42433	TFAM	CG4217	FBgn0038805	CTNNB1_bd, HMG_1/2, HMG_1/2_box, 2 CC	TFAM	
37042	thr	CG5785	FBgn0003701	LC	-	
35225	Top2	CG10223	FBgn0003732	ATP_bd_ATPase, CBFA_NFYB_topo, TopoII_euk, Topo_IIA_A/C, Topo_IIA_B/N, Topo_IIA_B_2, LC, 3 CC	TOP2B	
31565	Top3β	CG3458	FBgn0026015	DUF1738, Topo_IA, Topo_IA_cen, Toprim_dom, tRNA-synt_I, LC	TOP3B	
39430	tral	CG10686	FBgn0041775	LC, 1 CC	-	
35559	Trap1	CG3152	FBgn0026761	ATP_bd_ATPase, Hsp90	TRAP1	
38045	Tudor-SN	CG7008	FBgn0035121	Tudor, Snase, Maternal_tudor, LC, 2 CC	SND1	Epstein-Barr virus (EBV) nuclear antigen-2 (EBNA2) coactivator
36538	tum	CG13345	FBgn0033881	DAG_PE_bd, RhoGAP, LC	-	
47286	twin	CG31137	FBgn0011725	Exo_endo_phos, LRR_typ, LC	CNOT6	
42738	unk	CG4620	FBgn0004395	Znf_CCCH, Znf_RING, LC, 1 CC	UNK	
31349	Vap-33-1	CG5014	FBgn0029687	MSP, LC, Transmembrane, 1 CC	VAPB	AMYOTROPHIC LATERAL SCLEROSIS 8
45012	Vha68-2	CG3762	FBgn0020367	ATPase_a_b_C, ATPase_a_b_N, ATPase_a_b_nl-bd, Ubiq_surface	ATP6V1A	
34906	wor	CG4158	FBgn0001983	Znf_C2H2, Znf_C2H2_sub, LC	-	
38294	yellow-g	CG5717	FBgn0041709	Royaljelly, LC, Signal peptide	-	
38295	yellow-g2	CG13804	FBgn0035328	Royaljelly, Signal peptide	-	
32367	yl	CG1372	FBgn0004649	Asx_hydroxyl_S, EGF_3, EGF_Ca_bd, EGF_Ca_bd2, EGF_like_reg, EGF_like, LDLR , LDL_rcptr_A, Ribosomal_S14, LC	-	
31939	Yp1	CG2985	FBgn0004045	signal peptide, Lipase, LC	-	
31938	Yp2	CG2979	FBgn0005391	Lipase, LC	-	
32339	Yp3	CG11129	FBgn0004047	CPase_L_D2, Lipase, Signal peptide, LC, 1 CC	ABCG5	SITOSTEROLEMIA
39764	Zn72D	CG5215	FBgn0017453	DZF, Znf_C2H2, LC	KIAA1086	

centrosome / candidate / novel — Human centrosome (Andersen et al., Nature 2003)

centrosome related phenotype / spindle phenotype — Goshima et al., Science 2007

described as RNAi-phenotype in Bettencourt-Dias et al., Nature 2004
Chlamydomonas centriole homologue in Keller et al., Curr Biol, 2005
Chlamydomonas flagellar and basal body homologue , Li et al., Cell 2004

z-score +4 / z-score +3 / z-score -3 / z-score -4 — FACS

low mitotic index
high mitotic index
phenotype in category
more than one main phenotype in category

* candidate protein identified by peptide mass fingerprinting

Supplemental Table 2

	centrosome number phenotype			centrosome morphology phenotype		
GeneSymbol	1	0	>3	large	fuzzy	small
CG6905	■					
CG7033	■					
crn	■					
fzy	■					
gammaTub23C	■					
Grip75	■					
alphaTub67C	■			■		
alphaTub84D	■			■		
alphaTub85E	■			■		
betaTub56D	■			■		
betaTub97EF	■			■		
mts	■			■		
Nup153	■			■		
Pp2A-29B	■			■		
RacGAP50C	■			■		
Hsc70-3	■			■		
ida	■			■		
Klp10A	■			■		
Grip71	■			■		
thr	■			■		
CG7456				■		
feo				■		
His3				■		
His4r				■		
mask				■		
Myb				■		
Pen				■		
stg				■		
Grip163	■	■		■		
Klp61F	■	■		■		
pav	■	■		■		
Grip128	■	■		■		
CG31716	■	■				
l(3)s2214	■	■				
Mer	■	■				
Lam	■	■				
CG11943		■				
CG15524		■				
CG3173		■				
eIF-4a		■				
Grip84		■				
l(1)dd4		■				
Rae1		■				
scra		■				
Sop2		■				
Act57B		■				
CG17286		■				■
cnn		■				■
cort						■
cup						■
Fib						■
lat			■			■
ald			■			
His2A			■			
nuf			■			
ncd			■		■	
Act79B					■	
asp					■	
aur					■	
Total	**28**	**20**	**5**	**26**	**4**	**6**

Significant phenotypes relating to centrosome number and morphology
are listed for MS identified and selected control centrosome associated proteins.

Supplemental Table 3

														FACS-analysis						Bjoerklund et al.								
gene-Name	CG-ID	FBgn-ID	gene-ID	HFA_ID	Length	Primer_f	Primer_r	Target_CG	Target_Name	#siRNAs	#siRNAs_Gene_specific	#siRNAs_efficient	#siRNAs_Transcript_specific	z-score	z-score	z-score	z-score	z-score	targeted FBgn	G1-pl	G2-pl	subG1-p	overG2-p	cell size pl	cell size p	p-value chi-test		
																										significance threshold 0,0001		
14-3-3epsilon	CG31196	FBgn0020238	42186	HFA16370	462	AATGGTGGAGGCCATGAAG	TTCAATGCCAAGCCCAAAC	CG31196	14-3-3epsilon	442	442	64	442+442+442+442	3,21	0,15	0,66	-0,74	-0,13	FBgn0020238	G1+	G2-		overG2-			0,698486	0,958253	4,59E-05
26-29-p	CG8947	FBgn0028967	39547	HFA08742	514	GAGATGAGGGGCTATAACAC	GAGTGACAGCGCCGTATA	CG8947	26-29-p	494	494	92	494	-0,62	0,72	2,65	-0,79	-0,36								0,338763	0,213532	0,804199
Act42A	CG12051	FBgn0000043	35526	HFA04835	500	CTTACTGAGGCTCCTTTGAA	GCCTCCATGCCGAGGAA	CG12051&CG5178&CG7478&CG10067&CG18290&CG4027	Act42A&Act88F&Act79B&Act57B&Act87E&Act5C	480	480&32&28&6&6&3	63	480&32&28&6+6&6+6&3+3+3+3	3,64	1,21	-0,18	-2,57	1,84								0,308132	0,963828	0,194804
Act57B	CG10067	FBgn0000044	37368	HFA04042	510	CCGTCCTGCTGACTGAG	AGGATTCCATTCCCAGGAAG	CG10067&CG4027&CG18290&CG5178&CG7478&CG12051	Act57B&Act5C&Act87E&Act88F&Act79B&Act42A	490	490&103&101&49&45&6	43	490+490&103+103+103+103&101+101&49&45&6	1,49	-2,00	-1,15	-2,30	3,78	FBgn0000044	G1+	G2-			G1 FSC-A-		1,32E-05	0,005264	0,003779
Act5C	CG4027	FBgn0000042	31521	HFA17723	500	GAGGCCCCGCTGAACC	CCGCAAGCCTCCATTCC	CG4027&CG18290&CG10067&CG5178&CG7478&CG12051	Act5C&Act87E&Act57B&Act88F&Act79B&Act42A	480	480&174&103&60&21&3	37	480+480+480+480&174+174&103+103&60&21&3	3,90	-1,01	-1,01	-1,56	1,52								0,311995	0,07724	1,53E-09
Act79B	CG7478	FBgn0000045	40444	HFA11604	505	ACCGAGGCTCCCTTGAA	TGCCGCAGGACTCCAT	CG7478&CG5178&CG10067&CG18290&CG12051&CG4027	Act79B&Act88F&Act57B&Act87E&Act42A&Act5C	485	485&89&45&39&28&21	32	485&89&45+45&39+39&28&21+21+21+21	1,40	0,61	-0,05	-1,20	1,19								0,143457	1,35E-05	0,000875
Act87E	CG18290	FBgn0000046	48632	HFA14104	NA	TGTGTGACGATGAGGTTGC	ACCCGGAGTCGAGGACA	NA	NA	NA	NA	NA	NA	1,32	0,09	-0,96	-1,45	3,28								0,575396	0,263855	0,830808
Act88F	CG5178	FBgn0000047	41885	HFA14105	499	GACCGAGGCTCCACTGA	CGACTCCATGCCCAGGA	CG5178&CG7478&CG18290&CG4027&CG10067&CG12051&CG4013	Act88F&Act79B&Act87E&Act5C&Act57B&Act42A&Smr	479	479&89&68&60&49&32&1	27	479&89&68+68&60+60+60+60&49+49&32&1+1+1	2,02	0,15	-1,10	-1,46	2,82								0,048898	0,445147	0,271699
alpha-Spec	CG1977	FBgn0003470	38231	HFA08704	510	CCTGAAGGCCAACGAAGT	AAACGCTGCAGGTCGTAC	CG1977	alpha-Spec	490	490	27	490	-0,72	-0,83	0,31	1,49	0,31								0,194207	0,356215	0,128536
alphaTub67C	CG8308	FBgn0004236	39130	HFA11321	500	TTGCAGGGATTCCTCATCTT	GATTCGAAACAGGCATTGGT	CG8308&CG2512	alphaTub67C&alphaTub84D	480	480&6	83	480&6+6	5,18	-1,77	0,82	-0,10	0,22								8,09E-35	8,45E-31	0,117484
alphaTub84B	CG1913	FBgn0003884	40848	HFA12622	507	CTCGTTCGGTGGAGGTAC	CGGGGATCGCACTTGAC	CG1913&CG2512&CG9476	alphaTub84B&alphaTub84D&alphaTub85E	487	487&104&15	24	487&104+104&15	-0,60	-0,59	-0,40	1,96	-0,12	FBgn0003884			subG1+				0,922508	0,014677	0,205436
alphaTub84D	CG2512	FBgn0003885	40904	HFA12623	507	TTCGGTGGAGGTACCGG	GTGACGGGGATCCACCTT	CG2512&CG1913&CG8308	alphaTub84D&alphaTub84B&alphaTub67C	487	487&100&6	41	487+487&100&6	3.46	-1.72	-0.21	0.22	0.68	FBgn0003885			subG1+				1.84E-60	3.07E-21	0.184784
alphaTub85E	CG9476	FBgn0003886	41183	HFA16899	511	CTGTGGTCGAGCCATACAA	CCCGTGGGACACCAGTC	CG9476&CG1913&CG2512&CG8308	alphaTub85E&alphaTub84B&alphaTub84D&alphaTub67	491	491&25&6&3	49	491&25&6+6&3	6.49	-2.38	-0.69	-0.09	0.57	FBgn0003886		G2-	subG1+				3.67E-51	4.08E-52	0.312101
alt	CG18212	FBgn0038535	42127	HFA15315	488	CCAGGCCAACAACAAAACC	CAAGCGTCAACTTGTCATTC	CG18212	CG18212	468	468	97	468+468+468+468+468+468	-0,22	0,38	-0,53	1,62	-2,17								0,056017	0,039835	0,968347
Apc	CG1451	FBgn0015589	44642	HFA14114	488	ATGCAGCGGAAGCCAAC	TGTACGGCTGGCCCAAC	CG1451	Apc	468	468	78	468	-0,24	0,70	1,05	0,48	-0,49								0,752739	0,593229	0,060969
Apc2	CG6193	FBgn0026598	42871	HFA14115	496	TGCGACCCTCAACAGTCA	GAGTCGAAGCGACTGAAG	CG6193	Apc2	476	476	118	476	-1,39	0,10	1,49	0,50	0,22								0,203553	0,602787	0,259861
aralar1	CG2139	FBgn0028646	43616	HFA16901	509	CGAGGGATTCATGGGTCTC	ATCGGGCAACCACCTGAA	CG2139	aralar1	489	489	36	489+489+489+489	-0,67	-0,60	-0,27	1,01	0,44								0,488145	0,85891	0,704608
arm	CG11579	FBgn0000117	31151	HFA18738	510	GACTACGAGAAGCTTCTGT	TGGTGGATGCAATAGCTTTAC	CG11579	arm	490	490	65	490+490+490+490+490	-0,77	-0,75	-0,87	1,31	0,76								0,904635	0,73205	0,998247
Arp53D	CG5409	FBgn0011743	36879	HFA05923	505	GGATTTGCCGGCTCTACT	CACCTCCTGACCCAGCAA	CG5409	Arp53D	485	485	99	485	-1,00	-0,56	0,72	1,63	0,06								0,239499	0,139616	0,416079
asp	CG6875	FBgn0000140	42946	HFA16903	508	ACCCGAGTCATGGAGGTAA	AGCGCTGGATGGTGATAA	CG6875	asp	488	488	88	488	-1,42	-0,13	1,74	0,57	0,32								0,000136	6,59E-05	4,59E-05
ATPsyn-beta	CG11154	FBgn0010217	43829	HFA17194	508	CTCCTGGCTCCATACGC	ATATGGCCTGAACAGAAGTAAT	CG11154	ATPsyn-beta	488	488	114	254+488	1,62	-1,08	-0,19	1,22	0,04								0,244872	0,277138	0,021096
Atx2	CG5166	FBgn0041188	41883	HFA15727	434	CAGTACCGCAACCAATCTC	GGTGAAGTGTTGCTCGGG	CG5166&CG4013&CG32548&CG4744&CG12348&CG6043&CG32133& CG8118&CG5461&CG32778&CG13109&CG14351&CG9355&CG32466 &CG14307&CG32532&CG31243&CG1343&CG7958&CG14023&CG969 6&CG2083&CG16902&CG10107&CG5058&CG10555&CG14459&CG14 441&CG15365&CG15319&CG2530&CG30497&CG32139&CG12071&C G10543&CG7847&CG5488&CG7368&CG17724&CG33205&CG6824&C G9533&CG32767&CG2904&CG31761&CG7391&CG33261&CG17762& CG2368&CG32904&CG15532&CG32365&CG31738&CG4026&CG5466 &CG8127&CG30483&CG12072&CG32180&CG33141&CG11516&CG97 55&CG18023&CG12720&CG10572&CG31369&CG30361&CG33106&C G33473&CG15504&CG32062&CG14650&CG33980&CG1689&CG3696 &CG10325&CG33516&CG32688&CG1130&CG12653&CG3075&CG677 5&CG9653&CG3851&CG7951&CG30089&CG33183&CG32494&CG325 60&CG32717&CG13222&CG11194&CG18208&CG4722&CG32045&CG 32306&CG17888&CG9850&CG11711&CG3936&CG11172&CG17228&C G3497&CG11354&CG4059&CG5053&CG3905&CG6619&CG3327&CG1 3598&CG32394&CG6964&CG15470&CG3754&CG1775&CG11505&CG 2252&CG10732&CG18250&CG3638&CG1070&CG8639&CG17689&CG 10082&CG11352&CG11203&CG4297&CG11641&CG31302&CG10348& CG12236&CG11294&CG4136&CG32432&CG6376&CG3166&CG12690 &CG7015&CG15478&CG5905&CG5732&CG12772&CG32130&CG5674&	3&mam&bun&CG32778&tai&CG14351&dy&rn&fru&CG 32532&cpo&Sp1&tna&CG14023&dom&CG2083&Hr4& CG10107&grh&CG10555&CG14459&CG14441&CG15 365&nej&corto&CG30497&Sox21b&CG12071&CG1054 3&sr&B- H2&CG7368&CG17724&CG33205&ovo&rut&CG32767 &ec&bru- 2&Clk&Trl&tomosyn&psq&seq&hdc&CG32365&CG317 38&IP3K1&CG5466&Eip75B&Prosap&wts&Eip74EF&s ns&Ptp99A&pum&Eip78C&CG12720&Cdk8&PQBP- 1&mXr&mask&luna&dmrt99B&CG32062&CG14650&C G33980&lz&kis&abd- A&dpr3&Hk&scrt&btd&CG3075&rg&brk&odd&sima&CG 30089&Hr46&CG32494&CG32560&sdt&CG13222&Hey &CG18208&bib&fry&CG32306&Pdp1&CG9850&Mob1& N&NFAT&pros&Su(H)&Lim1&ftz- f1&CG5053&Su(z)2&CG6619&E23&sba&CG32394&Gu g&CG15470&CG3754&Med&CG11505&fs(1)h&CG107 32&Dg&CG3638&Alh&Cirl&CG17689&CG10082&jim& CG11203&CG4297&CG11641&CG31302&CG10348&C G12236&CG11294&CG4136&CG32432&E2f&aop&CH ES-1- like&CG7015&CG15478&Nep1&CG5732&CG12772&C G32130&CG5674&Magi&nAcRalpha- 7E&vvl&CG14995&bs&peb&CG17271&srp&CG13921&l md&Scr&CG33975&CG32606&CG11769&CG8924&Ets 96B&Samuel&CG32479&VAChT&cas&CG11940&CG1	414	438&116&90&52&38&37&34&33&32&32&31& 28&28&28&27&26&25&25&23&23&23&22&2 2&22&22&21&20&20&19&19&19&18&18&18 &18&18&18&17&17&17&17&16&16&16&15& 15&15&15&15&14&14&14&14&14&14&13&13 &13&13&12&12&12&12&12&12&12&12&12& 12&12&11&11&11&11&11&11&11&11&10&10 &10&10&10&10&10&10&10&10&10&10&9&9 &9&9&9&9&9&9&9&9&9&9&9&9&9&9&9&9& 9&8&8&8&8&8&8&8&8&8&8&8&8&8&8&8&7 &7&7&7&7&7&7&7&7&7&7&7&7&6&6&6&6& 6&6&6&6&6&6&6&6&6&6&6&6&6&6&6&6&6 &6&6&6&6&6&6&6&6&6&6&6&6&6&6&6&6& 6&6&6&6&6&6&6&6&6&6&6&6&5&5&5&5 &5&5&5&5&5&5&5&5&5&5&5&5&5&5&5& 4&4&4&4&4&4&4&4&4&4&4&4&4&4&4&4&4&4 &4&4&4&4&4&4&4&4&4&4&4&4&4&3&3&3& 3&3&3&3&3&3&3&3&3&3&3&3&3&3&3&3&3 &3&3&3&3&3&3&3&3&3&3&3&3&3&3&3&3& 3&3&3&3&3&3&3&3&3&3&3&3&3&3&3&3&3 &3&3&3&3&3&3&3&3&3&3&3&3&3&3&3&2& 2&2&2&2&2&2&2&2&2&2&2&2&2&2&2&2&2 &2&2&2&2&2&2&2&2&2&2&2&2&2&2&2&2& 1&1&1&1&1&1&1&1&1&1&1&1&1&1&1&1&1 &1&1&1&1&1&1&1&1&1&1&1&1&1&1&1&1& 1&1&1&1&1&1&1&1&1&1&1&1&1&1&1&1&1 &1&1&1&1&1&1&1&1&1&1&1	43	+0+9+0&37+37+37+37&34&25+1+25&3+0+28+0+ 0+28&32&31&28&28&26+20&14+0+0+2+0+0+2+0 +0+14+0+14+0&26&15+15+9+15+9+15&25+25&2 3+23&23&0+23+23&22&22&22+22+0&3+12+12+0 +15+15&21&20&20&19&19&19&10+10+10&18&1 8+18&18+18+18&14+14&3&17&14&1+1+1+0+11+ 11+1+11&17+17+17+17&16&16+16&16&6+6+6+6 &15+15+15+15+15+15&0+15+0+0+15+15+15+15 +0&0+15+0+0&9+9+9+9+9+9+9+9+9+9+9+9&14& 6+6+6&6&0+14&14&14&0+2+7+0&10&13&4+4+4 +4&11+11&0+9+0+0+0&12+12+3+12+3&1+7+7&1 2&12&3&0+0+12&12+12&3&12&11+11&11&1&7& 11+11&11+10&8&11+11&10&10&10&10+10+10&1 0&10&10&10&4+0+0&10&10&0+3+4+4+7+0&9&9 &1&9&9+9&0+6+0+6&6+0+0+0+0+0+0+3&2+0&0 +0+0+4&9&9&6+6+6&9&4&0+3&9&9&9&9+9+0&5 +5&8&8+8+8+8&8&8&8+8&0+8+8&0+0+0+0+8&8 +0&0+0+3&8+8+8+8&0+0+8+0&8&2+8&0+8&7+7 +7&7&7+7&7&7+7+7&7&7+7&7&7&7&7+7+7&7+7 &7&7&6&6+6&6&6&6+0+0+0&6+6+6&6&6&6&6+6 +6+6&3&6+6&6+0&6+0+6&6+6&6+6&6+6+6&6&6 &6&6+6&6+6&6&6&6&6&6+6&6&6&0+0+0+0+6&6 &6&6&6&6&1+0+0+0&6&6+0&6&6&0+0+6+0+0&6 &6&6&0+0+0+0+6+6+0+0+0+0+0+6+6+0+0&6+6+ 6&6&6+6&4&5+5+5+5+5&5&5+5&5+5&5&0+2+0+ 2+0+0+0+0+0+0+0+0+0&5&0+0+5&5&5&5&5+ 5&5&5+5&5&5+5&5+5&5&5&5&4&4+0+0&4+4+4&	1,32	-3,43	-2,47	3,43	0,89								0,859444	0,219973	0,591303
aur	CG3068	FBgn0000147	41446	HFA16905	509	CCCAGAAGCCGAAGAAGA	TGTCATGCGCATGGAGTT	CG3068	aur	489	489	63	489	0,41	-1,14	-0,37	1,82	0,11								0,153933	1,92E-09	7,71E-32
baz	CG5055	FBgn0000163	32703	HFA20309	500	GAAAGACGTGCTCGAATCT	AGCACTGCCACCACCTC	CG5055&CG8184	baz&CG8184	480	480&1	87	480+480&1	0,18	-0,08	0,19	-2,00	2,08								0,663009	0,052926	0,943724
BcDNA:GH0877	CG10345	FBgn0027562	42017	HFA14138	569	GTCTACAAGGAGGTCTTGAG	TCCTCATTGTACTGCCAACC	CG10345	CG10345	549	549	134	474	0,57	-0,82	0,20	1,58	-0,17								0,641993	0,215085	0,803042
bel	CG9748	FBgn0000171	45826	HFA16555	500	CACCGGTGCAGAAGCAC	GGTTGGCGGCATGTTTAG	CG9748&CG10777&CG3131	bel&CG10777&CG3131	480	480&9&1	52	480&9&1	0,76	-0,07	-1,07	1,14	-0,78	FBgn0000171	G1-						0,540001	0,694765	0,493113
betaTub56D	CG9277	FBgn0003887	37238	HFA07583	480	ACTGGCTCCGGTATGGG	GGCGGCCATCATGTTCTT	CG9277&CG9359&CG3401	betaTub56D&betaTub85D&betaTub60D	460	460&21&18	22	460+460+460+460&21&18	4,41	-1,97	0,30	-1,28	1,70	FBgn0003887			subG1+	overG2-	G1 FSC-A	G2 FSC-A	2,96E-22	2,18E-32	0,035971
betaTub97EF	CG4869	FBgn0003890	43359	HFA15666	131	CAACTCGACCGCCATCC	TCTCGGCCTCGGTGAAC	CG4869&CG3401&CG9277	betaTub97EF&betaTub60D&betaTub56D	111	111&33&32	11	111&33&32+32+32+32	6,18	-0,40	1,45	-1,53	-0,23	FBgn0003890			subG1+				5E-30	8,18E-16	4,42E-26
BicC	CG4824	FBgn0000182	34946	HFA02005	516	CAAAATCTACGAGGCCCG	CCCGGCAATTGGGCATAC	CG4824	BicC	496	496	56	496+496+496	-0,53	0,74	0,39	0,44	-1,21								0,051382	0,058677	0,871756
BicD	CG6605	FBgn0000183	35051	HFA02006	518	CGAACTTAAATCTCCTGACG	AGATGTGCGTAAGAGTTTGA	CG6605	BicD	498	498	110	498	0,60	-1,64	-0,75	-1,39	3,06								0,759436	0,423356	0,185732
blw	CG3612	FBgn0011211	37617	HFA04675	493	CATCGACACCATCATCAACC	GATGACGTTGGTTGGAATGTA	CG3612	blw	473	473	29	473	-0,10	-0,88	0,88	1,02	0,39								0,07426	0,277086	0,35
bnk	CG1480	FBgn0004389	43687	HFA16912	506	ACGGAGCCGGGTAATGG	ACGCCCATGGCTGGTAC	CG1480	bnk	486	486	65	486	-0,62	-0,19	-0,13	-1,92	4,78								0,056574	0,874938	0,003491
bol	CG4760	FBgn0011206	39049	HFA11329	134	CCGAGGCTGATCTAACCC	CAGTCTTTGCGCCTCCT	CG4760	bol	114	114	10	114+114+114+114	-1,12	-2,13	-0,48	3,48	0,21								0,818788	0,000541	0,852688
bor	CG6815	FBgn0040237	53565	HFA16915	512	GCTGGTACTGTTATCGGTG	GACCAGTCGAACACCTTGT	CG6815	bor	492	492	46	492	-0,36	-0,49	0,21	1,53	-0,09								0,395611	0,618864	0,885683
brat	CG10719	FBgn0010300	35197	HFA03497	504	AAGACCGAATTGCTCAAGG	CGCCTGCAGCTGTTGA	CG10719	brat	484	484	51	484+484+484	-0,21	-1,11	-0,97	1,55	0,66								0,215772	0,003837	0,000414
brm	CG5942	FBgn0000212	39744	HFA11330	520	GTTTCGCTGTACAATAACAATC	ATGTGGAGCAGGACTTAAAG	CG5942	brm	500	500	140	500+500+500+500	-1,35	-0,74	-0,88	2,37	0,07								0,012307	0,147839	0,401367
Cas	CG13281	FBgn0022213	35016	HFA03287	508	TGGTGATTTCAATGTCATCAA	CTTGGTGTGCAAACTTGTCT	CG13281	Cas	488	488	139	488	0,23	-1,31	-1,54	1,73	0,84	FBgn0022213	G1-						0,943945	0,548078	0,704608
Cctgamma	CG8977	FBgn0015019	42029	HFA16602	509	CCAAGGTGGAGAAGATCCC	CTCCTTGCACTCCGTCAC	CG8977	Cctgamma	489	489	60	489+489	-0,55	1,36	-0,74	0,23	-1,20								0,062463	0,195644	0,947152
cdc2	CG5363	FBgn0004106	34411	HFA03504	577	GTCTGTTTGGAGGATGTTTTG	AGTCGGGTAGCGAAGTAAC	CG5363	cdc2	557	557	165	482	1,57	-3,66	-1,99	-5,37	7,57	FBgn0004106	G1-	G2+	subG1+				0,006336	0,002603	4,81E-08
cdc2c	CG10498	FBgn0004107	42453	HFA16921	185	TATGCGCCGCTCCTTG	CGTGCGCCTCGTGTTC	CG10498	cdc2c	165	165	41	165+165	0,98	8,95	0,35	-7,94	-0,78	FBgn0004107	G1+	G2-			G1 FSC-A+		0,131686	0,860436	0,352304
CG10077	CG10077	FBgn0035720	38756	HFA09691	504	GCACCACCTCGTTGAAGA	GGGCAGCCACATCGGT	CG10077&CG10279	CG10077&Rm62	484	484&13	74	449+484&13+13+13+13+13+13	-0,45	1,39	-0,64	-0,90	0,67								0,056138	0,550472	0,998247
CG10732	CG10732	FBgn0036365	39513	HFA09790	493	CTTACCCCAACACCCACCC	TGGGGGGCGGCATGTA	CG10732&CG12330&CG10847	CG10732&CG12330&enc	473	473&6&3	65	473+473&6&3+3	-0,66	-0,45	-0,42	1,97	-0,20								0,261549	0,161621	0,023114
CG10777	CG10777	FBgn0029979	31707	HFA17755	506	AGACTATGGACATCTGTGCA	TCTCCACAAAGACGATAATTTT	CG10777&CG9748	CG10777&bel	486	486&9	108	486&9	-0,44	0,29	-0,15	1,72	-2,21								0,226379	0,709761	0,659346
CG10864	CG10864	FBgn0038621	42222	HFA14273	511	CCACGAACGATGTACTGAG	AAGTCGCCAAATCCAATCTT	CG10864	CG10864	491	491	81	491	0,33	-0,19	-1,32	0,72	0,52								0,138283	0,561127	0,587623
CG11092	CG11092	FBgn0027537	32350	HFA19344	509	GTATTGTTGGCGTGTGATCC	CGTCCGTTCTCGGATTTAA	CG11092	CG11092	489	489	77	489	0,94	0,71	0,64	-0,32	-0,18								0,262163	0,838395	0,021096
CG11148	CG11148	FBgn0039936	43842	HFA17202	514	ACTTTCAATTACACCCCATAAG	AATGAAATTATTAGCATCCAGTAA	CG11148	CG11148	494	494	174	494+494+494	5,76	2,96	3,28	-5,26	-0,57								0,932675	1,68E-25	0,000231
CG11763/micr	CG11763	FBgn0033522	36102	HFA06079	263	TGGAGAACGTCGAAGAGG	ATGTGGTGAATTCTCGCG	CG11763&CG11873&CG5058&CG32717&CG4807&CG5580	micr&CG11873&grh&sdt&ab&sbb	243	243&2&1&1&1&1	22	243+0+243&2&0+1+1+0+1+1&0+0+1+1+1+0&1+1	-0,82	-0,15	0,39	0,91	0,31								0,38731	0,418213	0,957874
CG11943	CG11943	FBgn0031078	33002	HFA19432	505	CCTGGCCGCCATTAAGA	CAACAGCACTACGGAGTTC	CG11943	CG11943	485	485	77	485+485	-0,29	-1,18	-0,93	0,86	1,14								2,73E-09	0,423985	0,148322
CG12503	CG32479	FBgn0052479	38103	HFA08282	513	GGACGGATGCGCGAAC	CTGGTGCCAGATCTGGGT	CG32479	CG32479	493	493	24	493	0,10	-1,09	-0,21	1,36	0,48								0,46852	0,115427	0,259861
CG14065	CG14065	FBgn0039579	43372	HFA14728	491	CCGTGGACAACAAAGAGAAC	ATCCTTGCGATCCTTGTGT	CG14065&CG32245	CG14065&CG32245	471	471&2	24	471&2+2+2	1,11	0,71	0,93	-0,13	-0,43								0,849652	0,985291	0,185732
CG14215	CG14215	FBgn0031052	32971	HFA19571	503	TGGAGCCCTACCAAAAGAC	CGCCTGGAGGAAATTTGG	CG14215	CG14215	483	483	92	483	1,12	-2,31	-0,78	1,63	1,02								0,806979	0,143015	0,051806
CG14235	CG14235	FBgn0031066	32989	HFA19590	227	CGCCTACAAGCTGGAGA	AGATGCGGCCGGGGA	CG14235	CG14235	207	207	9	207+207+207	0,50	-2,04	-0,84	0,83	1,56								2,99E-36	0,060452	1,15E-08
CG14309	CG14309	FBgn0038611	42212	HFA14788	511	CTGCCCGATGTCAATCTG	AGTCGAAAAGGGGCTTATTC	CG14309	CG14309	491	491	107	491	-0,42	-0,26	0,61	1,26	-0,21								0,826439	0,06003	0,463229
CG14391	CG14391	FBgn0038078	41567	HFA14850	398	CCATACCAGAGGCTCAGTA	TCATCTGAGATAGCTAGTGAC	CG14391	CG14391	378	378	72	378	-0,22	-0,04	0,49	0,86	0,02								0,76069	0,412839	0,185732
CG14682	CG32922	FBgn0037820	326242	HFA14906	499	ATAACGAAATCTTCGGAAATAA	GGCCGGGCAGTTTAACC	CG14681&CG33676	CG14681&Skeletor	479	479&479	60	444+0&444	-0,07	-1,36	-0,28	2,36	0,00								0,00061	0,074234	0,885683
CG15092	CG15092	FBgn0034388	37164	HFA06521	341	TCTTCTGCTCCCTTGGAAC	TCCGAATGGCGGACAAAC	CG15092	CG15092	321	321	40	321	-0,51	0,77	1,19	-2,01	2,60								0,011795	0,903578	0,471888
CG15350	CG15350	FBgn0030044	31785	HFA18034	515	CCGCCACGCTTTGTGAA	TCCACGAACTTGTAGTCCTC	CG15350	Cp7Fb	495	495	84	495	-0,89	-0,72	-0,01	-1,07	2,36								0,930805	0,188511	0,992105
CG15524	CG15524	FBgn0039731	43555	HFA15061	504	TTGAACACCGTACTCTTCTAC	CTTGAGGTCCTCGATTTTGT	CG15524	CG15524	484	484	131	484	-0,15	-0,43	0,15	1,33	-0,04								3,7E-11	0,790068	0,01232
CG17255	CG17255	FBgn0030205	31976	HFA18123	503	GGCAATAAGCGGGTAAGTC	TGTTGCTTGCCATATTCCTC	CG17255	CG17255	483	483	15	483+483	0,66	-0,34	1,01	0,68	-0,07								0,389522	0,763266	0,185732
CG17280	CG17280	FBgn0034877	37728	HFA04289	198	GAAGCGCCTGTCCTTCTT	GGCAGGGCGTTAACGTG	CG17280	CG17280	178	178	6	178	-0,84	0,49	2,00	0,35	-0,15								0,650496	0,122695	0,373274
CG17286	CG17286	FBgn0027500	39850	HFA09682	512	CATCCGCAAATCACCATCA	GTGGAACTGGCCTCACTAC	CG17286	CG17286	492	492	42	492	-0,67	-0,72	-0,17	1,99	-0,02								6,38E-31	7,84E-14	0,591303
CG18397	CG18397	FBgn0032723	35149	HFA02669	306	CTGTGGAGGGTCCTTTGTC	AGTCCTTGCTGAGGAACTC	CG18397	CG18397	286	286	52	286	-0,34	-1,14	0,92	1,59	0,27								0,046045	0,000244	0,675888
CG18610	CG30122	FBgn0050122	37146	HFA06776	484	GACAATCGCCGCAACTAC	CGCCTACAGCGGTGTTA	CG30122&CG15335&CG15307&CG32464&CG1412&CG5953&CG1207 5&CG11473&CG3606&CG2187&CG34050&CG32423&CG10272&CG32 541&CG17364&CG15028&CG6883&CG9983&CG2961&CG1143&CG22 56&CG10328&CG6534&CG17894&CG32972&CG17786&CG12502&CG 12726&CG15154&CG32694&CG13363&CG15225&CG15544&CG11112 &CG33547&CG13003&CG32434&CG1689&CG16752&CG9850&CG321 59&CG13131&CG9888&CG5812&CG3588&CG13535&CG5595&CG522 5&CG15532&CG6824&CG9559&CG10353&CG15319&CG7915&CG584 1&CG11219&CG7129&CG6305&CG6525&CG31247&CG9425&CG3982 &CG8502&CG32550&CG5172&CG8944&CG3800&CG11866&CG3884& CG30458&CG4038	CG30122&CG15335&CG15307&l(3)82Fd&RhoGAP19 D&CG5953&CG12075&CG11473&caz&CG2187&CG34 050&CG32423&gpp&CG32541&CG17364&CG15028&t rh&Hrb98DE&lpod&CG1143&CG2256&nonA- l&slou&cnc&CG32972&CG17786&CG12502&CG12726 &Socs36E&CG32694&Suv4- 20&CG15225&CG15544&CG11112&Rim&CG13003&si z&lz&CG16752&CG9850&CG32159&CG13131&Fib&G CR(ich)&CG3588&CG13535&Sce&CG5225&hdc&ovo& fog&CG10353&nej&Ect4&mib1&PIP82&l(3)05822&CG6 305&CG6525&tinc&CG9425&CG3982&CG8502&CG32 550&CG5172&CG8944&CG3800&CG11866&CG3884& CG30458&CG4038	464	466&17&17&12&11&10&10&10&9&9&9&9&8 &8&8&8&7&7&7&6&6&6&6&5&5&5&5&5&5& 4&4&4&4&4&4&4&4&4&4&4&3&3&3&3&3&3&3 &3&3&3&2&2&2&2&2&2&2&2&1&1&1&1&1& 1&1&1&1&1&1&1&1	33	466&17&17&0+0+0+0+0+0+0+0+12+0+0+0+0+ 0&11&10+10&10+10&10&9+9&9&9&0+0+9+0&8+ 8+8+8&8&8+8&0+7&7+7&7+7+7+7+7&6&6&6& 6&5&0+0+5+0+0+5+0&5+5&5&5&5&5+5&0+0+4+ 0&4&4&4&4+0&4&4&0+0+4&4&4&3+0&3&3&3&3 &0+0+3+0&3&3&3&0+3+3&2+2+2+2&2+2&2+2&2 &0+2&2&2&2+2&1&1&0+1+1+1&1+1&1&1+1&1&1 +1&1+1&1&1&1+0&1&1	1,53	-1,46	-0,20	1,15	0,45								0,872268	0,598076	0,861346
CG18811	CG18811	FBgn0042134	59172	HFA10346	520	GCTCCATCCCTGGAACATC	CGACATGGTTGGGCTGTT	CG18811	CG18811	500	500	44	500	0,29	-0,81	-0,70	1,30	0,13								0,005411	0,008328	0,03528
CG1962	CG1962	FBgn0032876	35330	HFA02704	494	TGACGATCGCAGCATACT	GGCGATTACGGAAATGAGAT	CG1962	CG1962	474	474	133	474+474+474	-0,59	-0,39	-0,59	0,01	2,06								0,266538	0,310669	0,089409
CG2158	CG2158	FBgn0033264	35784	HFA06827	510	CGTGAAAGCGTTGCTGA	CTTTTTAGTGGTCGTATCCTTT	CG2158	CG2158	490	490	118	490	0,51	-0,02	-0,26	0,29	0,31								0,084199	0,000175	1,42E-05
CG30159	CG30159	FBgn0050159	35611	HFA04981	500	GCTGGCCGTGGCCTAT	CCTTTTCCGCTGTGGTCT	CG30159	CG30159	480	480	33	480+480	-0,36	-0,78	0,94	0,85	0,19								0,032224	0,787037	0,134492
CG31716	CG31716	FBgn0051716	34416	HFA02831	514	CGCGATTCCATCGTCATC	CTTTTGTCTTATTGTACTCTCG	CG31716	CG31716	494	494	92	494+494+494+494+494+494	-0,47	-0,32	0,73	0,58	-0,08								3,97E-06	0,057017	0,871756
CG3173	CG3173	FBgn0034964	37840	HFA04343	495	GCACTCTGGCGACTTTGA	GGCATGTTGCTGTTGGAATA	CG3173	CG3173	475	475	138	475	-0,65	1,90	-0,03	-1,10	0,27								1,97E-05	0,914559	0,021096
CG31802	CG31802	FBgn0051802	318949	HFA02459	513	CAAGTCCCCAACTGTCGG	AGAAGGAAAAGGCCTTCATC	CG31802	CG31802	493	448	131	448	-1,35	-0,74	1,10	1,80	0,10								0,632133	0,036896	0,266829
CG32137	CG32137	FBgn0052137	39537	HFA10272	435	AGCTAGCGAATGCTATAACC	CAATTTTGCTCGAATAGTCCT	CG32137&CG9907&CG3992&CG11502&CG10605&CG4491&CG4119& CG6824&CG32529&CG18210&CG8787&CG18024&CG10897&CG9575 &CG2272&CG1921&CG5353&CG33558	CG32137&para&srp&svp&caup&noc&CG4119&ovo&C G32529&CG18210&Asx&SoxN&tou&Rab35&slpr&sty& Aats-thr&CG33558	415	415&2&2&2&2&2&2&2&2&2&2&2&2&1&1&1& 1&1	60	415+165&2+2+2&2+2+2&2+0+2&2&2&2&0+2+ 2&2+2+2&2&2+2&2&0+0+2+0&1&1&1+1&0+0+1& 1	-0,83	0,04	-0,10	1,56	-0,29								0,137786	0,172542	0,631586

Supplemental Table 4

Centrosomal phenotype						
	1	0	>3	large	fuzzy	small
CEP192		■				■
CENPJ	■				■	
CNOT4					■	
NUP205					■	
ANLN			■			

Experimental contributions:

Conception: B.M.H. Lange, H. Lehrach, M. Boutros
Mass spectrometry analysis: J. Gobom, N. Gustavsson, E. Mirgorodskaya
Production of dsRNA, FACS analysis, Supplementary Table 3: S. Steinbrink
Parts of cell culture (RNAi) and microscopic phenotype evaluation: K. Habermann, B.M.H. Lange, V. Lehmann

A Centrosome-Independent Role for γ-TuRC Proteins in the Spindle Assembly Checkpoint

Hannah Müller, Marie-Laure Fogeron, Verena Lehmann, Hans Lehrach,
Bodo M.H. Lange

Science, 2006. 314, pages 654-656, Publication available online:
DOI: 10.1126/science.1132834

Abstract

The spindle assembly checkpoint guards the fidelity of chromosome segregation. It requires the close cooperation of cell cycle regulatory proteins and cytoskeletal elements to sense spindle integrity. The role of the centrosome, the organizing center of the microtubule cytoskeleton, in the spindle checkpoint is unclear. We found that the molecular requirements for a functional spindle checkpoint included components of the large γ-tubulin ring complex (γ-TuRC). However, their localization at the centrosome and centrosome integrity were not essential for this function. Thus, the spindle checkpoint can be activated at the level of microtubule nucleation.

Experimental contributions:

Conception: B.M.H. Lange, H. Lehrach
Tandem-Affinity-Purification: M-L. Fogeron
Immunopreciptitation: D. Weichart
Parts of cell culture and microscopy: V. Lehmann

4 Discussion

In addition to its function in microtubule nucleation, the centrosome has been implicated in signalling pathways regulating cell cycle progression, differentiation, cell death and stress (Lange, 2002). To better understand the molecular basis of the connection of the centrosome to these pathways, the aim of this work was to identify the centrosomal proteome and to analyse its function. In the following sections, the obtained results will be discussed in relation to previously published work.

4.1 Comparison of centrosome isolation methods

The development and application of a new efficient centrosome isolation method was the prerequisite for the proteomic analysis of the centrosome. Centrosome isolation techniques from mammalian tissue culture cells (Mitchison & Kirschner, 1984; Moudjou & Bornens, 1994), calf thymus (Komesli *et al*., 1989), yeast (Rout & Kilmartin, 1990) and Spisula solidissima (Palazzo & Vogel, 1999) resulted in a 600-fold to 3000-fold enrichment of centrosomes. Previous isolation in sucrose gradients from *Drosophila* embryo extract resulted in 1000-fold enrichment of centrosomes in relation to total protein concentration, a total number of 0,5-2,5 x 10^7 centrosomes per gram embryos and 10% estimated yield (Moritz *et al*., 1995), taking into account that one embryo is 9,5 μg and contains 2500 centrosomes (Ashburner, 1989). Using the same isolation technique as described in Moritz *et al*. (1995) we calculated 250-fold enrichment with the total number of 10 x 10^7 centrosomes present in the isolated fraction and a 25% yield. The difference between the two calculations of centrosomal enrichment could be due to the fact, that Moritz *et al*. determined the enrichment in the centrosomal peak fraction, which is not representative for the complete preparation. The total numbers of centrosomes resulting from both preparations is similar, indicating comparable quantities of isolated centrosomes. Application of the immunoisolation technique established by Lange *et al.* (2000) and optimized as part of this thesis (Lehmann *et al*., 2005) results in a further 10-fold increase per ml. Therefore, immunoisolation results in an overall 2500-fold enrichment of centrosomes from embryo extract as analysed by quantitative immunofluorescence microscopy, western blotting and SDS-PAGE, showing reduction of contaminations like actin and enrichment of centrosomal proteins like Cnn, Dgrip84 and γ-tubulin in the immunoisolated preparations. In conclusion, we achieve higher enriched centrosomal

preparations by applying immunoisolation compared to isolation methods previously used to isolate centrosomes from *Drosophila* embryos.

4.2 Centrosome proteome analysis in *Drosophila*

Different estimates have been made for the total number of centrosomal proteins. It has been speculated that approximately 100 proteins are associated with the *Drosophila* centrosome (Moritz *et al*., 1995). More recently, the proteomic analysis of the human centrosome identified as many as 500 proteins (Andersen *et al*., 2003) while around 100 proteins (60 in interphase centrosome) have been identified with various methods (reviewed by Schatten, 2008). Database searches provide a list of only 31 proteins that localise to the centrosome in *Drosophila*. In our preparations we identified 260 proteins, of which 17 were previously known centrosomal proteins, thereby confirming the reliability of our isolation and mass spectrometry analysis.

In addition, immunofluorescence microscopy of GFP- and TAP-tagged expressed Cort, CG11148 and CG17286 and in SL2 cells has verified centrosomal localisation for three identified candidate proteins. Cort localises to one of the two centrioles in interphase, CG11148 to the PCM in mitosis and CG17286 to both centrioles. Recent work classified CG17286 (Spd-2) as a centriolar protein (Dix & Raff, 2007), corroborating the accuracy of our localisation studies. Centrosomal localisation of Cort and CG11148 has not been reported before. The identification of both centriolar and PCM proteins denotes (a) that intact centrosomes have been isolated and (b) the sensitivity of our approach in identifying low abundant centriolar proteins. To confirm an association with the centrosome for further candidate proteins, the localisation studies have to be pursued.

A few known centrosomal proteins, such as Asp, Cp190 or Cp60 were not detected in our proteomic analysis. Cp190 localises to centrosomes during mitosis (Whitfield *et al*., 1988) and centrosomal localisation of Cp60 peaks during anaphase and telophase (Kellogg *et al*., 1995). It has been shown that composition of the centrosome depends on the concentration of detergent used in the isolation procedure (Moritz *et al*., 1995). Centrosomal localisation of γ-tubulin was not effected by higher detergent (0,5 % Triton X-100) concentration, while Cp190 localisation was slightly and Cp60 significantly reduced. Sucrose gradients that we used for the first step of the centrosome isolation contained 0,3 % non-ionic detergent, which might have caused a displacement of

Cp190, Cp60 and probably other proteins from the centrosome. The protein Asp is associated with the microtubule minus ends and can easily be removed from the centrosome (Wakefield *et al*., 2001). Proteins with a transient association might also get strongly reduced during the isolation process and are therefore difficult to detect in the mass spectrometry analysis.

4.3 Comparison of centrosome proteome analyses in different species

To compensate for the lack of an isolation technique that efficiently reduces contaminations, a previous proteomic analysis of the human centrosome used protein correlation profiling to distinguish centrosomal proteins from contaminants in sucrose gradient fractions (Andersen *et al*., 2003). In this study, we applied a direct biochemical approach in which we performed mass spectrometry analysis from immunoisolated centrosomes. In a similar study, basal bodies of *Chlamydomonas* were isolated by gradient centrifugation and analysed via mass spectrometry (Keller *et al*., 2005). Figure 5 compares the *Drosophila* orthologues of the proteins resulting from the proteomic analysis of the human centrosome and the *Chlamydomonas* basal body with the centrosomal proteome of *Drosophila*.

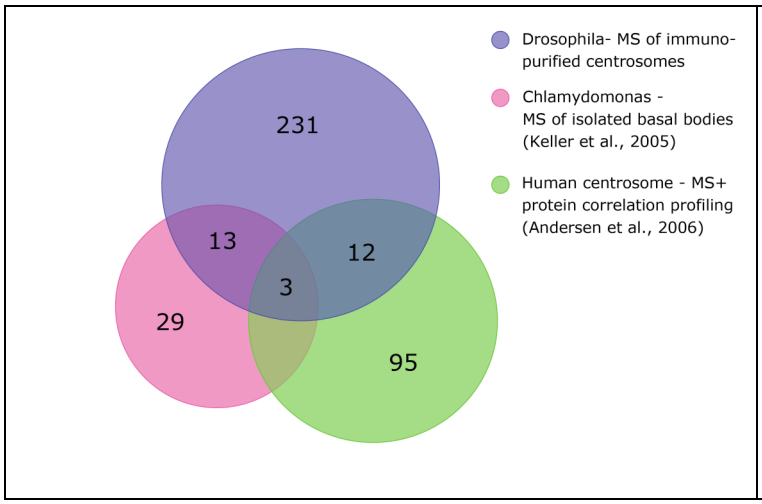

Figure 5: The *Drosophila* orthologues of the proteins resulting from the proteomic analysis of the human centrosome and the *Chlamydomonas* basal body are compared to the proteome of the *Drosophila* centrosome defined in this study.

Although these three studies used different approaches and organisms and the *Chlamydomonas* basal body represents only the centriole-part of the centrosome, the overlap of identified proteins evidences that proteins functioning in microtubule nucleation (γ-TuRC) and protein folding (chaperones) are conserved between species regarding their centrosomal function.

The microtubule monomers α-tubulin and β-tubulin as well as the chaperone Hsp90 were identified in all three organisms. α-tubulin and β-tubulin build the centriolar microtubule triplets, they are therefore likely to be present in all three analyses. Hsp90 was shown before to be essential for centrosome function in *Drosophila* and vertebrates (Lange *et al*., 2000). In consistency with previous studies that reported an important role in flagellar and cilia assembly for chaperones (Stolc *et al.*, 2005), two more chaperones (Hsp26, CG8863) were found in the centriole of *Chlamydomonas* and the *Drosophila* centrosome. The presence of chaperones at the centrosome in different species argues for a central role of these proteins in basic centrosomal function, probably mediated by modulating protein structure and facilitating interactions of centrosomal proteins (Lange *et al*., 2000). The importance of Hsp90 for centrosome function links the centrosome to human disease through its function in cilia assembly (Stolc *et al.*, 2005) and therefore ciliary diseases (reviewed by Badano *et al*., 2006) and through its implication in cancer (reviewed by Neckers, 2007).

The main protein group that was identified both in the centrosomal proteome of *Drosophila* and human is the γ-TuRC. All seven members were found in both organisms, demonstrating the conservation of the basic function of this complex for microtubule nucleation. Other components that are part of the *Drosophila* and the human centrosome proteome are involved in RNA processing or possess RNA helicase activity (CG10077, Rm62, Fib). A possible relevance for these proteins for centrosome structure is discussed below.

A common feature of 10 of the 15 proteins shared between *Drosophila* and human is the presence of at least one coiled-coil domain. Coiled-coil domains are protein-protein interaction motifs that are a common feature in centrosomal proteins (reviewed by Rose & Meier, 2004).

In conclusion, a set of centrosomal proteins is structurally and functionally conserved between *Chlamydomonas*, *Drosophila* and human, functioning in basic processes like microtubule nucleation.

4.4 The functional analysis of the centrosomal proteome

The accuracy of the phenotype analysis following mass spectrometry identification and RNAi is reflected by the identification of 24 previously identified proteins that have been associated with abnormal centrosomal phenotypes. Depletion of Grip75 (Vèrollet

et al., 2006), Grip 84 (Colombié *et al*., 2006), Grip 91 (Barbosa *et al*., 2003) and Cnn (Megraw *et al*., 1999) was shown to result in cells with single or no centrosomes. These previously shown phenotypes have been reproduced in the functional RNAi analysis, therefore substantiating our functional scoring. A further validation is provided by previous relation of the proteins Asp (do Carmo Avides & Glover, 1999), Ncd (Endow *et al*., 1994) and Aur (Giet *et al*., 2002) to centrosome integrity. In this study, depletion of these proteins also resulted in an abnormal centrosome shape indicating a disruption of centrosome integrity.

It has been proposed that the centrosome is integrated into multiple signalling pathways (Lange, 2002; Doxsey *et al*., 2005a). We identified for example the protein Pen (Küssel & Frasch, 1995), which is known to be an Importin alpha subunit that localises at the nucleus in a cell cycle-dependent manner. This study uncovers further functions of this protein: Pen depletion resulted in cells with large centrosomes and 8n DNA content. This indicates a function for Pen in both the regulation of cytokinesis and centrosomes segregation. The mechanism how centrosome duplication is limited to once per cell cycle is not fully understood. Recently, it has been proposed that DNA replication and centrosome replication are controlled by the same mechanism (Bettencourt-Dias & Glover, 2007). Support for this model is provided by our observation that depletion of the protein lat caused overduplication of centrosomes. Lat was previously described to play a role in DNA replication initiation (Chesnokov *et al*., 1999), suggesting a link between DNA replication and centrosome replication. Here we provided additional evidence for involvement of centrosomal proteins in cellular functions like nuclear transport and DNA replication.

4.5 The role of the centrosome in cell cycle control

The centrosome is required for several cell cycle transitions (Doxsey *et al*., 2005b). For example, increasing evidence relates the centrosome or centrosomal components to the spindle assembly checkpoint. In *Aspergillus nidulans*, a mutation in the γ-tubulin gene *mipA* disrupted the coordination of late mitotic events (Prigozhina *et al*., 2004). The authors suggest a role for γ-tubulin in establishing or maintaining a mitotic checkpoint block. The work of Vardy and Toda (2000) proposed that the fission yeast γ-tubulin complex members Alp4 and Alp6 are essential components of the spindle assembly checkpoint. An involvement of Dgrip84, which is part of the γ-TuRC, in mitotic

checkpoint regulation has been proposed in *Drosophila* (Colombiè *et al*., 2006) and was confirmed as part of this thesis. Here, implication of the γ-TuRC in the spindle assembly checkpoint in *Drosophila melanogaster* has been shown by providing evidence for a molecular and functional interaction of γ-TuRC proteins with spindle assembly checkpoint components.

4.6 A possible function of RNA for the centrosome

There has been a long debate on the presence of DNA and RNA in the centrosome. While the presence of DNA has not been confirmed (Johnson & Rosenbaum, 1990), RNA has been discovered in the centrosome recently (Alliegro *et al*., 2006, Alliegro & Alliegro, 2008). In relevance to this, our analysis identified a group of proteins that have previously been implicated in RNA-transport, RNA-processing or have RNA-binding domains. A subset of these proteins resulted in cells with no centrosomes or a single centrosome after RNAi mediated protein knock-down. This leads to the hypothesis that RNA and RNA-binding proteins might be involved in maintenance of centrosome structure and the regulation of the centrosome cycle. If RNA and RNA-binding proteins might act as a scaffold structure or play a role for centrosome regulation has to be validated by future studies. Furthermore, we identified ribosomal proteins in our immunoisolated centrosomes. 25 years ago it has been hypothesized that centrioles might contain ribosomes (Kallenbach, 1983), but more previously ribosomal proteins have been described to be a common contamination of centrosomal preparations (Andersen *et al*., 2003). In the functional analysis 70% of the identified ribosomal proteins caused a centrosomal phenotype after depletion. Whether this effect refers to impaired protein synthesis or reflects a physical link between centrosome and ribosome remains to be tested.

4.7 Conclusion

More and more evidence is provided for the implication of centrosomal proteins in the development of disease (Badano *et al.*, 2005; Fukasawa, 2005; Nigg, 2006). This is reflected by the fact that the centrosome is implicated in many essential cellular processes. A detailed description of the centrosomal proteome and molecular functions of its components is still missing. Through the proteomic and functional characterisation of the early *Drosophila* embryo centrosome this work provides

valuable insights and contributes to the molecular understanding of how the centrosome is connected to signalling pathways and how malfunction of such conserved proteins might lead to disease.

5 References

Andersen JS, Wilkinson CJ, Mayor T, Mortensen P, Nigg EA, Mann M. 2003. Proteomic characterization of the human centrosome by protein correlation profiling. *Nature*. 426: 570-4.

Alliegro MC, Alliegro MA, Palazzo RE. 2006. Centrosome-associated RNA in surf clam oocytes. *Proc Natl Acad Sci U S A*. **103**: 9034-8.

Alliegro MC, Alliegro MA. 2008. Centrosomal RNA correlates with intron-poor nuclear genes in Spisula oocytes. *Proc Natl Acad Sci U S A*. **105**: 6993-7.

Ansley SJ, Badano JL, Blacque OE, Hill J, Hoskins BE, Leitch CC, Kim JC, Ross AJ, Eichers ER, Teslovich TM *et al*. 2003. Basal body dysfunction is a likely cause of pleiotropic Bardet-Biedl syndrome. *Nature*. **425**: 628-33.

Ashburner, M. 1989. Drosophila, a laboratory handbook. Cold Spring Harbor Laboratory Press, Cold Spring Harbor. 216 pp.

Azimzadeh J, Bornens M. 2007. Structure and duplication of the centrosome. *J Cell Sci*. **120**: 2139-42.

Badano JL, Teslovich TM, Katsanis N. 2005. The centrosome in human genetic disease. *Nat Rev Genet.* **6**: 194-205.

Badano JL, Mitsuma N, Beales PL, Katsanis N. 2006. The ciliopathies: an emerging class of human genetic disorders. *Annu Rev Genomics Hum Genet.* **7**: 125-48.

Bahe S, Stierhof YD, Wilkinson CJ, Leiss F, Nigg EA. 2005. Rootletin forms centriole-associated filaments and functions in centrosome cohesion. *J Cell Biol. **171**: 27-33.*

Barbosa V, Gatt M, Rebollo E, Gonzalez C, Glover DM. 2003. Drosophila dd4 mutants reveal that gammaTuRC is required to maintain juxtaposed half spindles in spermatocytes. *J Cell Sci.* **116**: 929-41

Barros TP, Kinoshita K, Hyman AA, Raff JW. 2005. Aurora A activates D-TACC-Msps complexes exclusively at centrosomes to stabilize centrosomal microtubules. *J Cell Biol*. **170**: 1039-46.

Beales PL, Elcioglu N, Woolf AS, Parker D, Flinter FA. 1999. New criteria for improved diagnosis of Bardet-Biedl syndrome: results of a population survey. *J. Med. Genet.* **36**, 437–446.

Berdnik D, Knoblich JA. 2002. Drosophila Aurora-A is required for centrosome maturation and actindependent asymmetric protein localization during mitosis. *Curr. Biol*. **12**: 640–647.

Bertrand P, Lambert S, Joubert C, Lopez BS. 2003. Overexpression of mammalian Rad51 does not stimulate tumorigenesis while a dominant-negative Rad51 affects centrosome fragmentation, ploidy and stimulates tumorigenesis, in p53-defective CHO cells. *Oncogene* **22**: 7587–7592.

Bettencourt-Dias M, Rodrigues-Martins A, Carpenter L, Riparbelli M, Lehmann L, Gatt MK, Carmo N, Balloux F, Callaini G, Glover DM. 2005. SAK/PLK4 is required for centriole duplication and flagella development. *Curr Biol.* **15**: 2199-207.

Bettencourt-Dias M, Glover DM. 2007. Centrosome biogenesis and function: centrosomics brings new understanding. *Nat Rev Mol Cell Biol.* **8**: 451-63.

Bond J, Roberts E, Springell K, Lizarraga SB, Scott S, Higgins J, Hampshire DJ, Morrison EE, Leal GF, Silva EO *et al*. 2005. A centrosomal mechanism involving CDK5RAP2 and CENPJ controls brain size. *Nat Genet*. **37**: 353-5.

Boveri, T.1901. Über die Natur der Centrosomen. *Jena. Z. Med.Naturw.* **28**, 1–220.

Boveri T. Zur Frage der Entstehung maligner Tumoren. 1914. *Jena: Gustav Fischer*; 64 pp

Broadhead R, Dawe HR, Farr H, Griffiths S, Hart SR, Portman N, Shaw MK, Ginger ML, Gaskell SJ, McKean PG, Gull K. 2006. Flagellar motility is required for the viability of the bloodstream trypanosome. *Nature* **440**: 224-7.

Calarco-Gillam PD, Siebert MC, Hubble R, Mitchison T, Kirschner M. 1983. Centrosome development in early mouse embryos as defined by an autoantibody against pericentriolar material. *Cell*. **35**: 621-9.

Callaini G, Whitfield WG, Riparbelli MG. 1997. Centriole and centrosome dynamics during the embryonic cell cycles that follow the formation of the cellular blastoderm in Drosophila. *Exp Cell Res*. **234**: 183-90.

Castro A, Bernis C, Vigneron S, Labbé JC, Lorca T. 2005. The anaphase-promoting complex: a key factor in the regulation of cell cycle. *Oncogene*. **24**: 314-25.

Cheng KC, Loeb LA. 1997. Genomic stability and instability: a working paradigm. *Curr Top Microbiol Immunol.* **221**: 5-18.

Chesnokov I, Gossen M, Remus D, Botchan M. 1999. Assembly of functionally active Drosophila origin recognition complex from recombinant proteins. *Genes Dev.* **13**: 1289-1296.

Colombié N, Vérollet C, Sampaio P, Moisand A, Sunkel C, Bourbon HM, Wright M, Raynaud-Messina B. 2006. The Drosophila gamma-tubulin small complex subunit Dgrip84 is required for structural and functional integrity of the spindle apparatus. *Mol Biol Cell*. **17**: 272-82.

Dammermann A, Merdes A. 2002. Assembly of centrosomal proteins and microtubule organization depends on PCM-1. *J Cell Biol.* **159**: 255–266.

Delattre M, Canard C, Gönczy P. 2006. Sequential protein recruitment of C. elegans centriole formation. *Curr Biol*. **16**: 1844–1849.

Dix CI, Raff JW. 2007. *Drosophila* Spd-2 recruits PCM to the sperm centriole, but is dispensable for centriole duplication. *Curr Biol.* **17**: 1759-1764.

do Carmo Avides M, Glover DM. 1999. Abnormal spindle protein, Asp, and the integrity of mitotic centrosomal microtubule organizing centers. *Science*. **283**: 1733-5.

Doxsey S. 2001. Re-evaluating centrosome function. *Nat Rev Mol Cell Biol.* **2**: 688-98.

Doxsey S, McCollum D, Theurkauf W. 2005a. Centrosomes in cellular regulation. *Annu Rev Cell Dev Biol*. **21**: 411-34.

Doxsey S, Zimmerman W, Mikule K. 2005b. Centrosome control of the cell cycle. *Trends Cell Biol.* **15**: 303-11

Ekholm SV, Reed SI. 2000. Regulation of G(1) cyclin-dependent kinases in the mammalian cell cycle. *Curr Opin Cell Biol.* **12**: 676-684.

Endow SA, Chandra R, Komma DJ, Yamamoto AH, Salmon ED. 1994. Mutants of the Drosophila ncd microtubule motor protein cause centrosomal and spindle pole defects in mitosis. *J Cell Sci.* **107**: 859-67.

Engelender S, Sharp AH, Colomer V, Tokito MK, Lanahan A, Worley P, Holzbaur EL, Ross CA. 1997. Huntingtin-associated protein 1 (HAP1) interacts with the p150Glued subunit of dynactin. *Hum Mol Genet. 6*: 2205-12.

Fry AM, Meraldi P, Nigg EA. 1998. A centrosomal function for the human Nek2 protein kinase, a member of the NIMA family of cell cycle regulators. *EMBO J.* **17**: 470-81.

Fry AM, Mayor T, Nigg EA. 2000. Regulating centrosomes by protein phosphorylation. *Curr Top Dev Biol*. **49**: 291-312.

Fukasawa K, Choi T, Kuriyama R, Rulong S, Vande Woude GF. 1996. Abnormal centrosome amplification in the absence of p53. *Science*. **271**: 1744-7.

Fukasawa K, Wiener F, Vande Woude GF, Mai S. 1997. Genomic instability and apoptosis are frequent in p53 deficient young mice. *Oncogene*. **15**: 1295-302.

Fukasawa K. 2005. Centrosome amplification, chromosome instability and cancer development. *Cancer Lett*. **230**: 6-19.

Giet R, McLean D, Descamps S, Lee MJ, Raff JW, Prigent C, Glover DM. 2002. Drosophila Aurora A kinase is required to localize D-TACC to centrosomes and to regulate astral microtubules. *J Cell Biol.* **156**: 437-51.

Gillingham AK, Munro S. 2000. The PACT domain, a conserved centrosomal targeting motif in the coiled-coil proteins AKAP450 and pericentrin. *EMBO Rep.* **1**: 524-9.

Gleeson JG, Allen KM, Fox JW, Lamperti ED, Berkovic S, Scheffer I, Cooper EC, Dobyns WB, Minnerath SR, Ross ME, Walsh CA. 1998. Doublecortin, a brain-specific gene mutated in human X-linked lissencephaly and double cortex syndrome, encodes a putative signaling protein. *Cell*. **92**: 63-72.

Glotzer M, Murray AW, Kirschner MW. 1991. Cyclin is degraded by the ubiquitin pathway. *Nature*. **349**: 132-8.
Goshima G, Wollman R, Goodwin SS, Zhang N, Scholey JM, Vale RD, Stuurman N. 2007. Genes required for mitotic spindle assembly in Drosophila S2 cells. *Science*. **316**: 417-21.

Gutekunst CA, Levey AI, Heilman CJ, Whaley WL, Yi H, Nash NR, Rees HD, Madden JJ, Hersch SM. 1995. Identification and localization of huntingtin in brain and human lymphoblastoid cell lines with anti-fusion protein antibodies. *Proc Natl Acad Sci U S A*. **92**: 8710-4.

Habedanck R, Stierhof YD, Wilkinson CJ, Nigg EA. 2005. The Polo kinase Plk4 functions in centriole duplication. *Nat Cell Biol.* **7**: 1140-6.

Hanahan D, Weinberg RA. 2000. The hallmarks of cancer. Cell. **100**: *57-70*.

Hannak E, Kirkham M, Hyman AA, Oegema K. 2001. Aurora-A kinase is required for centrosome maturation in Caenorhabditis elegans. *J. Cell Biol.* ***155***: 1109–1116.

Heath JB. 1981. Nucleus-associated organelles in fungi. *Int. Rev. Cytol.* 191-221. Academic Press, New York.

Heuer JG, Li K, Kaufman TC. 1995. The Drosophila homeotic target gene centrosomin (cnn) encodes a novel centrosomal protein with leucine zippers and maps to a genomic region required for midgut morphogenesis. *Development*. **121**: 3861-76.

Hinchcliffe EH, Li C, Thompson EA, Maller JL, Sluder G. 1999. Requirement of Cdk2-cyclin E activity for repeated centrosome reproduction in Xenopus egg extracts. *Science*. **283**: 851-4.

Howell BJ, Moree B, Farrar EM, Stewart S, Fang G, Salmon ED. 2004. Spindle checkpoint protein dynamics at kinetochores in living cells. *Curr Biol*. **14**: 953-64.

Huang J, Raff JW. 1999. The disappearance of cyclin B at the end of mitosis is regulated spatially in Drosophila cells. *EMBO J*. **18**: 2184-95.

Johnson KA, Rosenbaum JL. 1990. The basal bodies of Chlamydomonas reinhardtii do not contain immunologically detectable DNA. *Cell*. **62**: 615-9.

Kallenbach RJ. 1983. Do centrioles contain ribosomes? *Biosci Rep.* **3**: 1155-62.

Kalt A, Schliwa M. 1993. Molecular components of the centrosome. *Trends Cell Biol*. **3**: 118-28.

Keller LC, Romijn EP, Zamora I, Yates JR 3rd, Marshall WF. 2005. Proteomic analysis of isolated chlamydomonas centrioles reveals orthologs of ciliary-disease genes. *Curr Biol*. **15**: 1090-8.

Kellogg DR, Oegema K, Raff J, Schneider K, Alberts BM. 1995. CP60: a microtubule-associated protein that is localized to the centrosome in a cell cycle-specific manner. *Mol Biol Cell*. **6**: 1673-84.

Kerr P, Ashworth A. 2001. New complexities for BRCA1 and BRCA2. *Curr Biol*. **11**: 668–676.

Kilburn C, Winey M. 2008. Basal bodies. *Curr Biol.* **18**: R56-R57.

Kim JC, Badano JL, Sibold S, Esmail MA, Hill J, Hoskins BE, Leitch CC, Venner K, Ansley SJ, Ross AJ *et al*. 2004. The Bardet-Biedl protein BBS4 targets cargo to the pericentriolar region and is required for microtubule anchoring and cell cycle progression. *Nat Genet*. **36**: 462-70.

Kim JC, Ou YY, Badano JL, Esmail MA, Leitch CC, Fiedrich E, Beales PL, Archibald JM, Katsanis N, Rattner JB, Leroux MR. 2005. MKKS/BBS6, a divergent chaperonin-like protein linked to the obesity disorder Bardet-Biedl syndrome, is a novel centrosomal component required for cytokinesis. *J Cell Sci*. **118**: 1007-20.

Komesli S, Tournier F, Paintrand M, Margolis RL, Job D, Bornens M. 1989. Mass isolation of calf thymus centrosomes: identification of a specific configuration. *J Cell Biol*. **109**: 2869-78.

Küssel P, Frasch M. 1995. Pendulin, a Drosophila protein with cell cycle-dependent nuclear localization, is required for normal cell proliferation. *J Cell Biol.* **129**: 1491-507.

Lange BM, Bachi A, Wilm M, González C. 2000. Hsp90 is a core centrosomal component and is required at different stages of the centrosome cycle in Drosophila and vertebrates. *EMBO J*. **19**: 1252-62.

Lange BM. 2002. Integration of the centrosome in cell cycle control, stress response and signal transduction pathways. *Curr Opin Cell Biol*. **14**: 35-43.

Li JB, Gerdes JM, Haycraft CJ, Fan Y, Teslovich TM, May-Simera H, Li H, Blacque OE, Li L, Leitch CC *et al*. 2004. Comparative genomics identifies a flagellar and basal body proteome that includes the BBS5 human disease gene. *Cell*. **117**: 541-52.

Lehmann V, Müller H, Lange BM. 2006. Immunoisolation of centrosomes from Drosophila melanogaster. *Curr Protoc Cell Biol.* Chapter 3: Unit 3.17.

Lingle WL, Barrett SL, Negron VC, D'Assoro AB, Boeneman K, Liu W, Whitehead CM, Reynolds C, Salisbury JL. 2002. Centrosome amplification drives chromosomal instability in breast tumor development. *Proc Natl Acad Sci U S A*. **99**: 1978-83.

Marshall WF, Nonaka S. 2006. Cilia: tuning in to the cell's antenna. *Curr Biol*. **16**: R604-14.

Martinez-Campos M, Basto R, Baker J, Kernan M, Raff JW. 2004. The Drosophila pericentrin-like protein is essential for cilia/flagella function, but appears to be dispensable for mitosis. *J Cell Biol.* **165**: 673-83.

Matsumoto Y, Hayashi K, Nishida E. 1999. Cyclin-dependent kinase 2 (Cdk2) is required for centrosome duplication in mammalian cells. *Curr Biol.* **9**: 429-32.

Mayor T, Stierhof YD, Tanaka K, Fry AM, Nigg EA. 2000. The centrosomal protein C-Nap1 is required for cell cycle-regulated centrosome cohesion. *J Cell Biol*. **151**: 837-46.

McCleland ML, O'Farrell PH. 2008. RNAi of mitotic cyclins in Drosophila uncouples the nuclear and centrosome cycle. *Curr Biol*. **18**: 245-54.

Megraw TL, Li K, Kao LR, Kaufman TC. 1999. The centrosomin protein is required for centrosome assembly and function during cleavage in Drosophila. *Development*. **126**: 2829-39.

Meraldi P, Lukas J, Fry AM, Bartek J, Nigg EA. 1999. Centrosome duplication in mammalian somatic cells requires E2F and Cdk2-cyclin A. *Nat Cell Biol.* **1**: 88-93.

Michaelis C, Ciosk R, Nasmyth K. 1997. Cohesins: chromosomal proteins that prevent premature separation of sister chromatids. *Cell*. **91**: 35-45.

Mitchison T, Kirschner M. 1984. Microtubule assembly nucleated by isolated centrosomes. *Nature.* **312**: 232-7.

Mizuta R, LaSalle JM, Cheng HL, Shinohara A, Ogawa H, Copeland N, Jenkins NA, Lalande M, Alt FW. 1997. RAB22 and RAB163/mouse BRCA2: proteins that specifically interact with the RAD51 protein. *Proc Natl Acad Sci U S A.* 94: 6927-32.

Moritz M, Braunfeld MB, Fung JC, Sedat JW, Alberts BM, Agard DA. 1995. Three-dimensional structural characterization of centrosomes from early Drosophila embryos. *J Cell Biol*. **130**: 1149-59.

Moritz M, Zheng Y, Alberts BM, Oegema K. 1998. Recruitment of the gamma-tubulin ring complex to Drosophila salt-stripped centrosome scaffolds. *J Cell Biol*. **142**: 775-86.

Moritz M, Braunfeld MB, Guenebaut V, Heuser J, Agard DA. 2000. Structure of the gamma-tubulin ring complex: a template for microtubule nucleation. *Nat Cell Biol*. **2**: 365-70.

Moudjou M, Bornens M. 1994. Method of centrosome isolation from cultured animal cells. *Cell Biology: A Laboratory Handbook. Academic Press, London.* **1**: 595-604.

Moynahan ME, Chiu JW, Koller BH, Jasin M. 1999. Brca1 controls homology-directed DNA repair. *Mol Cell.* **4**: 511-8.

Müller H, Fogeron ML, Lehmann V, Lehrach H, Lange BM. 2006. A centrosome-independent role for gamma-TuRC proteins in the spindle assembly checkpoint. *Science.* **314**: 654-7.

Musacchio A, Hardwick KG. 2002. The spindle checkpoint: structural insights into dynamic signalling. *Nat Rev Mol Cell Biol*. **3**: 731-41.

Nakagawa Y, Yamane Y, Okanoue T, Tsukita S. 2001. Outer dense fiber 2 is a widespread centrosome scaffold component preferentially associated with mother centrioles: its identification from isolated centrosomes. *Mol Biol Cell*. **12**: 1687-97.

Neckers L. 2007. Heat shock protein 90: the cancer chaperone. *J Biosci.* **32**: 517-30.

Nevins JR. 1992. E2F: a link between the Rb tumor suppressor protein and viral oncoproteins. *Science*. **258**: 424-9.

Nigg EA. 2001. Mitotic kinases as regulators of cell division and its checkpoints. *Nat Rev Mol Cell Biol.* **2**: 21-32.

Nigg EA. 2002. Centrosome aberrations: cause or consequence of cancer progression? *Nat Rev Cancer*. **2**: 815-25.

Nigg EA. 2006. Origins and consequences of centrosome aberrations in human cancers. *Int J Cancer.* **119**: 2717-2.

Okuda M, Horn HF, Tarapore P, Tokuyama Y, Smulian AG, Chan PK, Knudsen ES, Hofmann IA, Snyder JD, Bove KE, Fukasawa K. 2000. Nucleophosmin/B23 is a target of CDK2/cyclin E in centrosome duplication. *Cell.* **103**: 127-40.

Omura F, Fukui Y. 1985. Dictyostelium MTOC: structure and linkage to the nucleus. *Protoplasma.* **127**: 212-221.

Ostrowski LE, Blackburn K, Radde KM, Moyer MB, Schlatzer DM, Moseley A, Boucher RC. 2002. A proteomic analysis of human cilia: identification of novel components. *Mol Cell Proteomics*. **1**: 451-65.

Paintrand M, Moudjou M, Delacroix H, Bornens M. 1992. Centrosome organization and centriole architecture: their sensitivity to divalent cations. *J Struct Biol*. **108**: 107-28.

Palazzo RE, Vogel JM. 1999. Isolation of centrosomes from Spisula solidissima oocytes. *Methods Cell Biol*. **61**: 35-56.

Palazzo RE, Vogel JM, Schnackenberg BJ, Hull DR, Wu X. 2000. Centrosome maturation. *Curr Top Dev Biol.* **49**: 449–470.

Pazour GJ, Agrin N, Leszyk J, Witman GB. 2005. Proteomic analysis of a eukaryotic cilium. *J Cell Biol.* **170**: 103-13.

Pelletier L, O'Toole E, Schwager A, Hyman AA, Müller-Reichert T. 2006. Centriole assembly in Caenorhabditis elegans. *Nature*. **444**: 619-23.

Prigozhina NL, Oakley CE, Lewis AM, Nayak T, Osmani SA, Oakley BR. 2004. gamma-tubulin plays an essential role in the coordination of mitotic events. *Mol Biol Cell.* **15**: 1374-86.

Rajagopalan S, Bimbo A, Balasubramanian MK, Oliferenko S. 2004. A potential tension-sensing mechanism that ensures timely anaphase onset upon metaphase spindle orientation. *Curr Biol*. **14**: 69-74.

Rauch A, Thiel CT, Schindler D, Wick U, Crow YJ, Ekici AB, van Essen AJ, Goecke TO, Al-Gazali L, Chrzanowska KH et al. 2008. Mutations in the pericentrin (PCNT) gene cause primordial dwarfism. *Science*. **319**: 816-9.

Reinders Y, Schulz I, Gräf R, Sickmann A. 2006. Identification of novel centrosomal proteins in Dictyostelium discoideum by comparative proteomic approaches. *J Proteome Res.* **5**: 589-98.

Reiner O, Carrozzo R, Shen Y, Wehnert M, Faustinella F, Dobyns WB, Caskey CT, Ledbetter DH. 1993. Isolation of a Miller-Dieker lissencephaly gene containing G protein beta-subunit-like repeats. *Nature*. **364**: 717-21.

Riley T, Sontag E, Chen P, Levine A. 2008. Transcriptional control of human p53-regulated genes. *Nat Rev Mol Cell Biol.* **9**: 402-12.

Roos UP. 1975. Fine structure of an organelle associated with the nucleus and cytoplasmic microtubules in the cellular slime mould Polysphondylium violaceum. *J Cell Sci*. **18**: 315-26.

Rose A, Meier I. 2004. Scaffolds, levers, rods and springs: diverse cellular functions of long coiled-coil proteins. *Cell Mol Life Sci.* **61**: 1996-2009.

Rout MP, Kilmartin JV. 1990. Components of the yeast spindle and spindle pole body. *J Cell Biol*. **111**: 1913-27.

Salic A, Waters JC, Mitchison TJ. 2004. Vertebrate shugoshin links sister centromere cohesion and kinetochore microtubule stability in mitosis. *Cell*. **118**: 567-78.

Schatten H. 2008. The mammalian centrosome and its functional significance. *Histochem Cell Biol*. **129**: 667-86.

Schmit AC. 2002. Acentrosomal microtubule nucleation in higher plants. *Int Rev Cytol*. **220**: 257-89.

Schnackenberg BJ, Khodjakov A, Rieder CL, Palazzo RE. 1998. The disassembly and reassembly of functional centrosomes in vitro. *Proc Natl Acad Sci U S A*. **95**: 9295-300.
Scully R, Chen J, Plug A, Xiao Y, Weaver D, Feunteun J, Ashley T, Livingston DM. 1997. Association of BRCA1 with Rad51 in mitotic and meiotic cells. *Cell*. **88**: 265-75.

Scully R, Chen J, Plug A, Xiao Y, Weaver D, Feunteun J, Ashley T, Livingston DM. 1997. Association of BRCA1 with Rad51 in mitotic and meiotic cells. *Cell*. **88**: 265-75

Shen J, Eyaid W, Mochida GH, Al-Moayyad F, Bodell A, Woods CG, Walsh CA. 2005. ASPM mutations identified in patients with primary microcephaly and seizures. *Med Genet*. **42**: 725-9.

Shono M, Sato N, Mizumoto K, Maehara N, Nakamura M, Nagai E, Tanaka M. 2001. Stepwise progression of centrosome defects associated with local tumor growth and metastatic process of human pancreatic carcinoma cells transplanted orthotopically into nude mice. *Lab Invest.* **81**: 945-52.

Stolc V, Samanta MP, Tongprasit W, Marshall WF. 2005. Genome-wide transcriptional analysis of flagellar regeneration in Chlamydomonas reinhardtii identifies orthologs of ciliary disease genes. *Proc Natl Acad Sci U S A*. 102: 3703-7.

Szebeni A, Olson MO. 1999. Nucleolar protein B23 has molecular chaperone activities. *Protein Sci*. **8**: 905-912.

Szollosi D, Calarco P, Donahue RP. 1972. Absence of centrioles in the first and second meiotic spindles of mouse oocytes. *J Cell Sci*. **11**: 521-41.

Takahashi M, Yamagiwa A, Nishimura T, Mukai H, Ono Y. 2002. Centrosomal proteins CG-NAP and kendrin provide microtubule nucleation sites by anchoring gamma-tubulin ring complex. *Mol Biol Cell*. **13**: 3235-45.

Theurkauf WE, Hawley RS. 1992. Meiotic spindle assembly in Drosophila females: behavior of nonexchange chromosomes and the effects of mutations in the nod kinesin-like protein. *J Cell Biol.* **5**: 1167-80.

Tsou MF, Stearns T. 2006. Mechanism limiting centrosome duplication to once per cell cycle. *Nature*. **442**: 947-51.

Tutt A, Gabriel A, Bertwistle D, Connor F, Paterson H, Peacock J, Ross G, Ashworth A. 1999. Absence of Brca2 causes genome instability by chromosome breakage and loss associated with centrosome amplification. *Curr Biol*. **9**: 1107-10.

Uhlmann F, Lottspeich F, Nasmyth K. 1999. Sister-chromatid separation at anaphase onset is promoted by cleavage of the cohesin subunit Scc1. *Nature*. **400**: 37-42.

Vardy L, Toda T. 2000. The fission yeast gamma-tubulin complex is required in G(1) phase and is a component of the spindle assembly checkpoint. *EMBO J.* **19**: 6098-111.

Vérollet C, Colombié N, Daubon T, Bourbon HM, Wright M, Raynaud-Messina B. 2006. Drosophila melanogaster gamma-TuRC is dispensable for targeting gamma-tubulin to the centrosome and microtubule nucleation. *J Cell Biol.* **172**: 517-28.

Wakefield JG, Huang JY, Raff JW. 2000. Centrosomes have a role in regulating the destruction of cyclin B in early Drosophila embryos. *Curr. Biol*. **10**: 1367–1370.

Wakefield JG, Bonaccorsi S, Gatti M. 2001. The Drosophila protein asp is involved in microtubule organization during spindle formation and cytokinesis. *J Cell Biol*. **153**: 637-48.

Wang X, Yang Y, Duan Q, Jiang N, Huang Y, Darzynkiewicz Z, Dai W. 2008. sSgo1, a major splice variant of Sgo1, functions in centriole cohesion where it is regulated by Plk1. *Dev Cell*. **14**: 331-41.

Whitfield WG, Millar SE, Saumweber H, Frasch M, Glover DM. 1988. Cloning of a gene encoding an antigen associated with the centrosome in Drosophila. *J Cell Sci*. **89**: 467-80.

Wigge PA, Jensen ON, Holmes S, Souès S, Mann M, Kilmartin JV. 1998. Analysis of the Saccharomyces spindle pole by matrix-assisted laser desorption/ionization (MALDI) mass spectrometry. *J Cell Biol.* **141**: 967-77.

Wigley WC, Fabunmi RP, Lee MG, Marino CR, Muallem S, DeMartino GN, Thomas PJ. 1999. Dynamic association of proteasomal machinery with the centrosome. *J Cell Biol.* **145**: 481-90.

Xu X, Weaver Z, Linke SP, Li C, Gotay J, Wang XW, Harris CC, Ried T, Deng CX. 1999. Centrosome amplification and a defective G2-M cell cycle checkpoint induce genetic instability in BRCA1 exon 11 isoform-deficient cells. *Mol Cell*. **3**: 389-95.

Yu H. 2007. Cdc20: a WD40 activator for a cell cycle degradation machine. *Mol Cell.* **27**: 3-16.

Zhang J, Megraw TL. 2007. Proper recruitment of gamma-tubulin and D-TACC/Msps to embryonic Drosophila centrosomes requires Centrosomin Motif 1. *Mol Biol Cell.* **18**: 4037-49.

6 Appendix

6.1 Abstract

The centrosome is the primary microtubule-organizing centre in eukaryotic cells. In addition to its function in microtubule nucleation it is implicated in signalling pathways regulating fundamental processes like cell cycle progression, differentiation or cell stress. Centrosomal aberrations and dysfunction of centrosomal proteins frequently occur in various diseases such as cancer. To better understand these processes on a molecular level, precise functions of single centrosomal components have to be elucidated. Although a series of centrosomal proteins have already been characterised, the knowledge of centrosome composition and of function of its proteins remains incomplete. It was the aim of this project to identify the components of the centrosomal proteome in *Drosophila melanogaster* and to characterise their function for centrosome integrity, replication and cell cycle regulation. An immunoisolation technique was optimized to obtain highly enriched centrosomal preparations from *Drosophila* preblastoderm stage embryos for mass spectrometry protein identification. Using this approach, 260 centrosomal candidate proteins were identified and subsequently functionally characterised through RNAi in *Drosophila* SL2 cells. Analysing the resulting phenotypes by immunofluorescence microscopy and FACS revealed the existence of functional groups of centrosomal proteins playing a role in centrosome integrity, centrosome cycle or cell cycle progression. A new centrosome related function was assigned to 28 proteins. Among these proteins a conserved group of proteins were identified required for maintaining centrosome structure both in *Drosophila* and in human cells. Furthermore, this work provides evidence for a novel role of the microtubule nucleation proteins, the γ-TuRC proteins, in cell cycle control. A biochemical and functional interaction of γ-TuRC proteins with spindle assembly checkpoint proteins was shown by means of RNAi and immunoprecipitation in *Drosophila* and tandem-affinity purification in human cells. Depletion of γ-TuRC proteins triggers the spindle assembly checkpoint in addition to activation through lack of kinetochore-microtubule attachment. Simultaneous protein depletion of γ-TuRC and Cnn revealed that the γ-TuRC mediated activation of the spindle assembly checkpoint is independent of centrosome integrity.

In summary, a comprehensive proteomic analysis identified novel centrosomal candidate proteins functioning in centrosome integrity, centrosome replication and cell cycle progression. γ-TuRC proteins are implicated in the spindle assembly checkpoint. The interaction of γ-TuRC components with spindle assembly checkpoint proteins is evolutionary conserved between human and *Drosophila*.

6.2 Zusammenfassung

Das Zentrosom ist das Mikrotubuli-organisierende Zentrum in eukaryotischen Zellen. Neben Mikrotubuli-Nukleation spielt es eine Rolle in Signaltransduktionswegen, die fundamentelle zelluläre Prozesse wie das Fortschreiten des Zellzyklus, Differenzierung oder Zellstress regulieren. Zentrosomale Aberration oder Veränderung einzelner zentrosomaler Bestandteile ist häufig in der Entstehung von Krankheiten wie Krebs zu beobachten. Um diese Prozesse auf molekularer Ebene zu verstehen, ist es notwendig, die Funktionen einzelner zentrosomaler Proteine aufzuklären. Obwohl einige zentrosomale Proteine bereits charakterisiert wurden, ist die genaue Zusammensetzung dieses Zellorganells weitgehend unbekannt. Das Ziel dieser Arbeit war es, die zentrosomalen Proteine in *Drosophila melanogaster* zu identifizieren und deren Funktion in Integrität und Replikation des Zentrosoms, sowie Regulation des Zellzyklus zu charakterisieren. Ein Immunoisolationsansatz wurde optimiert, um hoch angereicherte zentrosomale Präparationen aus *Drosophila* Embryonen für die Analyse mittels Massenspektrometrie zu gewinnen. Mit diesem Ansatz wurden 260 zentrosomale Kandidatenproteine identifiziert und anschließend mittels RNAi in *Drosophila* SL2 Zellen funktionell untersucht. Die Immunfluoreszenzmikroskopie- und FACS-Analyse der resultierenden Phänotypen zeigte, dass sich die Funktion zentrosomaler Proteine in Erhaltung der zentrosomalen Struktur oder Regulation von Zentrosomenzyklus und Zellzyklus in Gruppen einordnen lassen. Eine neue zentrosomale Funktion wurde 28 identifizierten Proteinen zugeordnet. Darunter befand sich eine evolutionär konservierte Protein-Gruppe, die für die Aufrechterhaltung der Zentrosomenstruktur in *Drosophila* und im Menschen verantwortlich ist. Weiterhin konnte in dieser Arbeit der Nachweis erbracht werden, dass Proteine des γ-TuRC neben ihrer Funktion in Mikrotubuli-Nukleation eine Rolle im Zellzyklus-Kontrollsystem spielen. Unter Verwendung von RNAi, Immunopräzipitation in *Drosophila* und Tandem-Affinitäts-Aufreinigung in menschlichen Zellen wurde eine biochemische und

funktionelle Interaktion von γ-TuRC-Proteinen mit Spindelcheckpoint-Proteinen festgestellt. Reduzierung von γ-TuRC-Proteinen kann, zusätzlich zur Aktivierung durch fehlende Verbindung zwischen Kinetochor und Spindelmikrotubuli, den Spindelcheckpoint auslösen. Die gleichzeitige Proteinreduktion von γ-TuRC und Cnn belegte, dass γ-TuRC-vermittelte Spindelcheckpointaktivierung unabhängig von der Integrität des Zentrosoms ist.

Zusammenfassend kann gesagt werden, dass mit Hilfe einer umfassenden Proteomanalyse neue zentrosomale Kandidatenproteine identifiziert wurden, welchen eine Funktion in Aufrechterhaltung zentrosomaler Integrität, Zentrosomenreplikation und Zellzyklusregulation zugeordnet wurde. An der Aktivierung des Spindelcheckpoints sind γ-TuRC-Proteine beteiligt, deren evolutionär konservierte Interaktion mit Proteinen des Spindelcheckpoints gezeigt wurde.

6.4 Selbständigkeitserklärung

Ich versichere hiermit, diese Arbeit selbständig verfasst und nur die angegebenen Hilfsmittel und Hilfen in Anspruch genommen zu haben.
Experimente und Analysen wurden, sofern nicht anders gekennzeichnet, von mir durchgeführt.

Berlin, Juni 2008 Hannah Müller